

Article

Miscibility of Sphingomyelins and Phosphatidylcholines in Unsaturated Phosphatidylcholine Bilayers

Anders Kullberg,¹ Oscar Oz Ekhholm,¹ and J. Peter Slotte^{1,*}

¹Biochemistry, Faculty of Science and Engineering, Åbo Akademi University, Turku, Finland

ABSTRACT Polyunsaturated phospholipids are common in biological membranes and affect the lateral structure of bilayers. We have examined how saturated sphingomyelin (SM; palmitoyl and stearoyl SM (PSM and SSM, respectively)) and phosphatidylcholine (PC; dipalmitoyl PC and 1-palmitoyl-2-stearoyl PC (DPPC and PSPC, respectively)) segregate laterally to form ordered gel phases in increasingly unsaturated PC bilayers (*sn*-1: 16:0 and *sn*-2: 18:1...22:6; or *sn*-1 and *sn*-2: 18:1...22:6). The formation of gel phases was determined from the lifetime analysis of *trans*-parinaric acid. Using calorimetry, we also determined gel phase formation by PSM and DPPC in unsaturated PC mixed bilayers. Comparing PSM with DPPC, we observed that PSM formed a gel phase with less order than DPPC at comparable bilayer concentrations. The same was true when SSM was compared with PSPC. Furthermore, we observed that at equal saturated phospholipid concentration, the gel phases formed were less ordered in unsaturated PCs having 16:0 in *sn*-1, as compared to PCs having unsaturated acyl chains in both *sn*-1 and *sn*-2. The gel phases formed by the saturated phospholipids in unsaturated PC bilayers did not appear to achieve properties similar to pure saturated phospholipid bilayers, suggesting that complete lateral phase separation did not occur. Based on scanning calorimetry analysis, the melting of the gel phases formed by PSM and DPPC in unsaturated PC mixed bilayers (at 45 mol % saturated phospholipid) had low cooperativity and hence most likely were of mixed composition, in good agreement with *trans*-parinaric acid lifetime data. We conclude that both interfacial properties of the saturated phospholipids and their chain length, as well as the presence of 16:0 in *sn*-1 of the unsaturated PCs and the total number of *cis* unsaturations and acyl chain length (18 to 22) of the unsaturated PCs, all affected the formation of gel phases enriched in saturated phospholipids, under the conditions used.

INTRODUCTION

The role of lipids in the formation and maintenance of membrane lateral structure is of major interest, because it has been shown that certain membrane functions require ordered domains or platforms for optimal activity (1–4). The lipid raft hypothesis suggests that sphingomyelin (SM), glycosphingolipids, and cholesterol form dynamic, transient, and possibly very small domains that are functionally important (5–8). Many model membrane studies have focused on how saturated phosphatidylcholines (PCs) or SMs form ordered domains in unsaturated PC environments (9–14). Pertinent ternary phase diagrams have also been reported (15–19), which more quantitatively describe phase boundaries, phase coexistence regions, and phase compositions.

The formation of ordered domains by different SMs in 1-palmitoyl-2-oleoyl-*sn*-glycero-3-phosphocholine (POPC) and 1,2-dioleoyl-*sn*-glycero-3-phosphocholine (DOPC) bilayers has been examined extensively (20–25), and the relationship between SM structure and domain-forming properties has been discussed extensively (26). However, the role of the unsaturated phospholipids in determining

the properties of the more ordered PCs and SMs has received less attention, and complete ternary phase diagrams have been published for only a very limited set of unsaturated PCs. It has been shown that when the phospholipids have acyl chains that are highly polyunsaturated (e.g., with docosahexaenoic acid; 22:6), these may separate into cholesterol-devoid domains on their own (for recent reviews, see (27,28)). It is likely that cholesterol fails to interact favorably with polyunsaturated phospholipids because attractive van der Waals forces will not form efficiently between the planar sterol skeleton and the rough surface of the *cis*-double-bond-rich acyl chains. The unfavorable interaction between cholesterol and polyunsaturated phospholipid acyl chains also leads to a decreased bilayer solubility of cholesterol (29), a decreased bilayer affinity of cholesterol (30), and a potential displacement into the bilayer center of cholesterol itself (31). Even though cholesterol is not compatible with polyunsaturated acyl chains, 1-palmitoyl-2-docosahexaenoyl-*sn*-glycero-3-phosphocholine (PDPC) is apparently partially miscible with SM-rich domains and is thus able to interact with saturated phospholipids (32) and even to affect the cholesterol content of such domains. However, phosphatidylethanolamines with one saturated and one polyunsaturated acyl chain apparently phase-separate more efficiently from SM

Submitted May 28, 2015, and accepted for publication September 11, 2015.

*Correspondence: jpslotte@abo.fi

Editor: Heiko Heerklotz.

© 2015 by the Biophysical Society
0006-3495/15/11/1907/10



<http://dx.doi.org/10.1016/j.bpj.2015.09.009>

domains (33,34), suggesting that headgroup properties also affect miscibility.

In an effort to better understand the role of the unsaturated PCs in stabilizing/destabilizing ordered domains formed by a saturated PC or SM, Bakht and colleagues (35) examined domain stability using a TEMPO-based quenching assay in which diphenylhexatriene was the probe. They observed that the thermal stability of ordered dipalmitoyl PC domains was highest in bilayers containing polyunsaturated (20:4/20:4-PC) or methyl-branched (diphytanoyl) PCs and that it was significantly reduced when the bilayers contained 16:0/18:1-PC. The conclusion was that polyunsaturated phospholipid species had less ideal miscibility with the ordered phospholipids compared to 16:0/18:1-PC. The miscibility of mono- and polyunsaturated phosphatidylethanolamines with SM was also shown to be highly nonideal, leading to extensive phase separation, especially with the polyunsaturated species (34).

In this study, we examined the miscibility of saturated SMs (palmitoyl SM (PSM) and stearoyl SM (SSM)) and PCs (1,2-dipalmitoyl PC and 1-palmitoyl-2-stearoyl PC (DPPC and PSPC, respectively)) in bilayers formed from mono- or polyunsaturated PCs. The molecular structures of all phospholipids used in this study are shown in **Schemes S1–S3** in the **Supporting Material**. Immiscibility was deduced from the segregation into laterally ordered domains (gel phase) by the saturated phospholipids, as their concentration in the bilayer increased, and as the unsaturated PCs became increasingly polyunsaturated. The gel phase formation was detected either using time-resolved analysis of *trans*-parinaric acid (tPA) fluorescence, or DSC. Time-resolved tPA fluorescence is a powerful method for demonstrating the presence of ordered domains (or phases) in a fluid bilayer. First, tPA, because of its *all-trans* nature, prefers to partition into more ordered phases compared to more disordered phases (36,37). Second, the quantum yield of tPA increases significantly when tPA is localized in an ordered phase (36), in part because of less diffusion-dependent quenching (by oxygen and water). Although tPA emission decay is multicomponential, the longest lifetime component of tPA is a sensitive indicator of the appearance/disappearance of an ordered phase (as a function of concentration or temperature). However, lifetime data should be interpreted with some caution, because probe diffusion (between phases) during the excited-state lifetime will affect the observed lifetime. This effect is likely to be more significant if the ordered phase is composed of very small domains with significant molecular diffusion, or if the excited state lifetime is sufficiently long so that the probe may partition between ordered and more disordered phases.

We found that the saturated SMs and PCs were partially miscible with all the polyunsaturated fatty acid-containing PCs tested, in the sense that complete phase segregation was not observed. Increasing the chain length of the saturated phospholipids from 16:0 to 18:0 led to an increased

formation of a gel phase as the unsaturated acyl chains were increasingly unsaturated. Gel phases formed by SMs appeared to be less ordered than those formed by the matching PCs, as deduced from the longest lifetime component of tPA, and from the cooperativity of the gel phase melting by DSC. Only in the most unsaturated PC bilayers did a gel phase with properties similar to a pure gel phase coexist with a less ordered mixed phase of saturated phospholipid and unsaturated PC.

MATERIALS AND METHODS

Materials

The unsaturated (POPC, 1-palmitoyl-2-linoleoyl-*sn*-glycero-3-phosphocholine (PLPC), 1-palmitoyl-2-arachidonoyl-*sn*-glycero-3-phosphocholine (PAPC), PDPC, DOPC, 1,2-dilinoleoyl-*sn*-glycero-3-phosphocholine (DLPC), 1,2-diaraclidonoyl-*sn*-glycero-3-phosphocholine (DAPC), and 1,2-didocosahexaenoyl-*sn*-glycero-3-phosphocholine (DDPC)) as well as the saturated DPPC and PSPC were purchased from Avanti Polar Lipids (Alabaster, AL). PSM and SSM were purified from natural egg SM and brain SM, respectively (Avanti Polar Lipids) by preparative reverse-phase high-performance liquid chromatography (5 μm particle size, column dimensions of 250 mm × 21.1 mm, Supelco Discovery C18 (Bellefonte, PA)), using 100% methanol (Rathburn Chemicals, Walkerburn, Scotland) as an eluent. The identity of PSM and SSM was verified by mass spectrometry (Bruker HCT Ultra Ion Trap, Billerica, MA) and DSC (T_m :s were compared with literature values), and their purity was verified by analytical high-performance liquid chromatography (RP-C18 column eluted with methanol) and DSC. tPA was synthesized from methyl linolenate (Sigma-Aldrich, St. Louis, MO) as described previously (38). The identity of tPA was verified by mass spectrometry and by spectral analysis. The purity was ascertained using analytical high-performance liquid chromatography. Dry tPA was stored at –87°C in argon-purged vials containing 0.5 mol % butylated hydroxytoluene. Cholesterol was obtained from Sigma-Aldrich.

Stock solutions of phospholipids and cholesterol were made by dissolving the lipids in argon-purged methanol to ~2 mM concentration. tPA was dissolved in argon-purged methanol before use (remade every week). All unsaturated PC stock solutions were checked for oxidation products monthly, using electrospray ionization-mass spectrometry. Liposomes were only made from lipid stock solutions having intact polyunsaturated phospholipids and tPA. The lipids were stored at –20°C and warmed to ambient temperature before use. Water was used as the aqueous solvent in all studies and was purified by reverse osmosis through a Millipore UF Plus water-purification system. The resistivity of the water was 18.2 MΩcm.

Preparation of multilamellar vesicles

Multilamellar lipid vesicles (MLVs) used in fluorescence-lifetime measurements were prepared to a final lipid concentration of 0.2 mM and to a lipid/tPA ratio of 200:1. Various amounts of lipids were mixed and dried under a constant flow of argon at 40°C. The lipid mixtures were dispersed in argon-purged water and heated to a temperature above the chain-melting temperature (T_m) of the saturated phospholipid (to 65°C). The lipid suspension was then kept at this temperature for 30 min, vortexed, and sonicated with a FinnSonic M3 Bath Sonicator (40 kHz, ultrasonic power 80 W, FinnSonic Oy, Lahti, Finland) for 5 min to generate MLVs. All samples were kept shielded from light at 23°C before measurements. The integrity of polyunsaturated phospholipids in the MLV preparations was checked occasionally and no significant degradation of unsaturated PCs were observed in the samples from which data was used in our figures or tables. The size distribution of liposomes in the MLV preparations was also analyzed for some systems, using a Malvern Zetasizer Nano ZS. The MLV preparations

were polydisperse and large (for typical PDI and Z-average values of MLVs prepared from PSPC and unsaturated PCs, see Table S9).

Fluorescence experiments

The fluorescence-lifetime analysis was performed at 23°C with a FluoTime 100-spectrofluorimeter, using a PicoHarp 300E time-correlated single photon counting module (PicoQuant GmbH, Berlin, Germany). The tPA was excited with a 298 nm LED laser source (PLS300, PicoQuant) and the emission was measured above 350 nm. The samples were kept under constant stirring during the measurements. Data were analyzed with FluoFit Pro software (PicoQuant). Data were fitted to contain two (or sometimes three) lifetime components, whichever gave best unbiased residual plots and χ^2 closest to 1. The average lifetime was calculated as described in (39).

DSC

MLVs for DSC were prepared by mixing the desired lipids (saturated phospholipids together with unsaturated PCs, at 45 mol % saturated phospholipid) and evaporating the solvent under a stream of nitrogen. The samples were then kept under vacuum for 1 h to remove residual solvent. The resulting lipid films were hydrated with argon-purged MQ-water at 65°C for 30 min, followed by 5-min bath sonication at 65°C. Samples were cooled to room temperature and degassed for 10 min with a ThermoVac instrument (Microcal, Northampton, MA) before being loaded into the Microcal VP-DSC instrument. The saturated phospholipid concentration in the DSC cell was ~1 mM. Five up- and downscans were collected for each composition. Data analysis was performed using Origin software (OriginLab, Northampton, MA).

RESULTS

We examined the lateral segregation of PSM, DPPC, SSM, and PSPC in mono- and polyunsaturated PC bilayers as a function of bilayer composition at 23°C. Segregation was determined from the formation of an increasingly ordered gel phase, as deduced from the lifetime analysis of tPA fluorescence in the bilayer. We report both the intensity-weighted average lifetime (which takes into account the fractional contribution of all lifetime components (Figs. 1 and 2)) and the longest lifetime component (which reports from the most ordered phase present, but does not give information about the amount of phase, Figs. S1–S4 and Tables S1–S8). Because we do not know how tPA partitions among saturated and unsaturated phospholipids, we cannot use lifetime components (and preexponential factors) to calculate the amount of phases present in different systems. Finally, we provide thermograms of PSM and DPPC in mixed bilayers containing the unsaturated PCs (Figs. 3 and 4 and Table S10). For clarity, we refer to all PCs with different *sn*-1/*sn*-2 acyl chains as mixed chain PC and to those with identical *sn*-1/*sn*-2 acyl chains as equal chain PC.

Mixed bilayers containing mono- and polyunsaturated PCs and PSM

When PSM was added to mixed chain PCs, the average lifetime of tPA increased very moderately as the PSM concen-

tration increased (Fig. 1 A). Above 30 mol % PSM, the average lifetime increased more for PDPC bilayers than for the other mixed chain PC bilayers, but even at 45 mol % PSM, it remained at 20 ns, well below the average lifetime of tPA in pure PSM bilayers (~44 ns; shown as the dotted line in Fig. 1 A). These results suggest that although PSM formed a gel phase in these unsaturated PCs at sufficiently high concentration, these were not very densely packed or highly ordered (at least not when compared to pure PSM bilayers at the given temperature). The longest lifetime component never exceeded 40 ns in these mixed bilayers (Fig. S1), whereas pure PSM bilayers at 23°C had a longest lifetime component of ~67 ns. The longest lifetime component also revealed that the ordered phase started to appear at above 15 mol % and that the onset was unaffected by the *sn*-2 acyl chain composition (Fig. S1). For all lifetime components and their fractional intensities and amplitudes, please see Table S1.

The formation of gel phases by PSM was much enhanced in the equal chain PCs bilayers (Fig. 1 B). As unsaturation increased in the equal chain PCs, progressively less PSM was needed to increase the average tPA lifetime, suggesting that the miscibility of PSM in equal chain PC bilayers decreased as the unsaturation increased, resulting in the increased formation of PSM-enriched gel phases. The longest lifetime component reached values of 40–45 ns (at the highest PSM concentrations; Fig. S1) but did not reach the value of pure PSM bilayers. The onset of PSM segregation occurred at PSM concentrations above 15 mol % for all equal chain PCs except DDPC (at 10 mol %; Fig. S1). For all lifetime components and their fractional intensities and amplitudes, please see Table S2.

A comparison of the PSM gel phase formation in mixed chain and equal chain PC bilayers clearly demonstrated that the gel phase order was higher when PSM was mixed with equal chain PC as compared to the mixed chain PCs.

Mixed bilayers containing mono- and polyunsaturated PCs and DPPC

Even though DPPC is not the best acyl chain match for PSM (40), we used it for comparison, because DPPC is widely used in many model membrane studies and the data on DPPC properties are plentiful. Compared to PSM in mixed chain PC bilayers, the average lifetime of tPA increased to higher values and at somewhat lower concentrations when DPPC was mixed in mixed chain PC bilayers (Fig. 1 C). The highest average lifetimes at 45 mol % (around 30 ns) were still markedly lower than the average lifetime measured in pure DPPC bilayers (~51 ns). The longest lifetime component reached 50 ns in all equal chain PC bilayer systems (at 45 mol %) but was shorter than the 75 ns measured for pure DPPC bilayers. The onset of gel phase formation occurred at DPPC concentrations >15 mol % (Fig. S2), similarly as seen with PSM (Fig. S1). For all

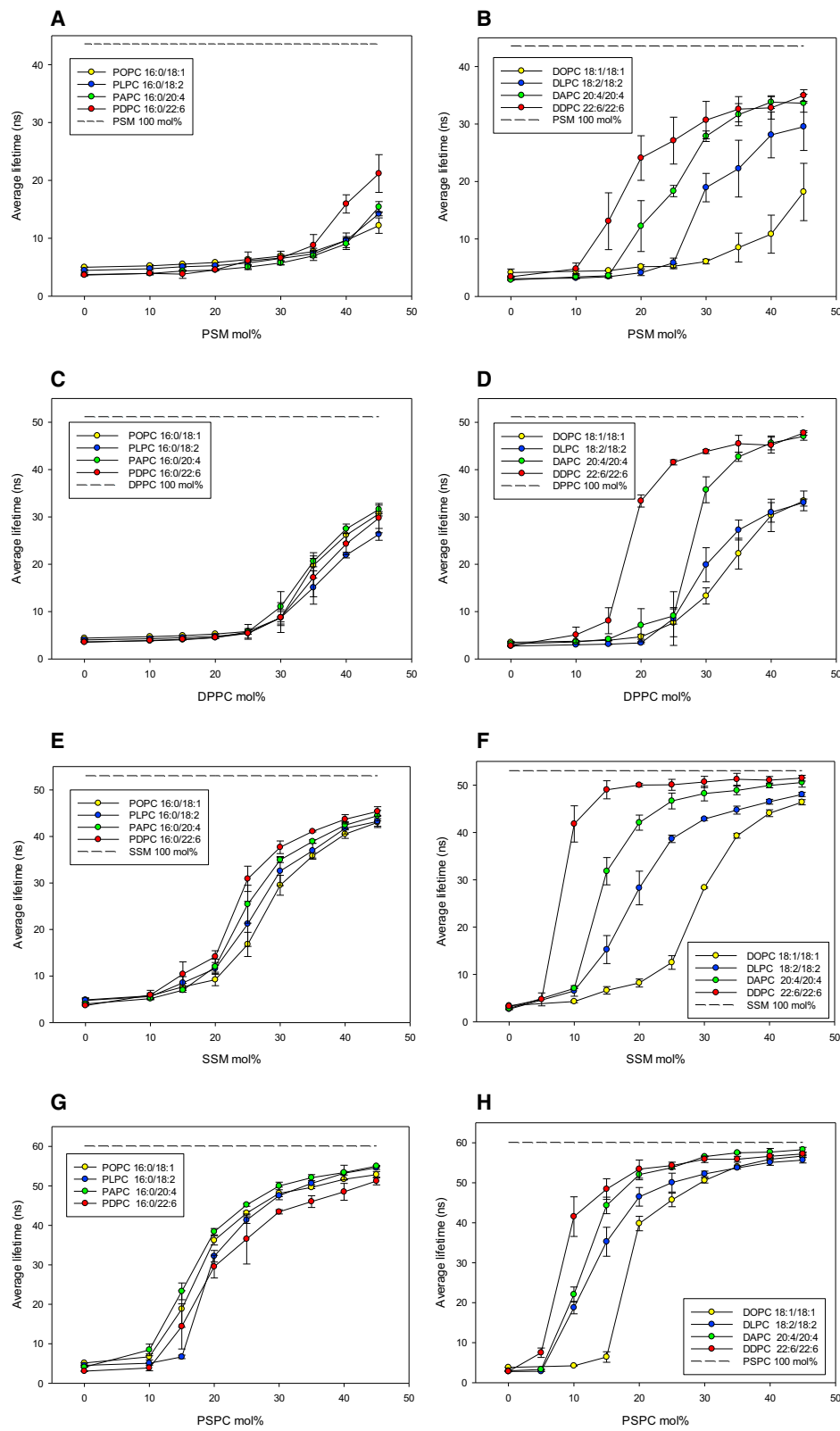


FIGURE 1 Intensity-weighted average lifetime of tPA in unsaturated phosphatidylcholine bilayers containing increasing concentrations of PSM, DPPC, SSM, or PSPC. Values are averages from $n = 2-3 \pm \text{SE}$. The dotted horizontal line in the top of each panel indicates the intensity-weighted average lifetime of tPA in a pure phospholipid bilayer of the respective saturated phospholipid. Left panels show data for mixed chain PC bilayers and right panels for equal chain PC bilayers. Panels from top to bottom are for PSM (*A* and *B*), DPPC (*C* and *D*), SSM (*E* and *F*), and PSPC (*G* and *H*), respectively. All compositions are indicated in the legend boxes and by the *x* axis legend. To see this figure in color, go online.

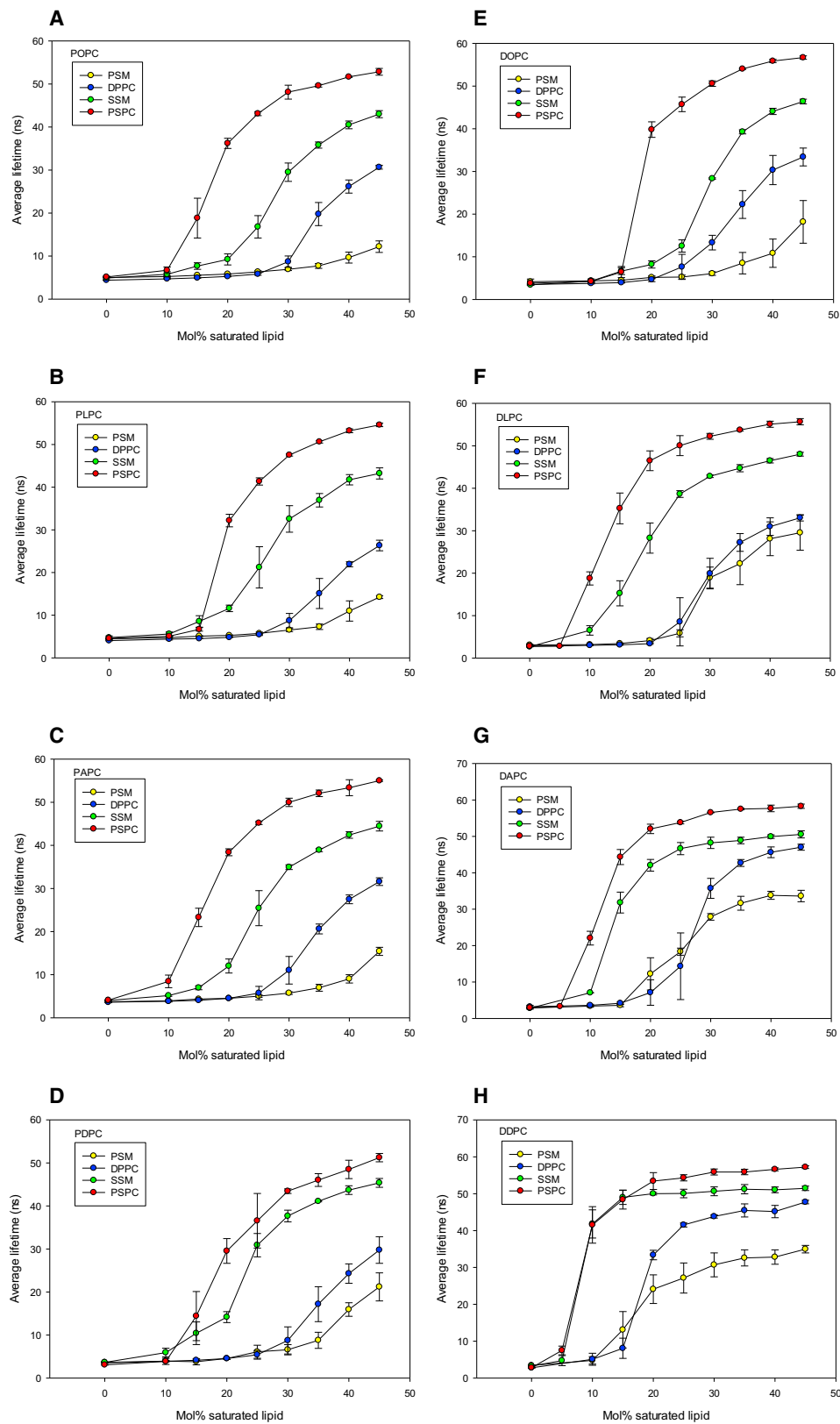


FIGURE 2 Intensity-weighted average lifetime of tPA in unsaturated phosphatidylcholine bilayers containing increasing concentrations of PSM, DPPC, SSM, or PSPC. Values from Fig. 1 are replotted to show individual panels with a single unsaturated phosphatidylcholine and all four saturated phospholipids. Panels show data for the following bilayers: (A) POPC, (B) PLPC, (C) PAPC, (D) PDPC, (E) DOPC, (F) DLPC, (G) DAPC, and (H) DDPC. Values are averages from $n = 3 \pm \text{SE}$. All compositions are indicated in the upper left corner of each panel. To see this figure in color, go online.

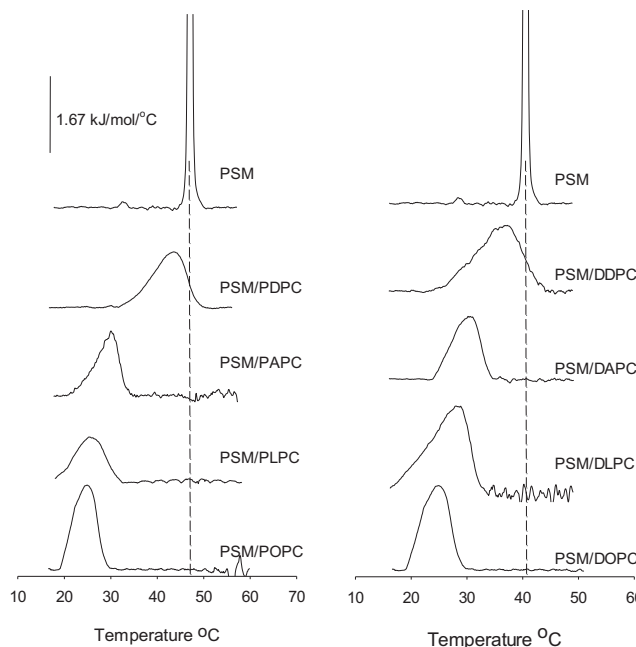


FIGURE 3 Scanning calorimetry thermograms of pure PSM and mixed unsaturated PC bilayers with PSM (at 45 mol %). Each trace is the fifth upscan. Thermograms have been normalized to the concentration of PSM present. Each composition is indicated next to the trace. The vertical dotted line indicates the T_m of pure PSM melting.

lifetime components and their fractional intensities and amplitudes, please see Table S3.

In equal chain PC bilayers, DPPC formed gel phases that gave longer average lifetimes for tPA (Fig. 1 D) when compared to each mixed chain PC bilayer (Fig. 1 C). The onset of ordered-phase formation occurred at or above 15 mol % for DOPC and DLPC, and at even lower concentrations of DPPC in DAPC and DDPC. For all lifetime components and their fractional intensities and amplitudes, please see Table S4.

Taken together, the gel phases formed by DPPC appeared to be more ordered (at each concentration and unsaturated PC) when compared to the gel phases formed by PSM, because both the average and longest lifetimes were shorter for PSM gel phases compared to DPPC gel phases at comparable bilayer compositions.

Mixed bilayers containing mono- and polyunsaturated PCs and SSM

Next, we examined how SSM behaved in the unsaturated PC bilayers. Its *N*-linked acyl chain has two extra methylene units compared to PSM, and its gel-liquid crystalline phase transition temperature is 4–5°C higher than the T_m for PSM (41,42). The addition of increasing amounts of SSM to mixed chain PC bilayers led to a sigmoidal increase in the average lifetime of tPA (Fig. 1 E). The POPC bilayers displayed the shortest tPA lifetime, whereas PDPC exhibited

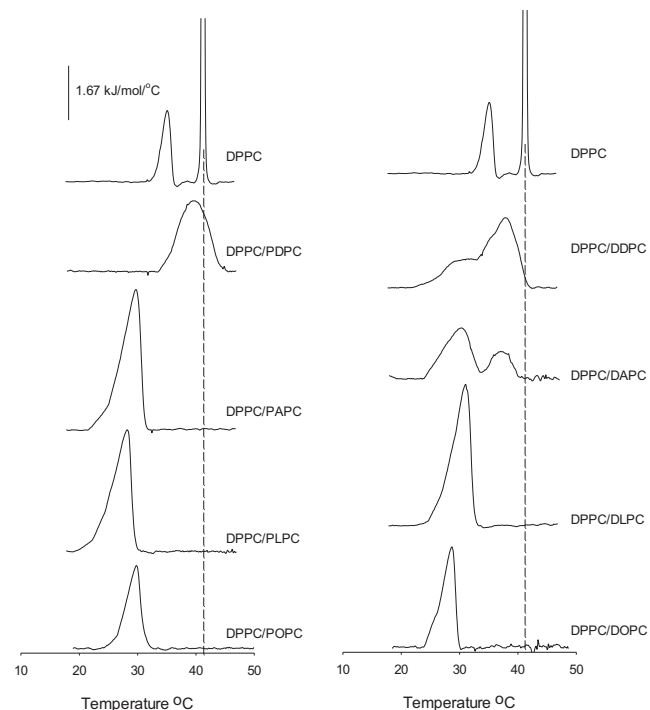


FIGURE 4 Scanning calorimetry thermograms of pure DPPC and mixed unsaturated PC bilayers with DPPC (at 45 mol %). Each trace is the fifth upscan. Thermograms have been normalized to the concentration of DPPC present. Each composition is indicated next to the trace. The vertical dotted line indicates the T_m of pure DPPC melting. The minor peak next to the main DPPC melting comes from the pretransition of DPPC.

the longest. The onset of gel phase formation occurred at above 10 mol % for POPC and PLPC bilayers and at an even lower concentration of SSM in PAPC and PDPC bilayers (Fig. S3). The highest average lifetime reached only 45 ns at 45 mol % SSM (whereas pure SSM had an average tPA lifetime of 53 ns), and even the longest lifetime component did not reach the value of pure SSM. In equal chain PC bilayers, SSM behaved much like PSM, although it formed gel phases at lower concentrations than PSM (Fig. 1 F). The onset of gel phase formation occurred at very low SSM concentrations (>0 to 10 mol %; Fig. S3). For all lifetime components and their fractional intensities and amplitudes, please see Tables S5 and S6.

The results with SSM show that extending the *N*-linked acyl chain of SM with two carbons (SSM versus PSM) had a substantial effect on the gel phase formation in each unsaturated PC bilayer.

Mixed bilayers containing mono- and polyunsaturated PCs and PSPC

PSPC has been used as a match for SSM in a recent study (43), and we have included it in this study, although the *sn*-1 palmitoyl residue together with the glycerol moiety probably is not equal in length to the sphingoid base of

SSM. Compared to DPPC, PSPC has two additional methylene units in the *sn*-2 acyl chain, and its T_m is 9°C higher than the T_m for DPPC (49 vs. 41°C, respectively). Compared to the addition of DPPC to mixed chain PC bilayers, the addition of PSPC caused the average lifetime of tPA to rise at lower PSPC concentrations and to higher absolute values (Fig. 1 G). The onset of gel phase formation occurred between >0 and 10 mol % in each mixed chain PC bilayer (Fig. S4). For all lifetime components and their fractional intensities and amplitudes, please see Table S7.

The miscibility of PSPC in equal chain PC bilayers was nonideal, as evidenced by the rapid onset of the gel phase formation as well as the high degree of order in the gel phase (long average lifetime (Fig. 1 H) and the longest lifetime component of tPA (Fig. S4). For all lifetime components and their fractional intensities and amplitudes, please see Table S8.

When tPA average lifetimes are plotted such that all saturated phospholipids are in the same panel for each unsaturated PC species, one can easily compare the lateral segregation of the gel phase as a function of the nature of the saturated phospholipid (Fig. 2). For the mixed chain PCs, the SMs formed less ordered gel phases compared to the matched saturated PCs, at equal concentration. The observed changes in average lifetime of tPA versus concentration of saturated phospholipid also followed clear trends, except in a few cases. For PDPC bilayers, the DPPC appeared to deviate somewhat from the trend (being closer to the PSM line). Deviation from the trend was also seen to some extent for DPPC in DPLC and DAPC bilayers, and for SSM in DDPC bilayers (Fig. 2). The reason for these deviations is not clear.

DSC analysis of mixed bilayers containing either PSM or DPPC and mono- and polyunsaturated PCs

To further analyze the formation and cooperativity of the gel phases formed by the saturated PSM and DPPC in the unsaturated PC bilayers, we obtained thermograms by DSC analysis (Figs. 3 and 4). The samples we measured contained 45 mol % saturated phospholipid. As shown in Fig. 3, PSM formed gel phases for which the melting occurred over a broad temperature range. The temperature range, in which the gel phase melted, shifted to higher temperatures as the degree of unsaturation increased. This was more clearly seen for equal chain PC bilayers. Only for PDPC and DDPC bilayers did the temperature range overlap with the T_m of pure PSM. The measured enthalpies of the melting of the gel phase in mixed chain PC bilayers were 25–30% of that for pure PSM, and ~40–60% in equal chain bilayers (Table S10).

The melting of gel phases formed by DPPC was more cooperative compared to PSM systems (narrower peak width at half height; Fig. 4). The melting temperatures

shifted very little in the mixed chain PCs (except for PDPC) but drifted to higher temperatures more clearly in equal chain PC bilayers. The gel phase formed by DPPC in DAPC and DDPC bilayers appeared to be more complex than for the other compositions. The melting enthalpies in mixed bilayers were 22–50% that of pure DPPC in both mixed chain and equal chain PC bilayers (Table S10).

DISCUSSION

Of the saturated phospholipids we have investigated, both PSM and SSM are biologically very relevant lipids. PSM is the major species in human fibroblasts, and SSM is a dominant molecular species in cultured neurons (44). Although DPPC is found in lung surfactant fractions (45), it is present only in very small amounts in eukaryotic cell membranes. One exception appears to be the bovine rod outer segment membrane, which could contain as much as 20% DPPC, together with polyunsaturated PCs (46). PSPC is a highly ordered lipid that does not have a significant presence in most cell membranes. However, these lipids were chosen not only on the basis of biological significance, but also because they have been extensively studied in model membrane systems. Of the polyunsaturated phospholipids, phosphatidylethanolamines are believed to be more prevalent in cell membranes compared to PC species (47), but both are present. In addition, some phosphatidylserines have also been reported to contain polyunsaturated acyl chains (47). In specialized cells, such as sperm cells, even SM may contain very long polyunsaturated acyl chains (48).

Phospholipids with mismatched acyl chain length (49) or unsaturation (50) are known to interact poorly and favor lateral segregation when possible. Previous studies have demonstrated that SM and cholesterol phase-separate from 22:6-containing phospholipids (e.g., phosphatidylethanolamine (51)). One reason for the segregation is believed to be cholesterol's aversion for the highly unsaturated acyl chains of the cophospholipids (29), which would in part drive the formation of cholesterol/SM domains. However, few studies have conducted a direct comparison of the effect of acyl chain unsaturation on the phase separation of saturated phospholipids in the absence of cholesterol. One such is by Curatolo and coworkers (52), who showed that PCs with a delta T_m of 33°C or higher (T_m difference between low and high melting PCs in a binary bilayer) show gel phase immiscibility. In this study, we have systematically examined how saturated PSM, DPPC, SSM, and PSPC behave in increasingly unsaturated PC bilayers. We have used both lifetime analysis of tPA and calorimetry. Time-resolved tPA fluorescence is a useful method for demonstrating the presence of ordered domains (or phases) in a fluid bilayer (see Introduction).

The result trends we present in Fig. 1 are not unexpected, in the sense that an ordered (gel) phase should be formed as

a saturated phospholipid is increasingly added to an unsaturated PC bilayer. Partial phase diagrams for PSM, DPPC, SSM, and PSPC in POPC and/or DOPC have been published (15–19,52), giving the concentration of saturated lipid needed for gel phase formation. In other studies, it has been shown that both 16:0/18:1 and 16:0/22:6 phosphatidylethanolamine phase-separate from SM, and that 16:0/22:6 phosphatidylethanolamine display greater nonideal mixing with SM (34). This concentration-dependent phase separation (Fig. 1) resulted most likely both from unfavorable interactions between saturated and unsaturated acyl chains, from acyl chain length mismatch, and from possible cohesive interactions between hydrogen bonding phospholipids (SM). Phase separation can also be induced by head-group effects, and this may also play some role in the current setup, because the rotational freedom of the headgroups may differ in PCs and SMs (53,54). Interestingly, both SMs appeared to form a less ordered gel phase with unsaturated PCs compared to their saturated PC matches, as seen from the shorter tPA lifetimes at equal concentration. It is unlikely that this fairly large difference depends on the fact that DPPC is not the best match for PSM (nor is PSPC for SSM), because the *sn*-1 chain length + glycerol is longer than the long-chain base of SM. The length difference between PSM and DPPC is fairly small compared to the large ordered phase forming effect we observed. It is more likely that the hydrogen-bonding properties of PSM and SSM allow them to better interact with unsaturated PC, compared to both DPPC and PSPC. It has also been suggested that SM interaction in monolayers does not lead to long-range crystalline in plane order, as compared to other nonsphingolipid phospholipids (55). If such lateral packing is replicated also in bilayer membranes, it could affect the miscibility with colipids in a way seen in our study. The SMs are hydrogen bond donors (from 2NH and 3OH in the long-chain base), whereas the glycerophospholipids only are acceptors for hydrogen bonds. A different degree of water penetration into the interfacial region may also explain differences between SMs and PCs with regard to miscibility in unsaturated and laterally expanded PC bilayers (56).

The observation that a saturated acyl chain (16:0) in the *sn*-1 position of the unsaturated PCs had a large effect on gel phase formation is of interest. The gel phases formed in diunsaturated PC bilayers were as a rule more ordered than the corresponding phases formed in 1-16:0/2-unsaturated-PC bilayers. Phospholipids with mixed saturated/unsaturated acyl chains are known to act as hybrid lipids in laterally phase-segregated bilayers (57). They may interact with both the ordered phase (via the saturated acyl chain) and the disordered phase (via the unsaturated acyl chain) and thus influence domain boundary properties. The other interesting feature of our results was the observed large effect on gel phase formation by increasing the length of the saturated phospholipid by 2 methylene units (SSM versus

PSM and PSPC versus DPPC). The increased chain length of SSM and PSPC provides for additional van der Waals interactions compared to the shorter saturated phospholipids, but also introduce intramolecular acyl chain mismatch, which most likely counteracts the attractive hydrophobic interactions. The more ordered gel phases formed by both SSM and PSPC suggest that the attractive interactions are more important than acyl chain disorder caused by their mismatch.

Based on tPA lifetime data (the longest lifetime component) it appeared that none of the saturated phospholipids formed a gel phase in unsaturated PC bilayers that had properties similar to a pure saturated phospholipid phase. This conclusion is also supported by DSC analysis (Fig. 3). The gel phase meltings were broad and noncooperative, suggesting multiple components and complex melting behavior. PSM at 45 mol % in both PDPC and DDPC appeared to have an ordered phase component, which melted above 40°C, suggestive of a gel phase component very similar to pure PSM gel phase. A similar discrepancy can also be seen for DPPC in PDPC, in which the longest lifetime component of tPA did not reach the level measured in pure DPPC, but the DSC thermogram reported a gel phase melting reaching above 41°C (Fig. 4). Apparently, the partly conflicting information provided by tPA (Figs. S1–S4) and DSC (Figs. 3 and 4) may suggest that the long lifetime of tPA did not report pure gel phase lifetimes because the long-lived excited state permitted tPA to also report from less ordered gel phases present during its excited lifetime (because of diffusion between ordered and less ordered environments). It is also possible that the gel phase formed actually contained traces of the unsaturated PC, thus giving broad multicomponent melting transitions and tPA lifetimes below that observed in pure saturated phospholipid.

The onset of gel phase formation was probably not abrupt but gradual, occurring as the concentration of the saturated phospholipid increased and containing a spectrum of different ratios of saturated to unsaturated phospholipids. This is suggested by the noncooperative melting of the ordered phase formed by both PSM and DPPC in unsaturated PC bilayers (Figs. 3 and 4). The reduced cooperativity of melting of PSM gel phases compared to DPPC gel phases also suggests that PSM displayed better miscibility with unsaturated PCs than DPPC. The phase separation of PSM or DPPC from the most unsaturated DDPC was never complete, as demonstrated by both the noncooperative gel-phase melting (Figs. 3 and 4) and the loss of melting enthalpy (Table S10) as compared to pure PSM or DPPC melting.

Taken together, our results show that all four saturated phospholipids displayed partial miscibility with all unsaturated PCs used in the study, even though miscibility became increasingly nonideal as the degree of unsaturation increased.

Biological significance

In cell membranes, SMs are mostly localized in the exoleaflet (58,59), whereas polyunsaturated phospholipids are predominantly found in the endoleaflet (27). However, this segregation is probably not absolute, and SMs may encounter polyunsaturated phospholipids during various events in cell membrane remodeling. In such instances, the mismatch in acyl chain unsaturation between SM and other colipids will lead to lateral segregation, which is further enforced by cholesterol's aversion for polyunsaturated acyl chains (31) and its affinity for SM domains (60). The role of this process in transient lipid raft formation is, however, unclear. It is also of interest to note that the saturated SMs used in this study, which are also the most prevalent SM species in cell membranes, were more miscible in unsaturated PC bilayers compared to their saturated PC counterparts. The fact that both DPPC and PSPC could form harmful gel phases in highly unsaturated PC bilayers may be one reason they are missing from the cell membrane lipidome. Finally, our results clearly show that all unsaturated PCs are not alike. A consequence of this is that simple model systems with one low melting and one high melting phospholipid is never a good model for complex biological membranes where a multitude of molecular species are present and interacting with each other in complex ways.

SUPPORTING MATERIAL

Four figures, three schemes, and ten tables are available at [http://www.biophysj.org/biophysj/supplemental/S0006-3495\(15\)00943-1](http://www.biophysj.org/biophysj/supplemental/S0006-3495(15)00943-1).

AUTHOR CONTRIBUTIONS

J.P.S. designed research. A.K. and O.E. performed research. A.K., E.O., and J.P.S. analyzed data and wrote the article.

ACKNOWLEDGMENTS

We thank Dr. Terhi Maula for constructive comments on the manuscript.

Financial support was generously provided by the Sigrid Juselius Foundation, the Academy of Finland, the Magnus Ehrnrooth Foundation, and the Åbo Akademi Foundation.

REFERENCES

- Feigenson, G. W. 2006. Phase behavior of lipid mixtures. *Nat. Chem. Biol.* 2:560–563.
- Simons, K., and W. L. Vaz. 2004. Model systems, lipid rafts, and cell membranes. *Annu. Rev. Biophys. Biomol. Struct.* 33:269–295.
- Lingwood, D., and K. Simons. 2010. Lipid rafts as a membrane-organizing principle. *Science*. 327:46–50.
- Brown, D. A., and E. London. 2000. Structure and function of sphingo-lipid- and cholesterol-rich membrane rafts. *J. Biol. Chem.* 275:17221–17224.
- Simons, K., and E. Ikonen. 1997. Functional rafts in cell membranes. *Nature*. 387:569–572.
- Simons, K., and E. Ikonen. 2000. How cells handle cholesterol. *Science*. 290:1721–1726.
- Simons, K., and D. Toomre. 2000. Lipid rafts and signal transduction. *Nat. Rev. Mol. Cell Biol.* 1:31–39.
- Pike, L. J. 2006. Rafts defined: a report on the Keystone Symposium on Lipid Rafts and Cell Function. *J. Lipid Res.* 47:1597–1598.
- London, E., D. A. Brown, and X. Xu. 2000. Fluorescence quenching assay of sphingolipid/phospholipid phase separation in model membranes. *Methods Enzymol.* 312:272–290.
- London, E. 2002. Insights into lipid raft structure and formation from experiments in model membranes. *Curr. Opin. Struct. Biol.* 12:480–486.
- Xu, X., and E. London. 2000. The effect of sterol structure on membrane lipid domains reveals how cholesterol can induce lipid domain formation. *Biochemistry*. 39:843–849.
- Björkbom, A., T. Rög, ..., J. P. Slotte. 2011. N- and O-methylation of sphingomyelin markedly affects its membrane properties and interactions with cholesterol. *Biochim. Biophys. Acta*. 1808:1179–1186.
- Björkqvist, Y. J. E., T. K. M. Nyholm, ..., B. Ramstedt. 2005. Domain formation and stability in complex lipid bilayers as reported by cholestatrienol. *Biophys. J.* 88:4054–4063.
- Halling, K. K., B. Ramstedt, ..., T. K. Nyholm. 2008. Cholesterol interactions with fluid-phase phospholipids: effect on the lateral organization of the bilayer. *Biophys. J.* 95:3861–3871.
- de Almeida, R. F., A. Fedorov, and M. Prieto. 2003. Sphingomyelin/phosphatidylcholine/cholesterol phase diagram: boundaries and composition of lipid rafts. *Biophys. J.* 85:2406–2416.
- Ionova, I. V., V. A. Livshits, and D. Marsh. 2012. Phase diagram of ternary cholesterol/palmitoylspingomyelin/palmitoyloleoyl-phosphatidylcholine mixtures: spin-label EPR study of lipid-raft formation. *Biophys. J.* 102:1856–1865.
- Marsh, D. 2009. Cholesterol-induced fluid membrane domains: a compendium of lipid-raft ternary phase diagrams. *Biochim. Biophys. Acta*. 1788:2114–2123.
- Veatch, S. L., and S. L. Keller. 2005. Miscibility phase diagrams of giant vesicles containing sphingomyelin. *Phys. Rev. Lett.* 94:148101–148104.
- Feigenson, G. W., and J. T. Buboltz. 2001. Ternary phase diagram of dipalmitoyl-PC/dilauroyl-PC/cholesterol: nanoscopic domain formation driven by cholesterol. *Biophys. J.* 80:2775–2788.
- Björkbom, A., T. Rög, ..., J. P. Slotte. 2010. Effect of sphingomyelin headgroup size on molecular properties and interactions with cholesterol. *Biophys. J.* 99:3300–3308.
- Björkbom, A., B. Ramstedt, and J. P. Slotte. 2007. Phosphatidylcholine and sphingomyelin containing an elaidoyl fatty acid can form cholesterol-rich lateral domains in bilayer membranes. *Biochim. Biophys. Acta*. 1768:1839–1847.
- Jaikishan, S., and J. P. Slotte. 2011. Effect of hydrophobic mismatch and interdigitation on sterol/sphingomyelin interaction in ternary bilayer membranes. *Biochim. Biophys. Acta*. 1808:1940–1945.
- Jaikishan, S., A. Björkbom, and J. P. Slotte. 2010. Sphingomyelin analogs with branched N-acyl chains: the position of branching dramatically affects acyl chain order and sterol interactions in bilayer membranes. *Biochim. Biophys. Acta*. 1798:1987–1994.
- Nyholm, T. K., D. Lindroos, ..., J. P. Slotte. 2011. Construction of a DOPC/PSM/cholesterol phase diagram based on the fluorescence properties of trans-parinaric acid. *Langmuir*. 27:8339–8350.
- Sergelius, C., and J. P. Slotte. 2011. Membrane properties of and cholesterol's interactions with a biologically relevant three-chain sphingomyelin: 3O-palmitoyl-N-palmitoyl-D-erythro-sphingomyelin. *Biochim. Biophys. Acta*. 1808:2841–2848.
- Slotte, J. P. 2013. Molecular properties of various structurally defined sphingomyelins – correlation of structure with function. *Prog. Lipid Res.* 52:206–219.

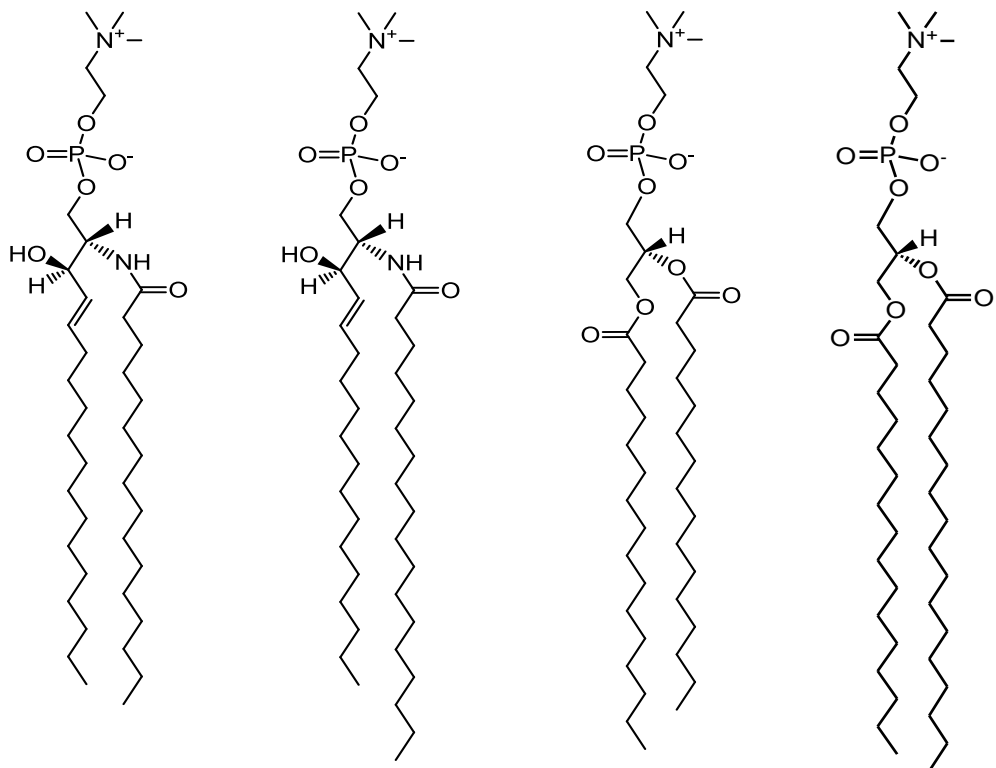
27. Wassall, S. R., and W. Stillwell. 2009. Polyunsaturated fatty acid-cholesterol interactions: domain formation in membranes. *Biochim. Biophys. Acta.* 1788:24–32.
28. Shaikh, S. R., J. J. Kinnun, ..., S. R. Wassall. 2015. How polyunsaturated fatty acids modify molecular organization in membranes: insight from NMR studies of model systems. *Biochim. Biophys. Acta.* 1848 (1 Pt B):211–219.
29. Shaikh, S. R., V. Cherezov, ..., S. R. Wassall. 2006. Molecular organization of cholesterol in unsaturated phosphatidylethanolamines: x-ray diffraction and solid state ²H NMR reveal differences with phosphatidylcholines. *J. Am. Chem. Soc.* 128:5375–5383.
30. Niu, S. L., and B. J. Litman. 2002. Determination of membrane cholesterol partition coefficient using a lipid vesicle-cyclodextrin binary system: effect of phospholipid acyl chain unsaturation and headgroup composition. *Biophys. J.* 83:3408–3415.
31. Kucerka, N., D. Marquardt, ..., J. Katsaras. 2010. Cholesterol in bilayers with PUFA chains: doping with DMPC or POPC results in sterol reorientation and membrane-domain formation. *Biochemistry.* 49:7485–7493.
32. Williams, J. A., S. E. Batten, ..., S. R. Wassall. 2012. Docosahexaenoic and eicosapentaenoic acids segregate differently between raft and non-raft domains. *Biophys. J.* 103:228–237.
33. Shaikh, S. R., M. R. Brzustowicz, ..., S. R. Wassall. 2002. Monounsaturated PE does not phase-separate from the lipid raft molecules sphingomyelin and cholesterol: role for polyunsaturation? *Biochemistry.* 41:10593–10602.
34. Shaikh, S. R., D. S. Locascio, ..., W. Stillwell. 2009. Oleic- and docosahexaenoic acid-containing phosphatidylethanolamines differentially phase separate from sphingomyelin. *Biochim. Biophys. Acta.* 1788:2421–2426.
35. Bakht, O., P. Pathak, and E. London. 2007. Effect of the structure of lipids favoring disordered domain formation on the stability of cholesterol-containing ordered domains (lipid rafts): identification of multiple raft-stabilization mechanisms. *Biophys. J.* 93:4307–4318.
36. Sklar, L. A., G. P. Miljanich, and E. A. Dratz. 1979. Phospholipid lateral phase separation and the partition of *cis*-parinaric acid and *trans*-parinaric acid among aqueous, solid lipid, and fluid lipid phases. *Biochemistry.* 18:1707–1716.
37. Welti, R., and D. F. Silbert. 1982. Partition of parinaroyl phospholipid probes between solid and fluid phosphatidylcholine phases. *Biochemistry.* 21:5685–5689.
38. Kuklev, D. V., and W. L. Smith. 2004. Synthesis of four isomers of parinaric acid. *Chem. Phys. Lipids.* 131:215–222.
39. Lakowicz, J. R. 1999. Principles of Fluorescence Spectroscopy. Kluwer Academic/Plenum Publishers, New York.
40. Térová, B., J. P. Slotte, and T. K. Nyholm. 2004. Miscibility of acyl-chain defined phosphatidylcholines with *N*-palmitoyl sphingomyelin in bilayer membranes. *Biochim. Biophys. Acta.* 1667:182–189.
41. Maulik, P. R., and G. G. Shipley. 1996. *N*-palmitoyl sphingomyelin bilayers: structure and interactions with cholesterol and dipalmitoylphosphatidylcholine. *Biochemistry.* 35:8025–8034.
42. Maulik, P. R., P. K. Sripada, and G. G. Shipley. 1991. Structure and thermotropic properties of hydrated *N*-stearoyl sphingomyelin bilayer membranes. *Biochim. Biophys. Acta.* 1062:211–219.
43. Yasuda, T., M. Kinoshita, ..., N. Matsumori. 2014. Detailed comparison of deuterium quadrupole profiles between sphingomyelin and phosphatidylcholine bilayers. *Biophys. J.* 106:631–638.
44. Valsecchi, M., L. Mauri, ..., S. Sonnino. 2007. Ceramide and sphingomyelin species of fibroblasts and neurons in culture. *J. Lipid Res.* 48:417–424.
45. Guthmann, F., R. Haupt, ..., B. Rüstow. 1995. Alveolar surfactant subfractions differ in their lipid composition. *Int. J. Biochem. Cell Biol.* 27:1021–1026.
46. Miljanich, G. P., L. A. Sklar, ..., E. A. Dratz. 1979. Disaturated and di-polyunsaturated phospholipids in the bovine retinal rod outer segment disk membrane. *Biochim. Biophys. Acta.* 552:294–306.
47. Emmelot, P., and R. P. Van Hoeven. 1975. Phospholipid unsaturation and plasma membrane organization. *Chem. Phys. Lipids.* 14:236–246.
48. Sandhoff, R. 2010. Very long chain sphingolipids: tissue expression, function and synthesis. *FEBS Lett.* 584:1907–1913.
49. Ipsen, J. H., and O. G. Mouritsen. 1988. Modelling the phase equilibria in two-component membranes of phospholipids with different acyl-chain lengths. *Biochim. Biophys. Acta.* 944:121–134.
50. Wassall, S. R., and W. Stillwell. 2008. Docosahexaenoic acid domains: the ultimate non-raft membrane domain. *Chem. Phys. Lipids.* 153:57–63.
51. Shaikh, S. R., V. Cherezov, ..., S. R. Wassall. 2003. Interaction of cholesterol with a docosahexaenoic acid-containing phosphatidylethanolamine: trigger for microdomain/raft formation? *Biochemistry.* 42:12028–12037.
52. Curatolo, W., B. Sears, and L. J. Neuringer. 1985. A calorimetry and deuterium NMR study of mixed model membranes of 1-palmitoyl-2-oleylphosphatidylcholine and saturated phosphatidylcholines. *Biochim. Biophys. Acta.* 817:261–270.
53. Niemelä, P., M. T. Hyvönen, and I. Vattulainen. 2004. Structure and dynamics of sphingomyelin bilayer: insight gained through systematic comparison to phosphatidylecholine. *Biophys. J.* 87:2976–2989.
54. Malcolm, I. C., J. C. Ross, and J. Higinbotham. 2005. A study of the headgroup motion of sphingomyelin using ³¹P NMR and an analytically soluble model. *Solid State Nucl. Magn. Reson.* 27:247–256.
55. Vaknin, D., M. S. Kelley, and B. M. Ocko. 2001. Sphingomyelin at the air-water interface. *J. Chem. Phys.* 115:7697–7704.
56. Nyholm, T., M. Nylund, ..., J. P. Slotte. 2003. Properties of palmitoyl phosphatidylcholine, sphingomyelin, and dihydro sphingomyelin bilayer membranes as reported by different fluorescent reporter molecules. *Biophys. J.* 84:987–997.
57. Heberle, F. A., M. Doktorova, ..., G. W. Feigenson. 2013. Hybrid and nonhybrid lipids exert common effects on membrane raft size and morphology. *J. Am. Chem. Soc.* 135:14932–14935.
58. Barenholz, Y., and T. E. Thompson. 1980. Sphingomyelins in bilayers and biological membranes. *Biochim. Biophys. Acta.* 604:129–158.
59. Ohvo-Rekilä, H., B. Ramstedt, ..., J. P. Slotte. 2002. Cholesterol interactions with phospholipids in membranes. *Prog. Lipid Res.* 41:66–97.
60. Lönnfors, M., J. P. Doux, ..., J. P. Slotte. 2011. Sterols have higher affinity for sphingomyelin than for phosphatidylcholine bilayers even at equal acyl-chain order. *Biophys. J.* 100:2633–2641.

Supplemental information
(3 Schemes, 4 figures with multiple panels, 10 tables)

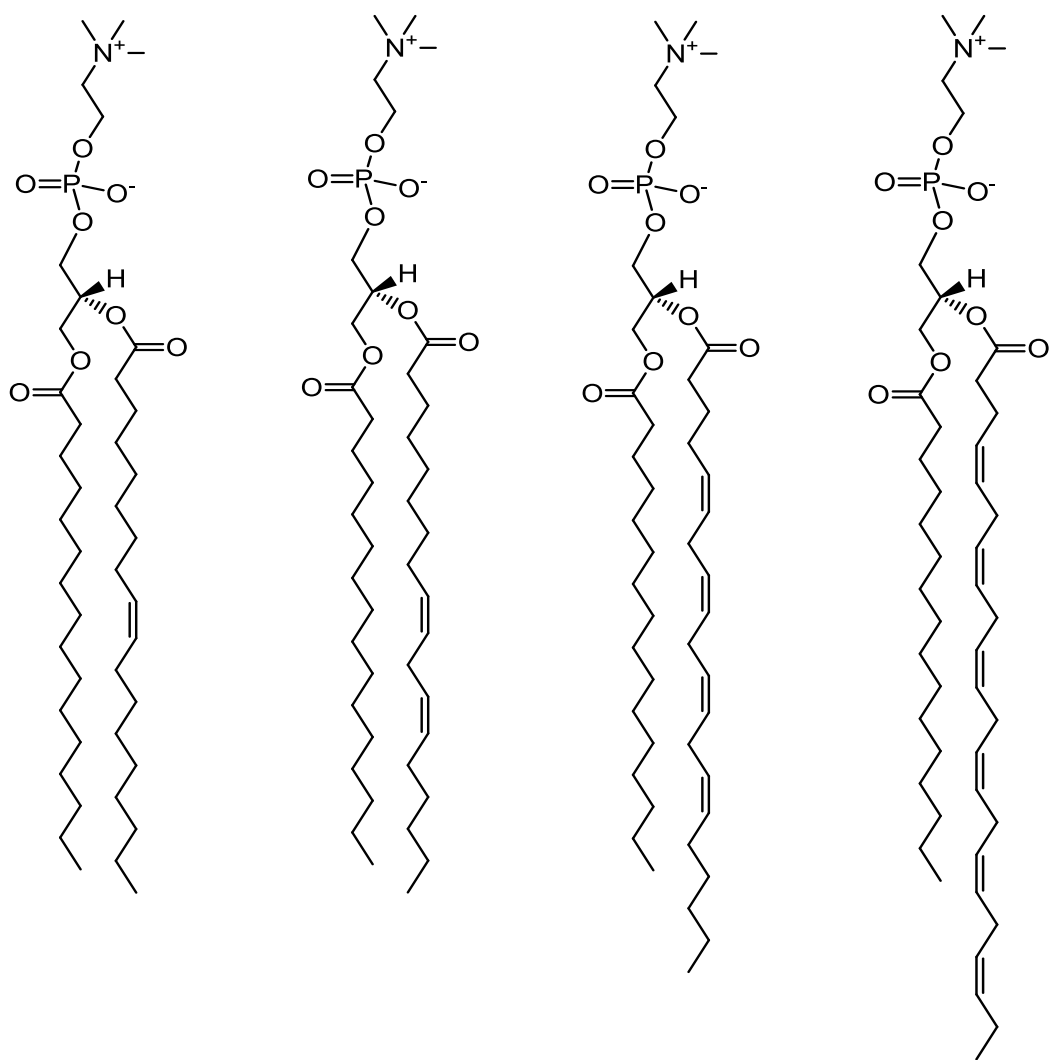
Miscibility of Sphingomyelins and Phosphatidylcholines in Unsaturated Phosphatidylcholine Bilayers

Anders Kullberg, Oscar Oz Ekholm and J.Peter Slotte*

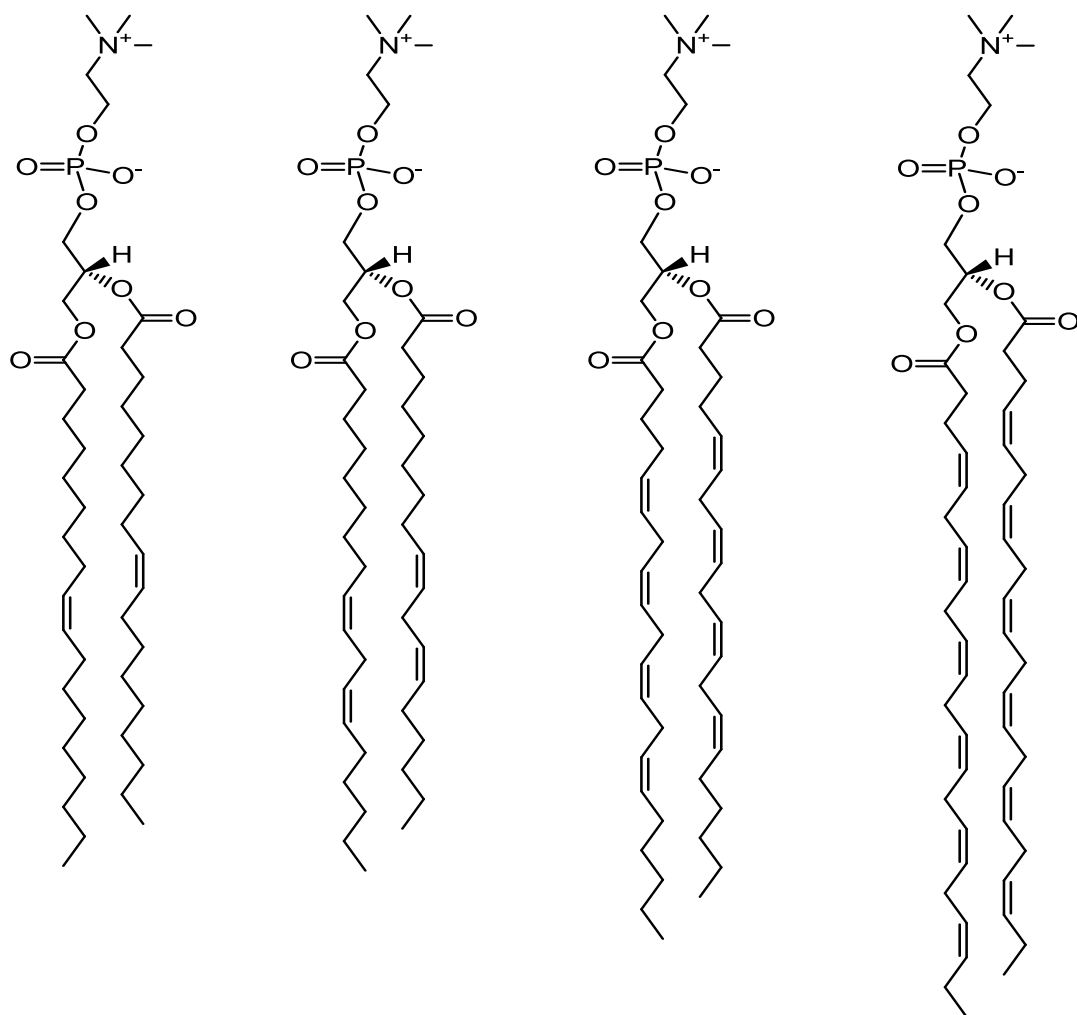
*Biochemistry, Faculty of Science and Engineering, Åbo Akademi University, 20520 Turku,
Finland*



Scheme S1. Molecular structures of (from left to right) PSM, SSM, DPPC, and PSPC

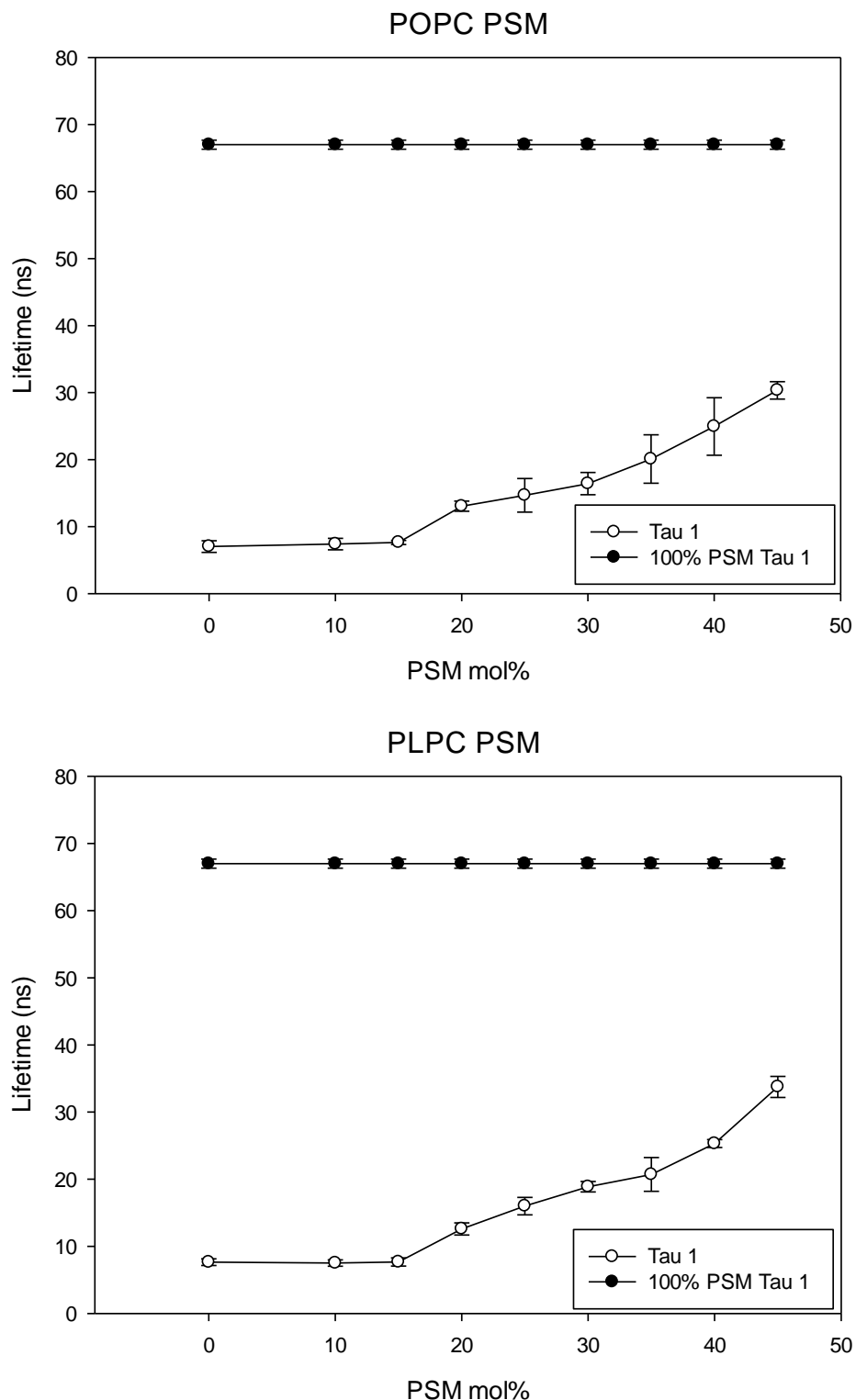


Scheme S2. Molecular structures of (from left to right) POPC, PLPC, PAPC and PDPC

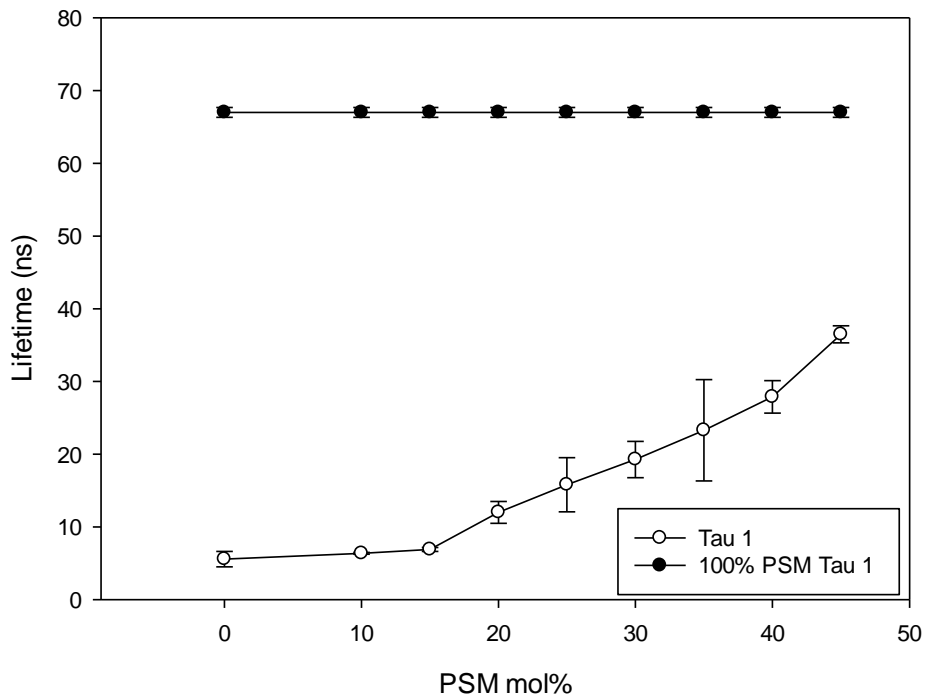


Scheme S3. Molecular structures of (from left to right) DOPC, DLPC, DAPC and DDPC

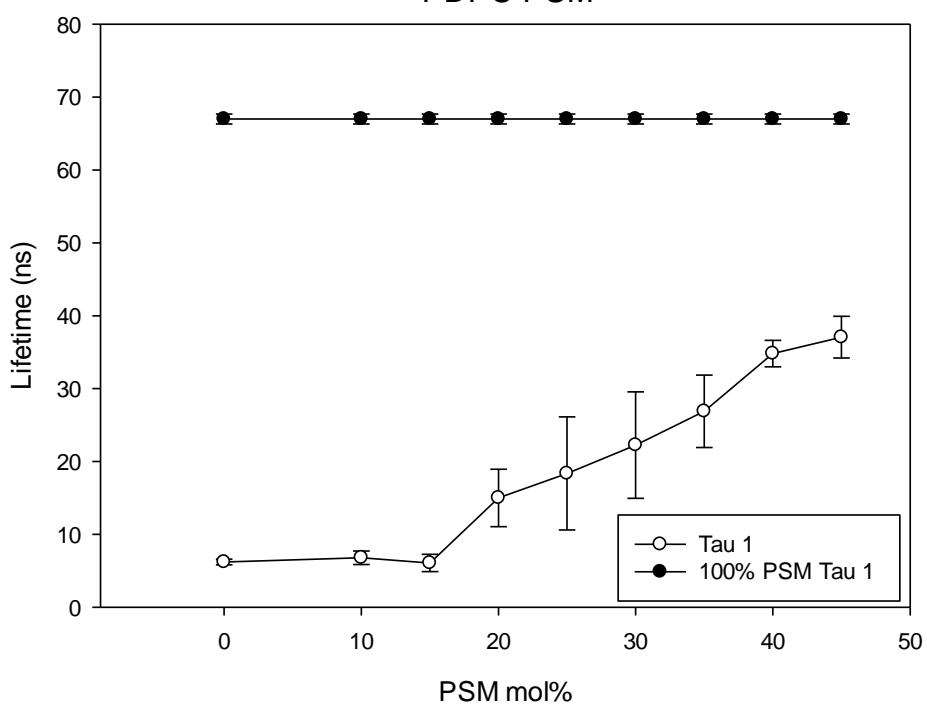
Figure S1. The longest lifetime component (τ_1) of tPA is given for pure PSM (filled symbols), and for PSM in unsaturated phosphatidylcholine bilayers (open symbols).



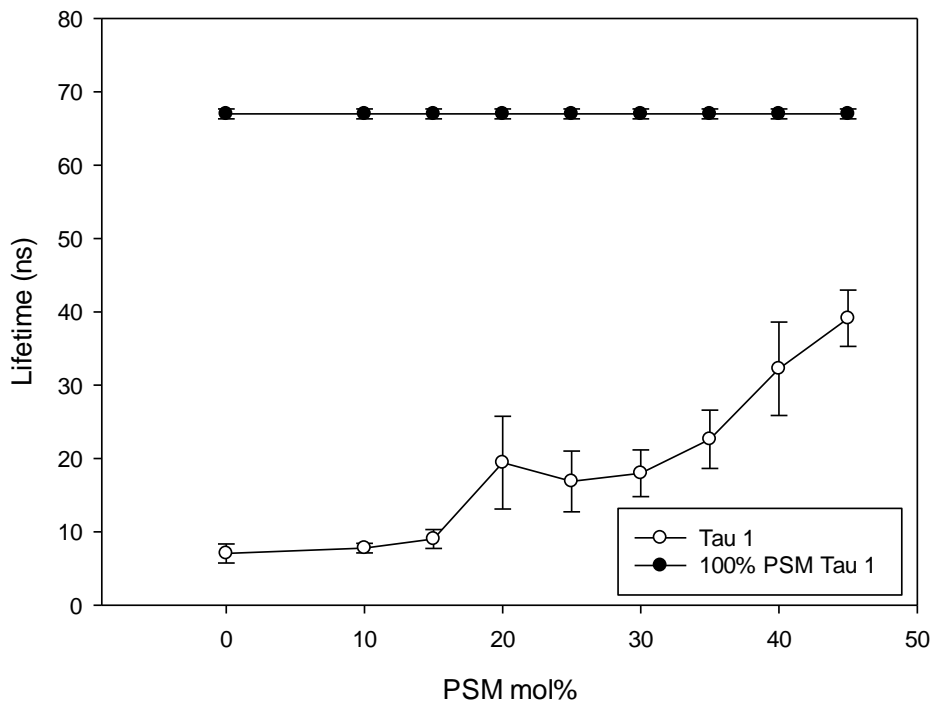
PAPC PSM



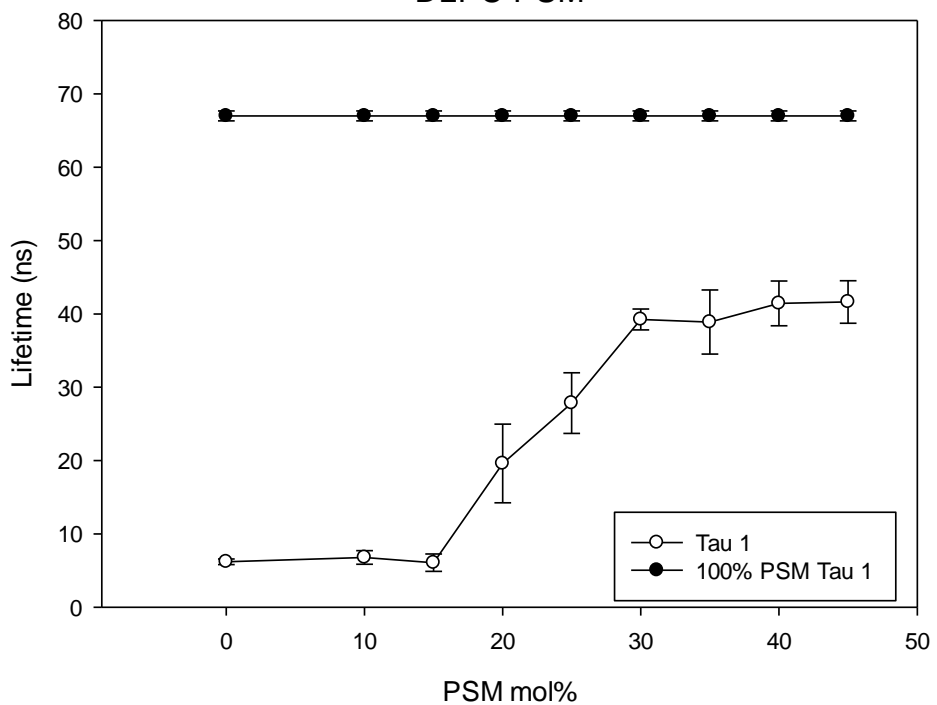
PDPC PSM



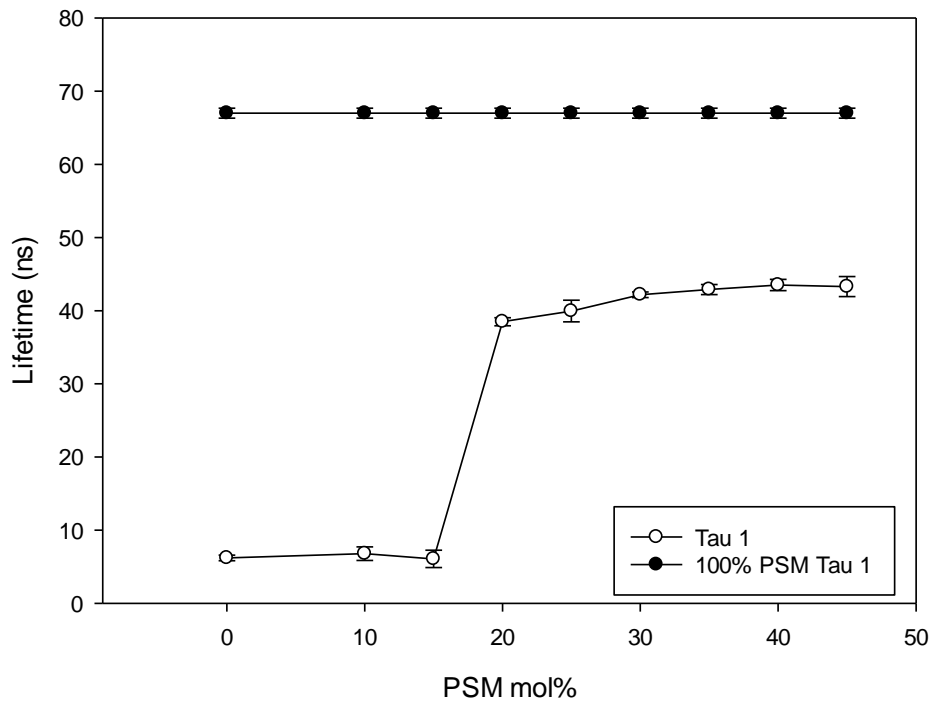
DOPC PSM



DLPC PSM



DAPC PSM



DDPC PSM

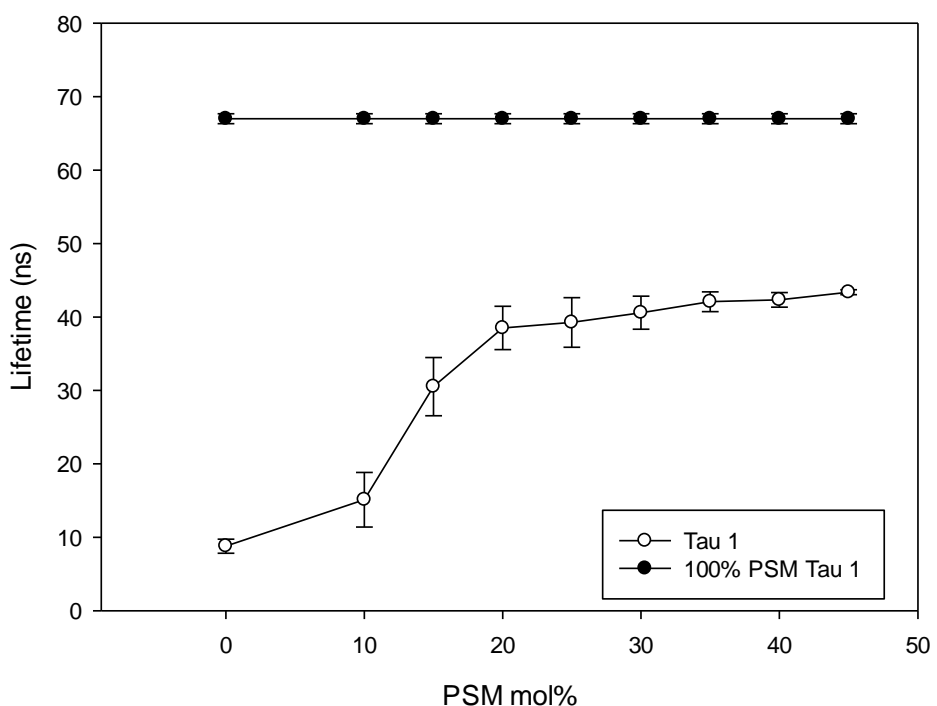
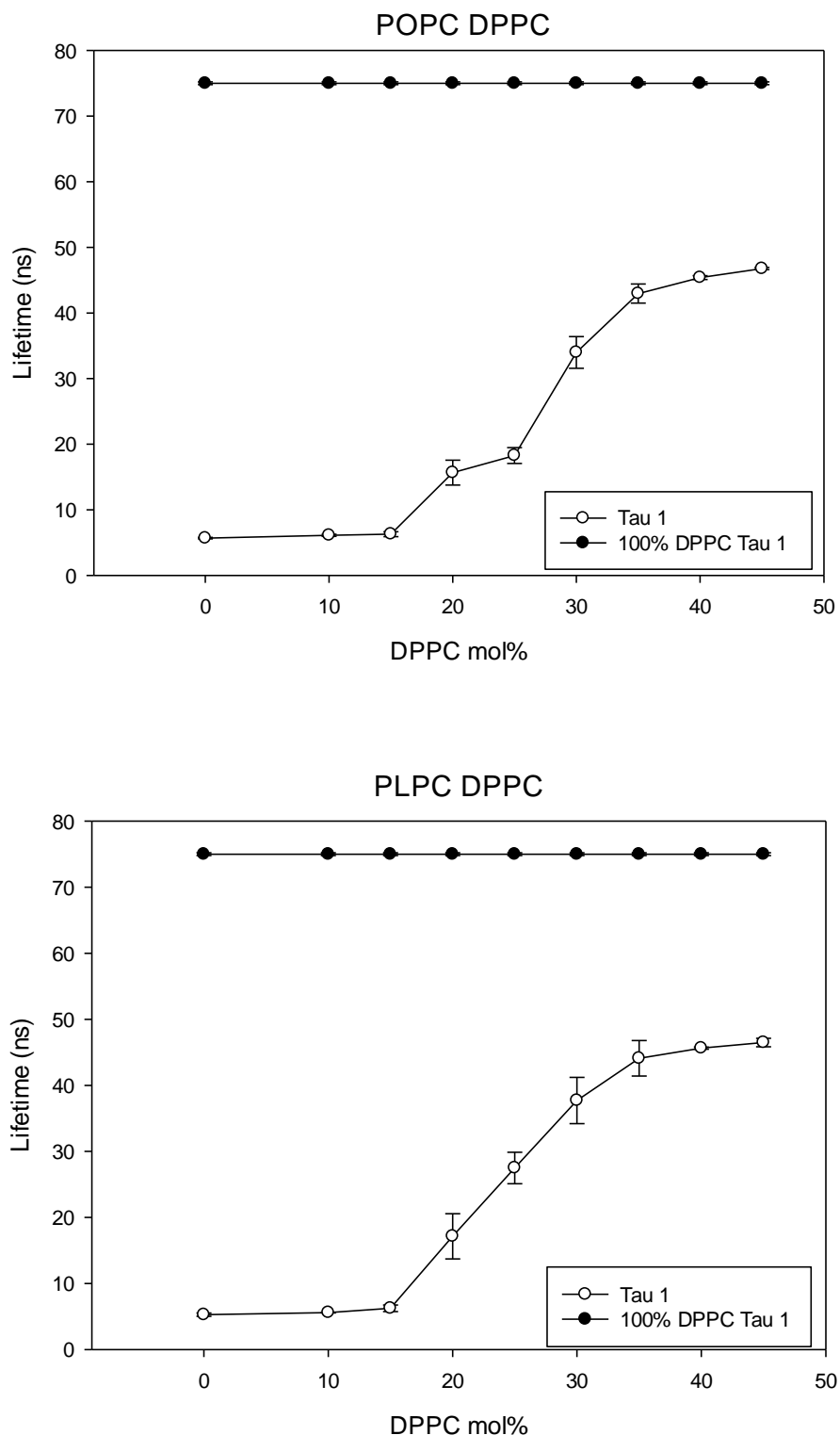
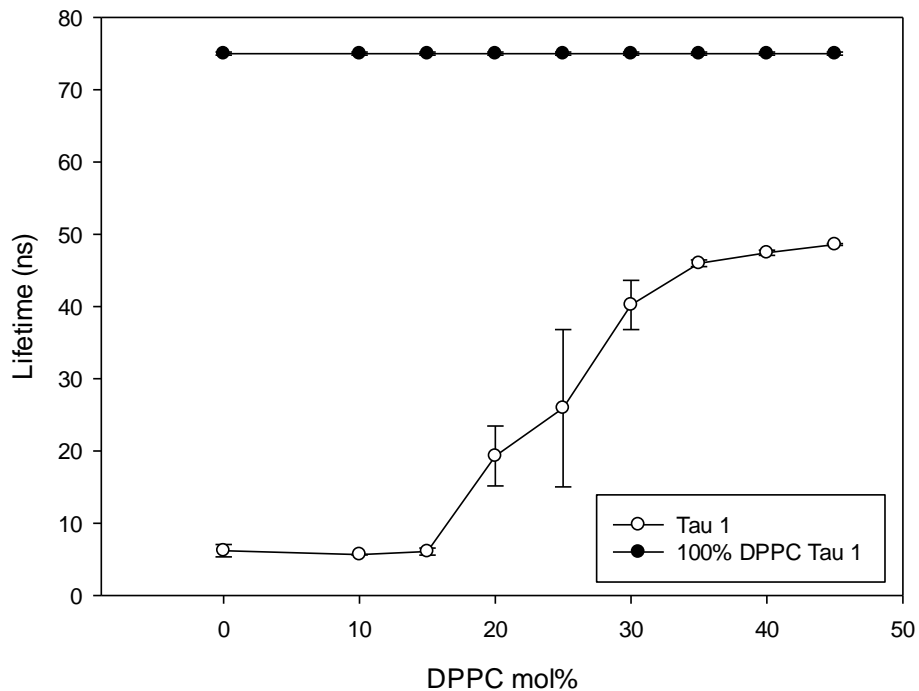


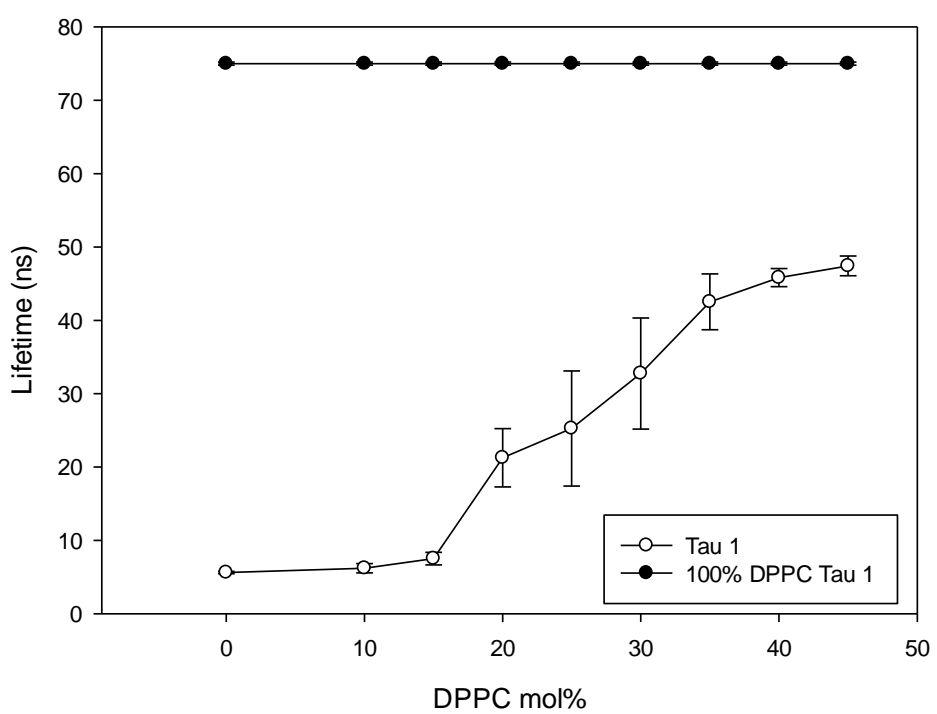
Figure S2. The longest lifetime component (τ_1) of tPA is given for pure DPPC (filled symbols), and for DPPC in unsaturated phosphatidylcholine bilayers (open symbols).

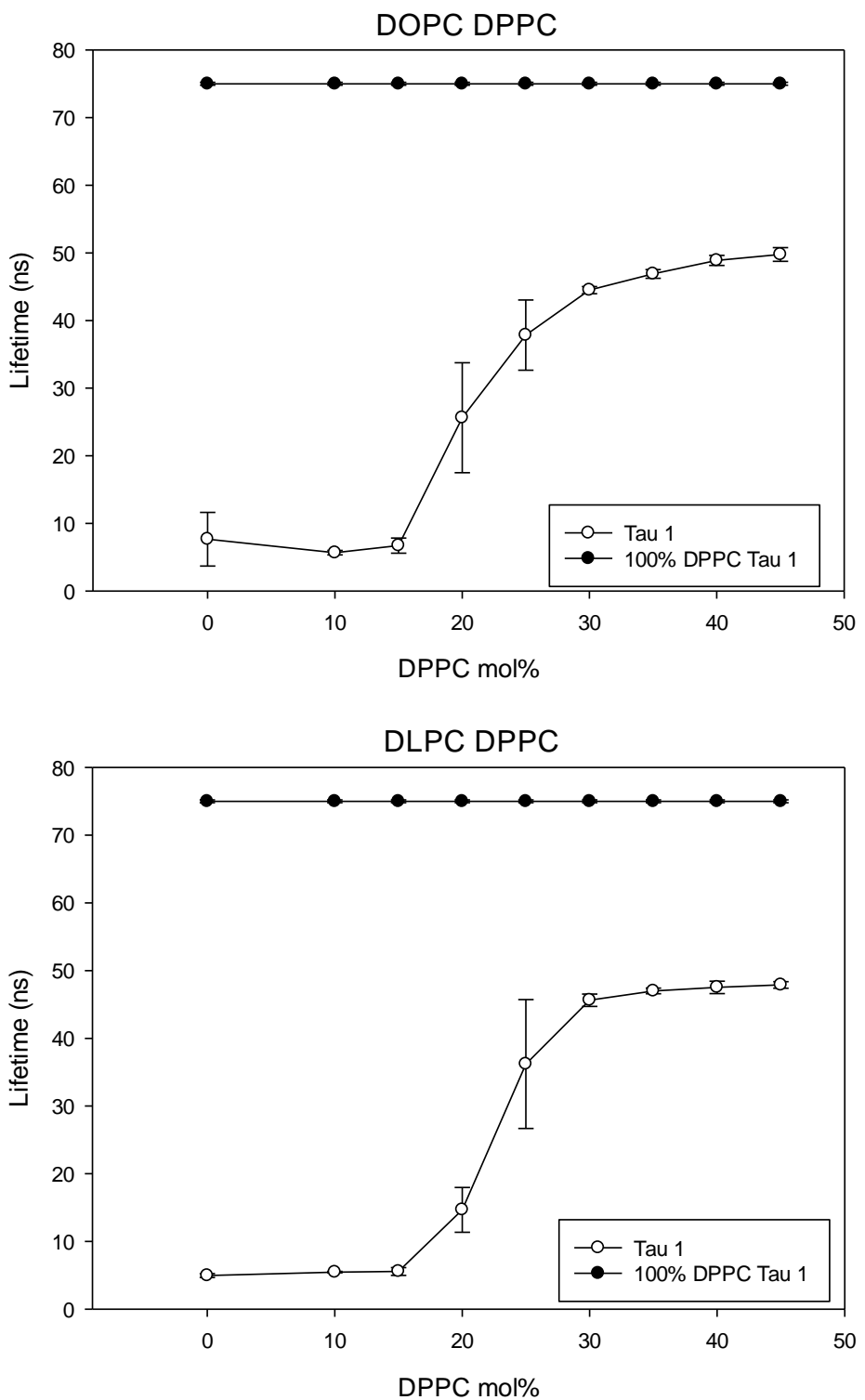


PAPC DPPC



PDPC DPPC





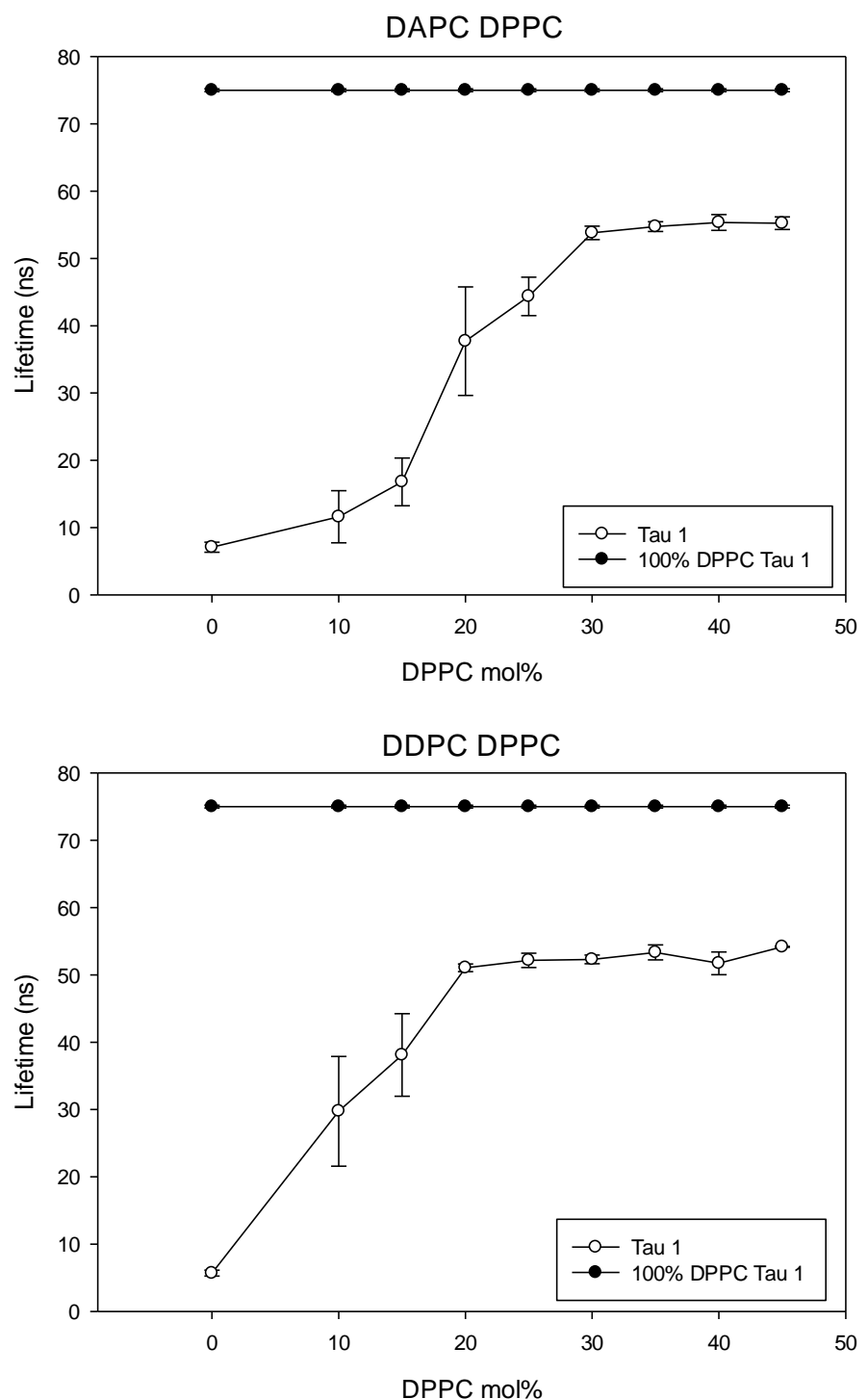
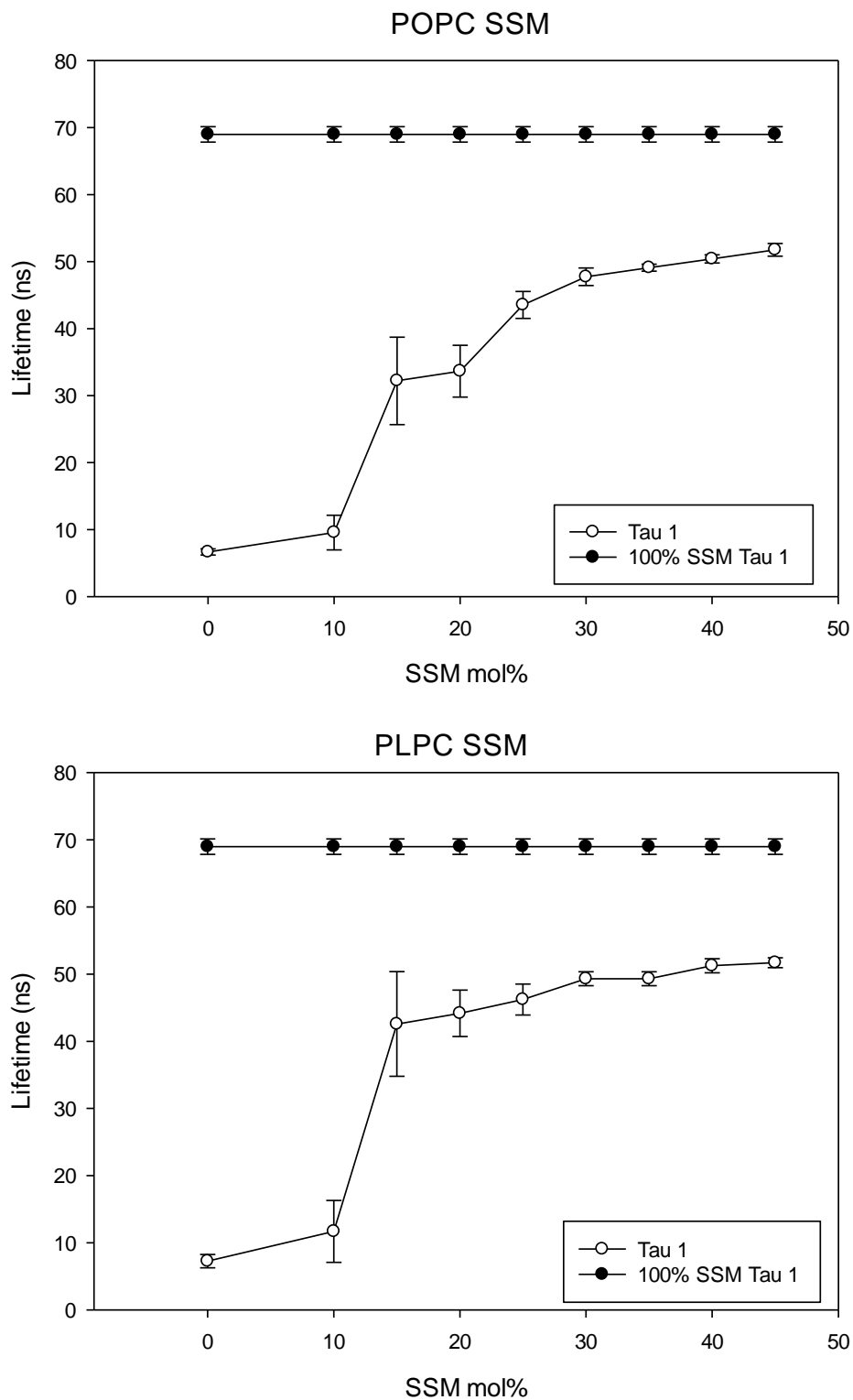
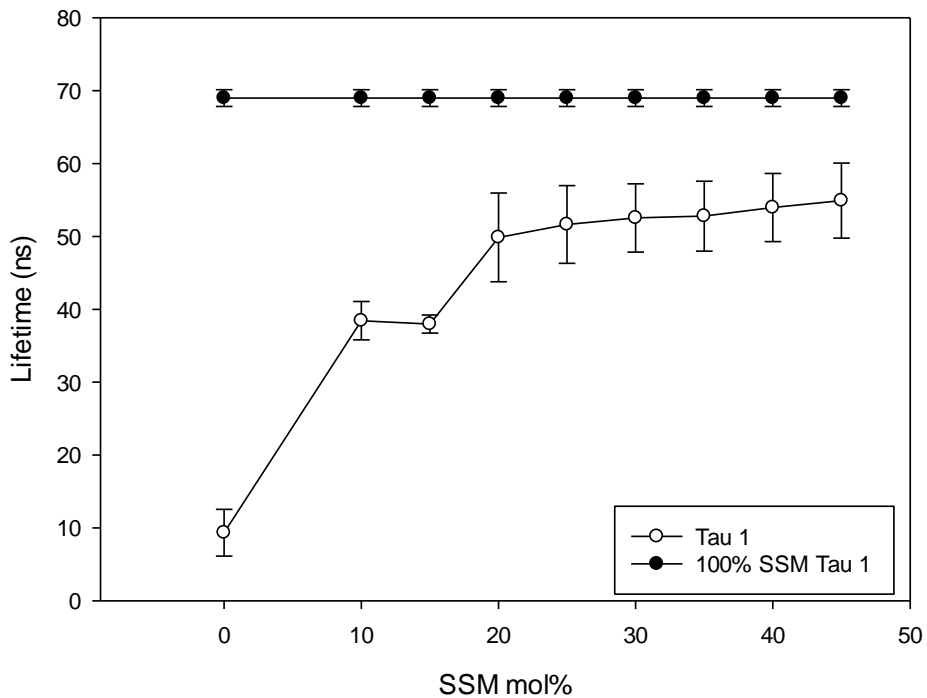


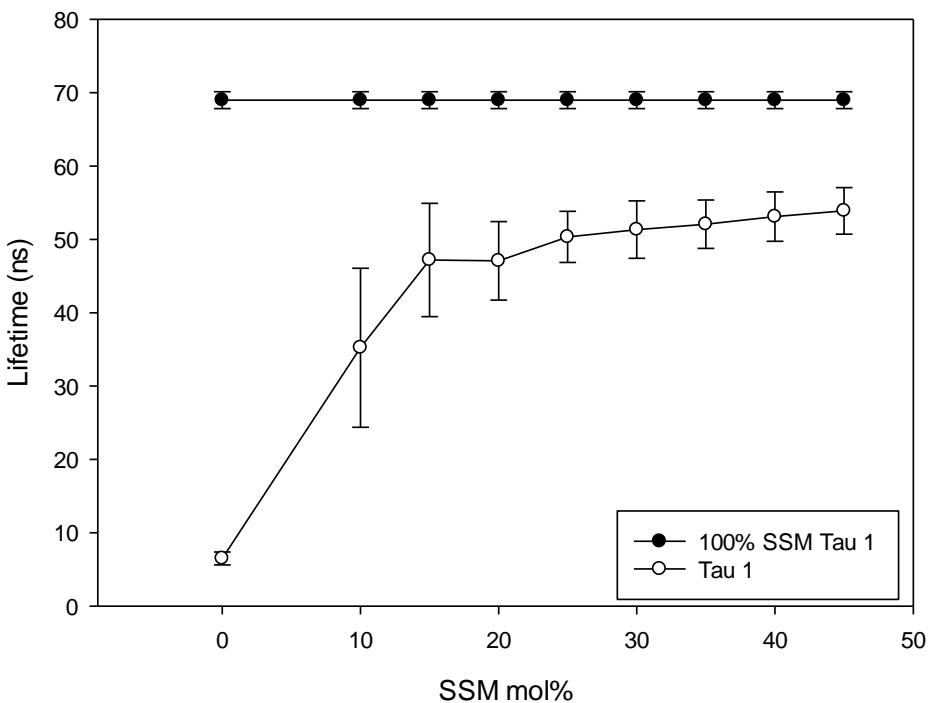
Figure S3. The longest lifetime component (τ_1) of tPA is given for pure SSM (filled symbols), and for SSM in unsaturated phosphatidylcholine bilayers (open symbols).



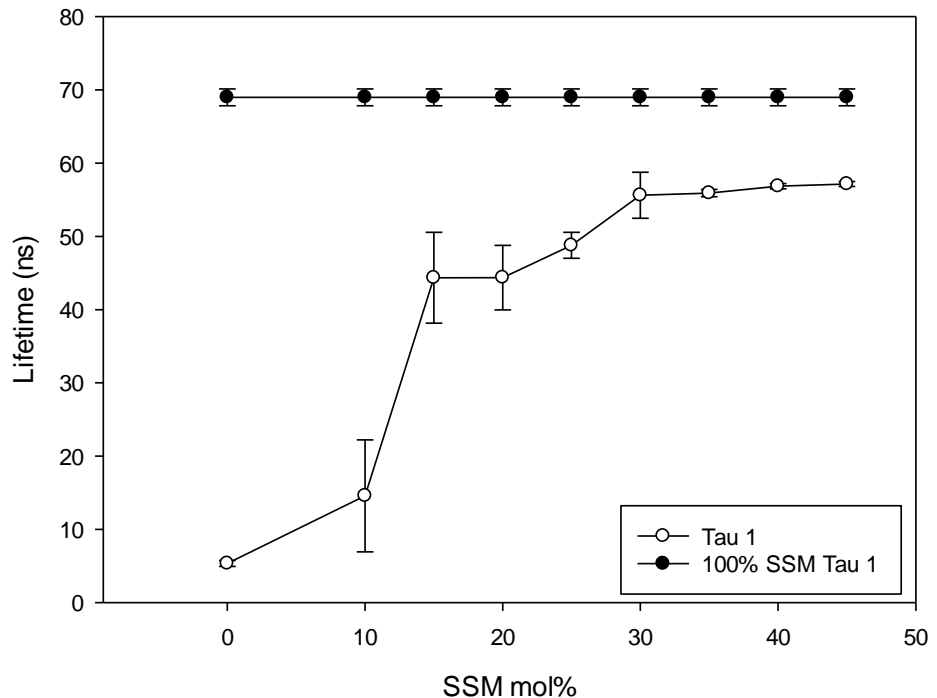
PAPC SSM



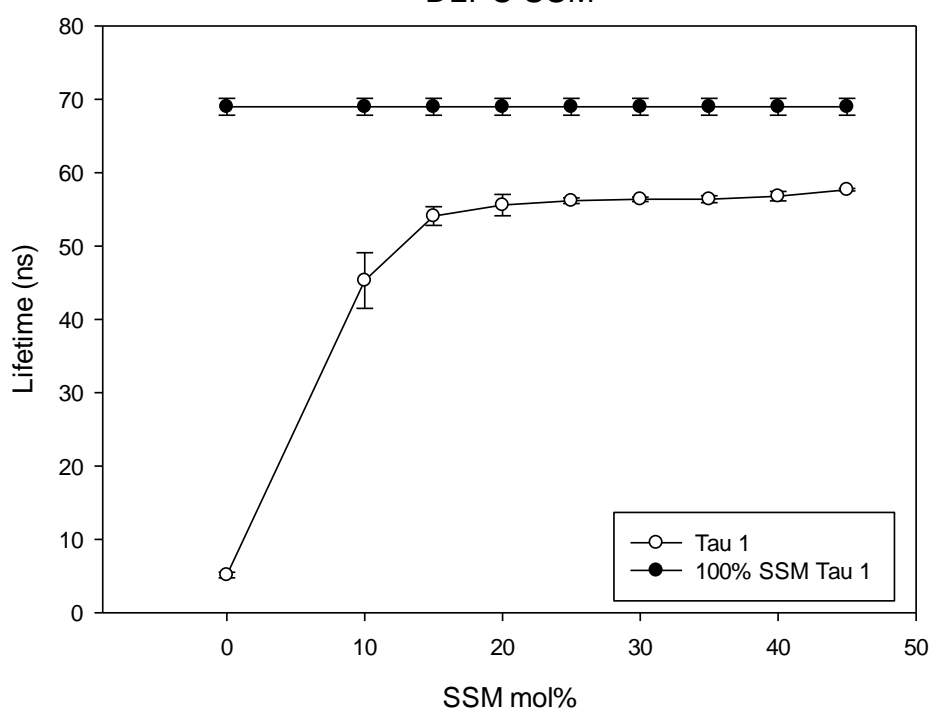
PDPC SSM



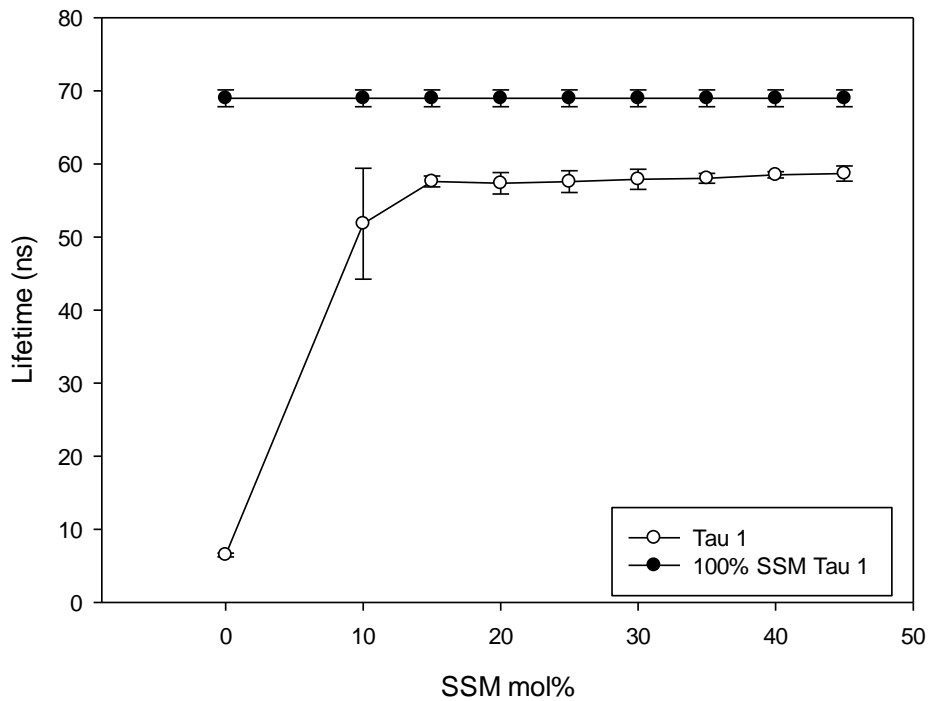
DOPC SSM



DLPC SSM



DAPC SSM



DDPC SSM

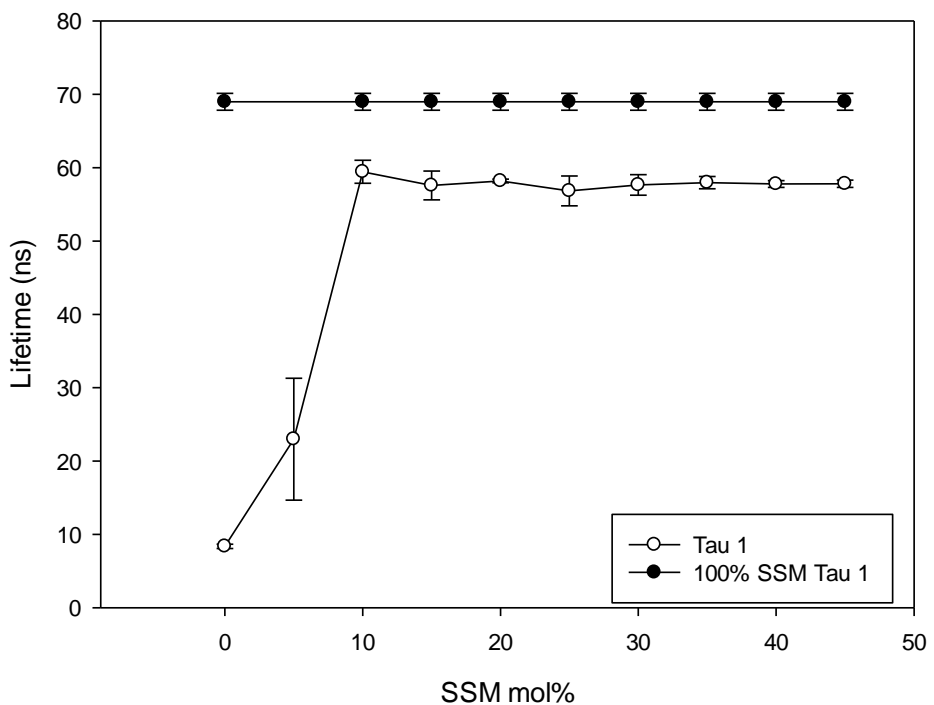
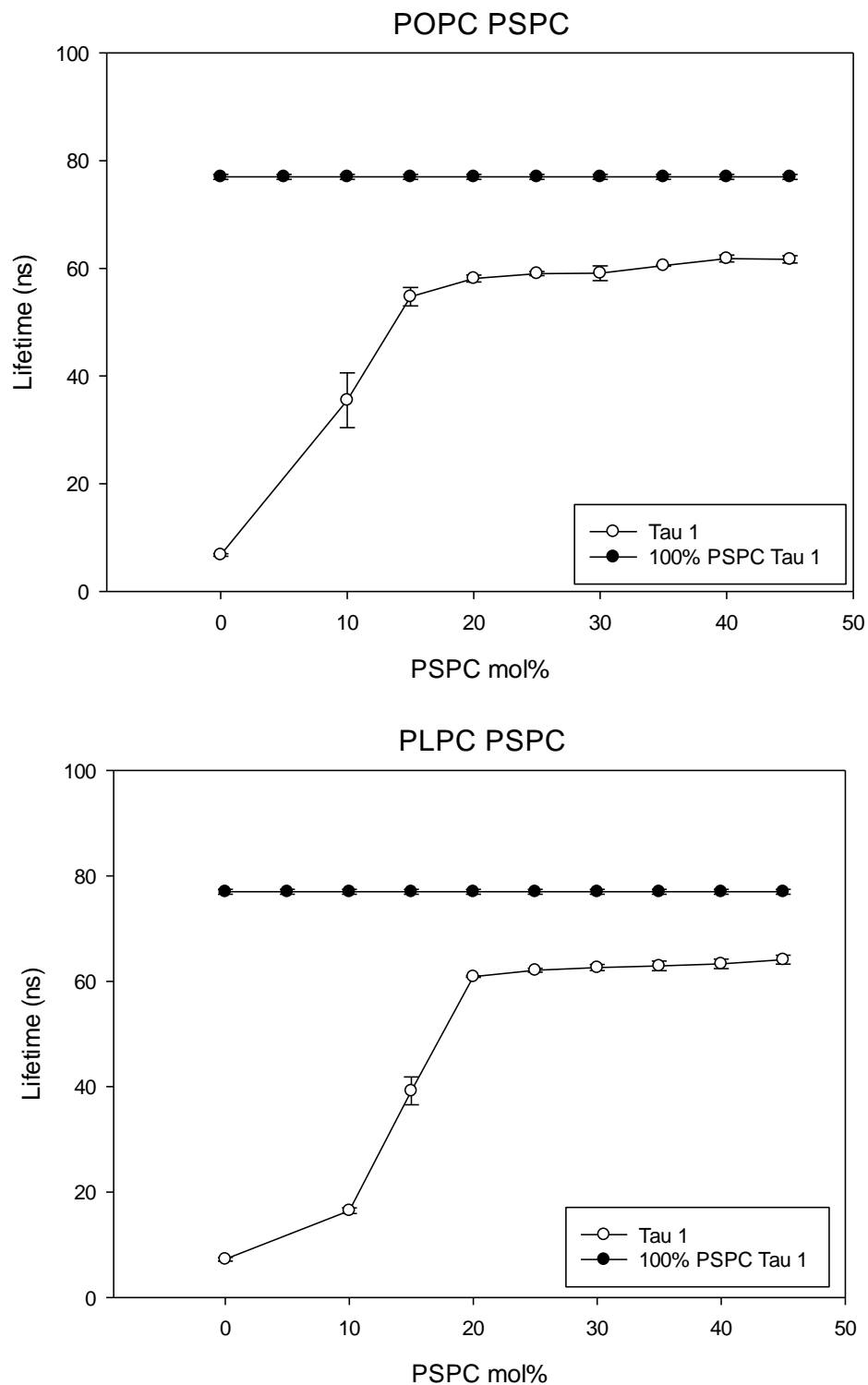
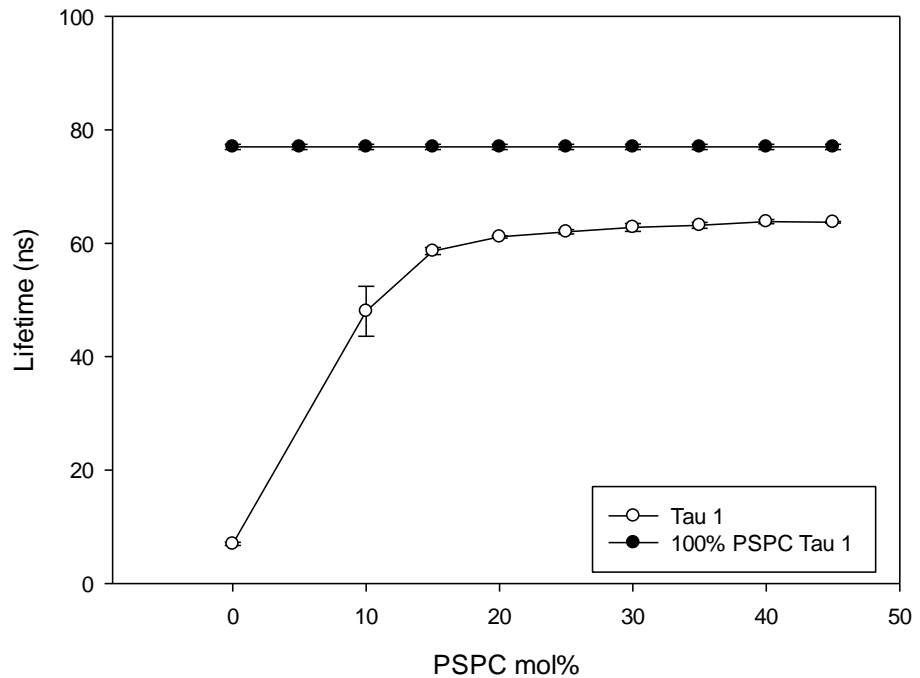


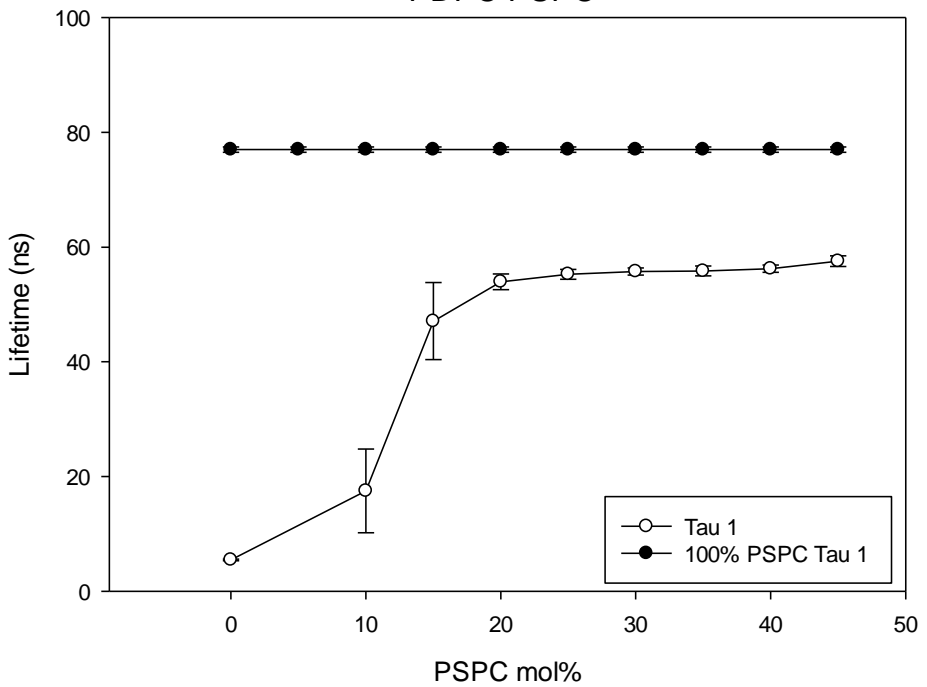
Figure S4. The longest lifetime component (τ_1) of tPA is given for pure PSPC (filled symbols), and for PSPC in unsaturated phosphatidylcholine bilayers (open symbols).



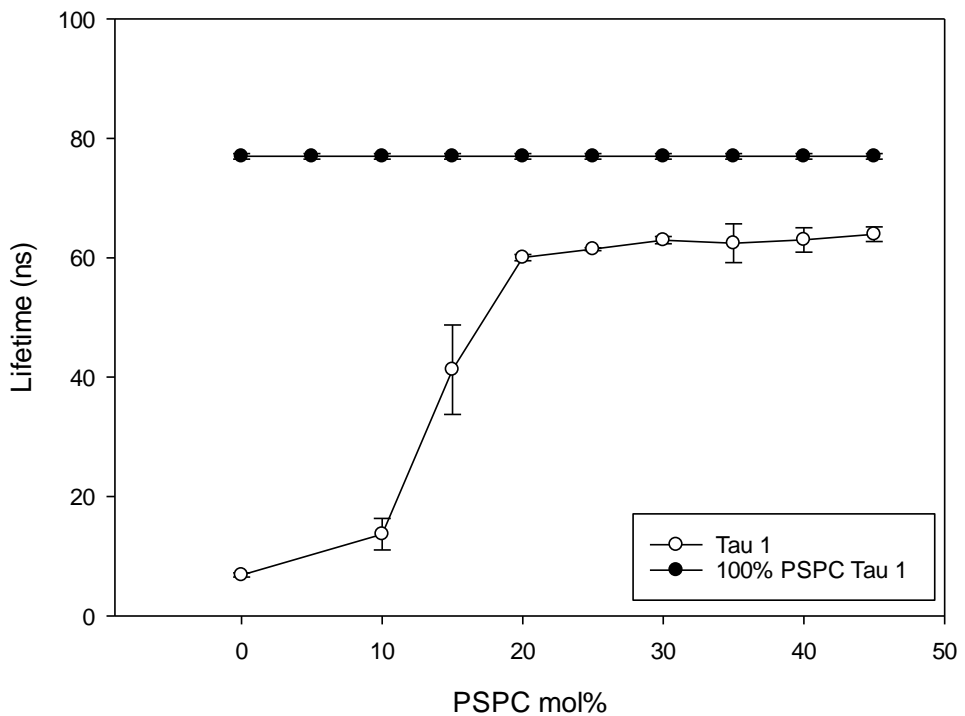
PA_{PC} PSPC



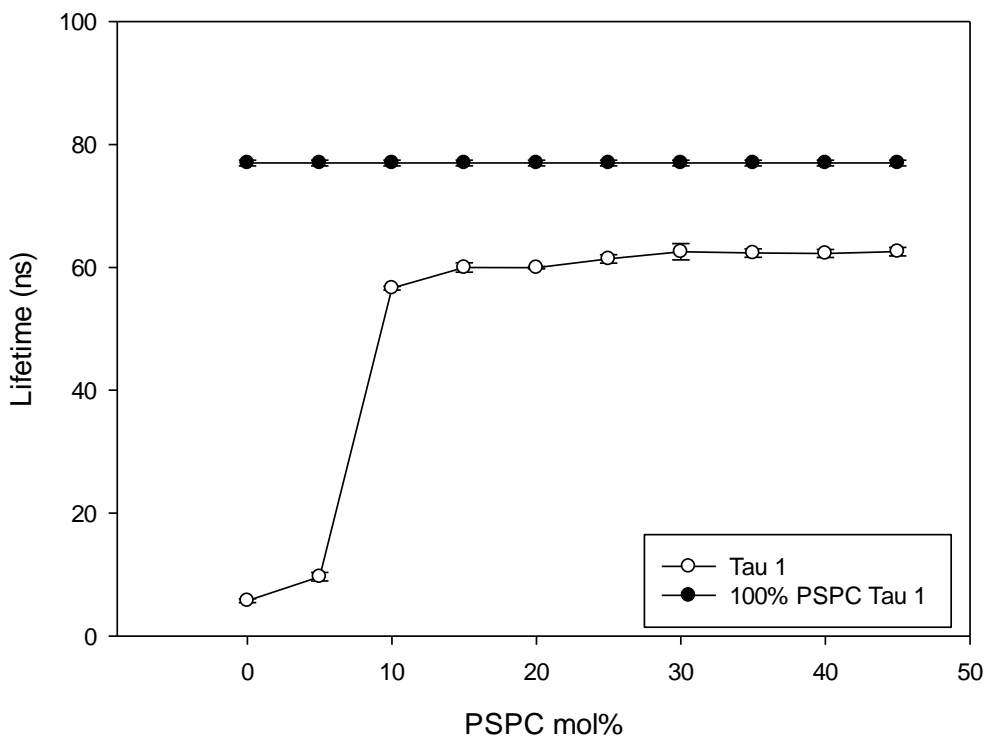
PD_{PC} PSPC



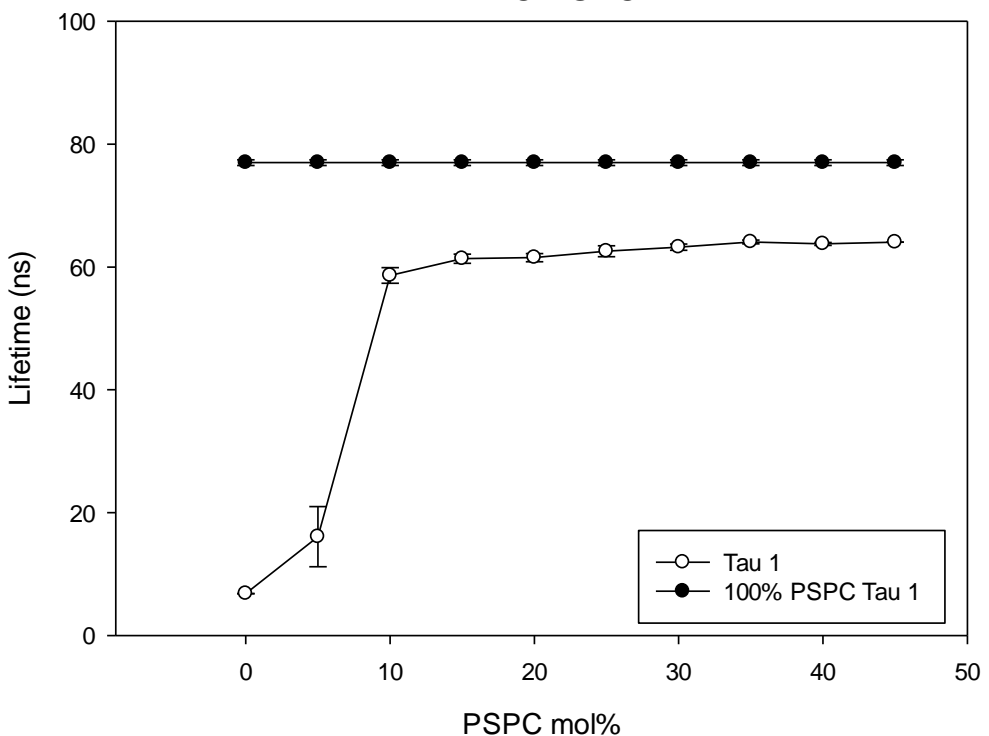
DOPC PSPC



DLPC PSPC



DAPC PSPC



DDPC PSPC

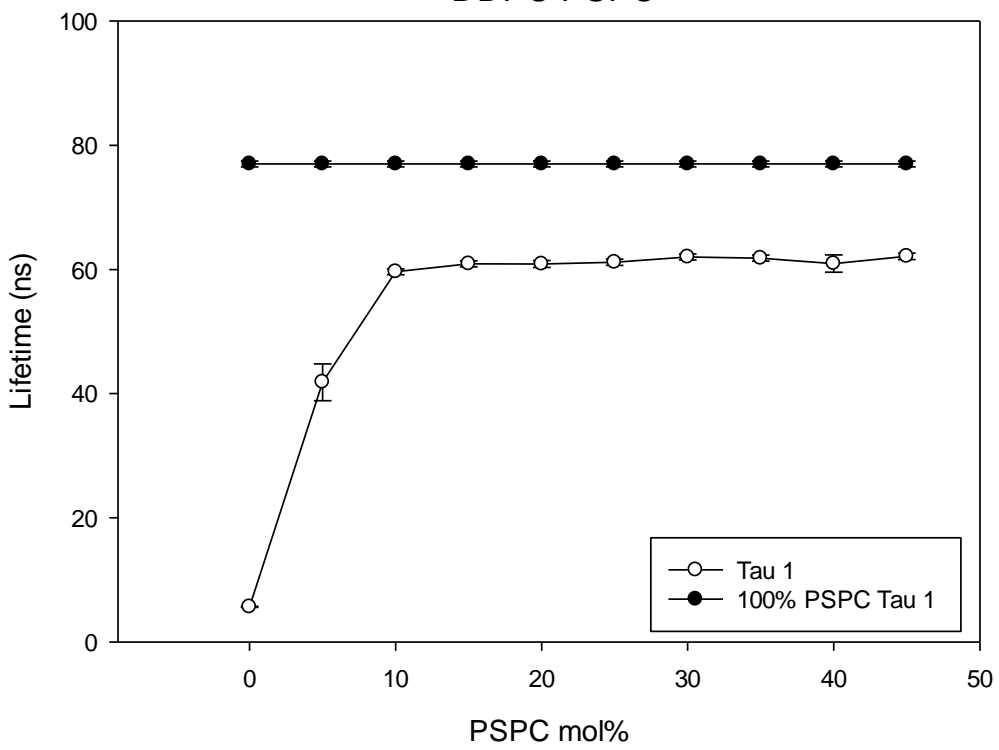


Table S1

Comparison of time-resolved fluorescence decays of tPA (1 mol%) in different bilayers at 23 °C

Sample	τ_1	f_1	α_1	τ_2	f_2	α_2	τ_3	f_3	α_3	τ_{AV}
POPC				6.5 ± 0.2	50.5 ± 3.5	34.5 ± 3.5	3.4 ± 0.0	49.5 ± 3.5	65.5 ± 3.5	5.0 ± 0.0
POPC/PSM (90:10)				6.9 ± 0.2	45.5 ± 3.5	30.5 ± 2.1	3.7 ± 0.1	54.5 ± 3.5	69.5 ± 2.1	5.2 ± 0.1
POPC/PSM (85:15)				7.8 ± 0.3	44.0 ± 1.4	27.5 ± 2.1	3.7 ± 0.1	56.0 ± 1.4	72.5 ± 2.1	5.5 ± 0.0
POPC/PSM (80:20)	13.4 ± 0.6	7.5 ± 0.7	2.5 ± 0.7	5.5 ± 0.0	82.5 ± 0.7	72.0 ± 1.4	1.9 ± 0.2	10.0 ± 1.4	25.0 ± 1.4	5.8 ± 0.1
POPC/PSM (75:25)	14.9 ± 3.5	10.0 ± 4.2	4.0 ± 2.8	6.1 ± 0.5	77.0 ± 0.0	66.5 ± 3.5	2.3 ± 0.4	13.0 ± 4.2	29.5 ± 6.4	6.4 ± 0.2
POPC/PSM (70:30)	16.1 ± 2.2	11.0 ± 1.4	4.0 ± 1.4	6.0 ± 0.0	78.0 ± 2.8	69.0 ± 1.4	2.1 ± 0.1	10.5 ± 0.7	27.0 ± 0.0	6.7 ± 0.1
POPC/PSM (65:35)	20.9 ± 4.7	13.0 ± 0.0	3.5 ± 0.7	6.8 ± 0.0	71.5 ± 0.7	62.0 ± 0.0	2.6 ± 0.1	15.5 ± 0.7	34.5 ± 0.7	7.9 ± 0.6
POPC/PSM (60:40)	26.4 ± 4.9	17.5 ± 0.7	4.5 ± 0.7	8.2 ± 0.6	60.0 ± 7.1	49.0 ± 8.5	3.2 ± 0.3	22.5 ± 6.4	46.5 ± 9.2	10.2 ± 1.1
POPC/PSM (55:45)	30.2 ± 1.8	22.5 ± 0.7	6.0 ± 0.0	9.6 ± 0.7	53.5 ± 0.7	43.5 ± 0.7	3.6 ± 0.2	24.0 ± 0.0	50.5 ± 0.7	12.9 ± 0.7
PLPC				7.4 ± 0.3	27.0 ± 2.8	15.0 ± 1.4	3.4 ± 0.1	72.5 ± 2.1	85.0 ± 1.4	4.5 ± 0.2
PLPC/PSM (90:10)				7.8 ± 0.2	26.0 ± 0.0	13.5 ± 0.7	3.5 ± 0.0	74.0 ± 0.0	86.5 ± 0.7	4.6 ± 0.0
PLPC/PSM (85:15)				7.3 ± 0.1	44.5 ± 4.9	27.0 ± 2.8	3.4 ± 0.2	55.5 ± 4.9	73.0 ± 2.8	5.2 ± 0.1
PLPC/PSM (80:20)	13.0 ± 0.8	7.5 ± 0.7	2.5 ± 0.7	5.0 ± 0.0	78.5 ± 2.1	67.5 ± 2.1	2.0 ± 0.0	13.5 ± 0.7	29.5 ± 2.1	5.2 ± 0.0
PLPC/PSM (75:25)	15.3 ± 0.2	8.5 ± 0.7	2.5 ± 0.7	5.3 ± 0.2	75.0 ± 0.0	61.0 ± 1.4	1.9 ± 0.4	16.5 ± 2.1	36.5 ± 0.7	5.6 ± 0.1
PLPC/PSM (70:30)	19.0 ± 1.0	8.0 ± 0.0	2.0 ± 0.0	6.1 ± 0.4	71.0 ± 1.4	57.0 ± 1.4	2.5 ± 0.2	21.0 ± 1.4	40.5 ± 2.1	6.4 ± 0.3
PLPC/PSM (65:35)	20.8 ± 3.5	10.5 ± 0.7	2.5 ± 0.7	6.2 ± 0.3	66.5 ± 4.9	53.5 ± 6.4	2.6 ± 0.1	23.0 ± 4.2	43.5 ± 6.4	7.0 ± 0.5
PLPC/PSM (60:40)	25.3 ± 0.6	17.0 ± 1.4	4.0 ± 0.0	7.6 ± 0.4	61.5 ± 0.7	50.0 ± 0.0	2.8 ± 0.1	21.0 ± 1.4	46.5 ± 0.7	9.6 ± 0.6
PLPC/PSM (55:45)	34.6 ± 0.9	24.0 ± 0.0	5.0 ± 0.0	10.5 ± 0.2	46.0 ± 1.4	32.0 ± 1.4	3.6 ± 0.1	30.0 ± 1.4	62.0 ± 1.4	14.3 ± 0.5
PAPC				5.6 ± 1.1	47.0 ± 15.6	26.5 ± 10.6	2.2 ± 0.5	53.0 ± 15.6	73.5 ± 10.6	3.7 ± 0.3
PAPC/PSM (90:10)				6.4 ± 0.1	42.0 ± 4.2	19.5 ± 2.1	2.2 ± 0.6	58.0 ± 4.2	80.5 ± 2.1	3.9 ± 0.3
PAPC/PSM (85:15)				6.8 ± 0.4	37.0 ± 1.4	19.5 ± 0.7	2.8 ± 0.1	63.0 ± 1.4	80.5 ± 0.7	4.3 ± 0.1
PAPC/PSM (80:20)	12.8 ± 0.5	7.5 ± 2.1	2.0 ± 0.0	4.4 ± 0.1	75.5 ± 3.5	57.5 ± 7.8	1.5 ± 0.3	17.0 ± 1.4	40.5 ± 7.8	4.5 ± 0.0
PAPC/PSM (75:25)	13.7 ± 0.6	8.0 ± 1.4	2.0 ± 0.0	4.6 ± 0.0	77.5 ± 0.7	61.5 ± 2.1	1.6 ± 0.2	15.5 ± 0.7	37.0 ± 1.4	4.9 ± 0.1
PAPC/PSM (70:30)	19.3 ± 2.5	8.0 ± 1.4	1.5 ± 0.7	5.4 ± 0.4	71.0 ± 1.4	52.5 ± 2.1	1.9 ± 0.6	36.5 ± 24.7	46.5 ± 2.1	5.7 ± 0.3
PAPC/PSM (65:35)	23.3 ± 7.0	10.5 ± 2.1	2.5 ± 0.7	6.2 ± 0.7	65.0 ± 4.2	48.0 ± 4.2	2.3 ± 0.6	24.5 ± 6.4	49.5 ± 4.9	7.0 ± 0.8
PAPC/PSM (60:40)	29.0 ± 1.4	16.0 ± 1.4	3.0 ± 0.0	7.4 ± 0.5	57.5 ± 3.5	42.5 ± 3.5	2.7 ± 0.5	26.5 ± 4.9	54.5 ± 3.5	9.6 ± 0.1
PAPC/PSM (55:45)	36.6 ± 1.6	29.5 ± 0.7	6.0 ± 0.0	9.8 ± 0.1	44.5 ± 0.7	18.0 ± 21.2	3.2 ± 0.2	26.5 ± 0.7	61.0 ± 0.0	15.9 ± 0.6
PDPC				6.0 ± 0.2	34.5 ± 0.7	17.5 ± 0.7	2.4 ± 0.2	65.5 ± 0.7	82.5 ± 0.7	3.6 ± 0.0
PDPC/PSM (90:10)				6.3 ± 0.0	36.5 ± 6.4	18.5 ± 2.1	2.4 ± 0.2	63.5 ± 6.4	81.5 ± 2.1	3.8 ± 0.1
PDPC/PSM (85:15)				6.7 ± 0.5	40.5 ± 2.1	20.5 ± 4.9	2.5 ± 0.3	59.5 ± 2.1	79.5 ± 4.9	4.2 ± 0.1
PDPC/PSM (80:20)	14.7 ± 5.5	10.0 ± 2.8	2.5 ± 2.1	4.3 ± 0.1	69.0 ± 5.7	49.0 ± 11.3	1.3 ± 0.1	21.0 ± 8.5	48.0 ± 12.7	4.6 ± 0.1
PDPC/PSM (75:25)	18.4 ± 7.8	9.5 ± 3.5	2.0 ± 1.4	4.7 ± 0.1	69.0 ± 2.8	51.0 ± 4.2	1.6 ± 0.2	21.5 ± 6.4	46.5 ± 6.4	5.2 ± 0.2
PDPC/PSM (70:30)	18.5 ± 4.6	13.0 ± 4.2	3.0 ± 1.4	5.0 ± 0.2	67.5 ± 0.7	49.5 ± 0.7	1.5 ± 0.3	19.5 ± 4.9	48.5 ± 2.1	5.9 ± 0.1
PDPC/PSM (65:35)	29.7 ± 1.1	18.5 ± 2.1	3.0 ± 0.0	6.9 ± 0.3	55.0 ± 2.8	38.0 ± 4.2	2.2 ± 0.2	26.5 ± 0.7	59.5 ± 3.5	9.8 ± 0.4
PDPC/PSM (60:40)	35.8 ± 1.1	35.5 ± 0.7	6.5 ± 0.7	8.5 ± 0.4	41.0 ± 1.4	31.0 ± 2.8	2.3 ± 0.1	23.5 ± 2.1	63.0 ± 2.8	16.8 ± 0.2
PDPC/PSM (55:45)	38.7 ± 0.9	49.0 ± 1.4	11.5 ± 0.7	10.9 ± 0.4	33.5 ± 2.1	28.5 ± 3.5	2.7 ± 0.1	17.5 ± 0.7	60.0 ± 2.8	23.0 ± 0.9

Each value is the average from at least two separate experiments ± SEM. τ , lifetimes (ns); f , fractional intensities (%); α , fractional amplitudes (%); τ_{AV} , intensity-weighted average lifetimes (ns).

Table S2

Comparison of time-resolved fluorescence decays of tPA (1 mol%) in different bilayers at 23 °C

Sample	τ_1	f_1	α_1	τ_2	f_2	α_2	τ_3	f_3	α_3	τ_{AV}
DOPC				7.2 ± 1.8	31.5 ± 6.4	16.0 ± 0.0	2.9 ± 0.1	68.5 ± 6.4	84.0 ± 0.0	4.3 ± 0.8
DOPC/PSM (90:10)				8.0 ± 0.7	16.0 ± 2.8	7.5 ± 2.1	3.4 ± 0.1	84.0 ± 2.8	92.5 ± 2.1	4.1 ± 0.1
DOPC/PSM (85:15)				9.7 ± 0.9	15.0 ± 4.2	6.5 ± 2.1	3.6 ± 0.1	84.5 ± 3.5	93.5 ± 2.1	4.5 ± 0.0
DOPC/PSM (80:20)	25.3 ± 1.9	4.0 ± 0.0	1.0 ± 0.0	5.2 ± 0.0	70.0 ± 4.2	55.5 ± 3.5	2.4 ± 0.1	25.5 ± 3.5	44.0 ± 4.2	5.4 ± 0.0
DOPC/PSM (75:25)	16.9 ± 4.2	5.5 ± 0.7	1.5 ± 0.7	5.1 ± 0.5	77.0 ± 4.2	65.0 ± 7.1	2.1 ± 0.2	16.5 ± 4.9	33.5 ± 7.8	5.3 ± 0.4
DOPC/PSM (70:30)	24.7 ± 6.4	6.5 ± 0.7	1.5 ± 0.7	6.1 ± 0.4	66.0 ± 7.1	51.0 ± 8.5	2.7 ± 0.3	27.5 ± 7.8	47.5 ± 9.2	6.3 ± 0.3
DOPC/PSM (65:35)	22.6 ± 4.0	9.5 ± 0.7	2.0 ± 0.0	6.5 ± 0.8	64.0 ± 7.1	50.0 ± 8.5	2.8 ± 0.4	26.5 ± 6.4	48.0 ± 8.5	7.1 ± 0.8
DOPC/PSM (60:40)	35.8 ± 2.3	19.0 ± 8.5	3.5 ± 2.1	8.8 ± 0.4	47.5 ± 4.9	35.0 ± 1.4	3.5 ± 0.0	33.0 ± 2.8	62.0 ± 0.0	12.3 ± 3.0
DOPC/PSM (55:45)	41.2 ± 1.9	37.0 ± 9.9	8.5 ± 3.5	11.5 ± 0.9	36.5 ± 6.4	28.5 ± 2.1	3.8 ± 0.2	27.0 ± 4.2	63.5 ± 0.7	20.4 ± 4.4
DLPC				7.7 ± 1.0	20.5 ± 0.7	6.5 ± 0.7	2.0 ± 0.0	79.5 ± 0.7	93.5 ± 0.7	3.2 ± 0.2
DLPC/PSM (90:10)				7.7 ± 0.3	20.0 ± 1.4	6.5 ± 0.7	2.1 ± 0.0	80.0 ± 1.4	93.5 ± 0.7	3.2 ± 0.1
DLPC/PSM (85:15)				8.2 ± 0.2	20.5 ± 0.7	7.0 ± 0.0	2.3 ± 0.0	79.5 ± 0.7	93.0 ± 0.0	3.5 ± 0.0
DLPC/PSM (80:20)	21.9 ± 5.0	6.5 ± 0.7	1.0 ± 0.0	4.4 ± 0.2	47.5 ± 6.4	29.5 ± 4.9	1.8 ± 0.1	46.0 ± 5.7	69.5 ± 4.9	4.3 ± 0.5
DLPC/PSM (75:25)	25.7 ± 2.4	9.5 ± 3.5	1.0 ± 0.0	4.5 ± 0.2	52.0 ± 1.4	33.0 ± 1.4	1.7 ± 0.2	38.0 ± 1.4	66.0 ± 1.4	5.5 ± 0.7
DLPC/PSM (70:30)	40.0 ± 0.8	44.5 ± 0.7	6.0 ± 0.0	7.0 ± 0.4	28.5 ± 3.5	21.5 ± 3.5	2.0 ± 0.1	27.0 ± 2.8	72.5 ± 3.5	20.4 ± 0.1
DLPC/PSM (65:35)	41.4 ± 0.8	53.5 ± 2.1	10.0 ± 0.0	10.8 ± 1.2	23.0 ± 0.0	17.0 ± 2.8	2.5 ± 0.1	23.5 ± 2.1	73.0 ± 2.8	25.1 ± 0.9
DLPC/PSM (60:40)	43.2 ± 1.0	62.0 ± 1.4	16.5 ± 0.7	13.9 ± 0.2	22.5 ± 0.7	18.5 ± 0.7	2.7 ± 0.0	15.5 ± 0.7	65.0 ± 0.0	30.4 ± 1.0
DLPC/PSM (55:45)	43.3 ± 0.8	64.5 ± 3.5	20.5 ± 2.1	15.0 ± 0.3	23.5 ± 2.1	21.5 ± 0.7	2.8 ± 0.1	12.0 ± 1.4	58.0 ± 1.4	31.8 ± 1.7
DAPC				6.3 ± 0.1	23.5 ± 7.8	7.0 ± 0.0	2.0 ± 0.1	81.0 ± 1.4	93.0 ± 0.0	2.8 ± 0.1
DAPC/PSM (90:10)				8.4 ± 2.2	19.0 ± 2.8	6.5 ± 2.1	2.3 ± 0.0	81.0 ± 2.8	93.5 ± 2.1	3.4 ± 0.3
DAPC/PSM (85:15)				9.5 ± 2.8	17.5 ± 7.8	5.5 ± 3.5	2.2 ± 0.1	82.5 ± 7.8	94.5 ± 3.5	3.4 ± 0.0
DAPC/PSM (80:20)	38.5 ± 0.6	25.5 ± 13.4	2.0 ± 1.4	5.0 ± 0.1	34.0 ± 4.2	22.5 ± 2.1	1.8 ± 0.4	40.5 ± 9.2	75.0 ± 1.4	12.2 ± 4.4
DAPC/PSM (75:25)	39.1 ± 0.3	39.5 ± 0.7	4.5 ± 0.7	6.5 ± 0.4	26.0 ± 0.0	17.5 ± 0.7	2.0 ± 0.1	34.5 ± 0.7	78.0 ± 0.0	17.8 ± 0.0
DAPC/PSM (70:30)	42.4 ± 0.1	60.0 ± 1.4	12.5 ± 0.7	11.4 ± 1.4	20.5 ± 0.7	16.5 ± 0.7	2.4 ± 0.0	19.0 ± 1.4	71.0 ± 0.0	28.3 ± 0.6
DAPC/PSM (65:35)	42.5 ± 0.2	64.0 ± 0.0	17.5 ± 0.7	13.8 ± 0.2	22.0 ± 0.0	19.0 ± 0.0	2.5 ± 0.0	14.0 ± 0.0	64.0 ± 0.0	30.5 ± 0.0
DAPC/PSM (60:40)	43.1 ± 0.0	69.5 ± 2.1	23.5 ± 2.1	14.8 ± 0.1	22.0 ± 1.4	21.5 ± 0.7	2.3 ± 0.1	8.5 ± 0.7	54.5 ± 0.7	33.3 ± 0.8
DAPC/PSM (55:45)	44.1 ± 0.4	68.5 ± 0.7	28.0 ± 1.4	17.0 ± 0.6	24.0 ± 1.4	25.0 ± 1.4	2.9 ± 0.3	7.5 ± 0.7	47.5 ± 0.7	34.5 ± 0.7
DDPC				9.1 ± 1.1	21.5 ± 0.7	5.5 ± 0.7	1.8 ± 0.0	78.5 ± 0.7	94.5 ± 0.7	3.4 ± 0.1
DDPC/PSM (90:10)				17.2 ± 1.3	21.0 ± 4.2	3.0 ± 0.0	2.1 ± 0.3	79.0 ± 4.2	97.0 ± 0.0	5.3 ± 0.7
DDPC/PSM (85:15)				32.2 ± 3.8	44.0 ± 7.1	5.5 ± 0.7	2.3 ± 0.1	56.0 ± 7.1	94.5 ± 0.7	15.5 ± 3.7
DDPC/PSM (80:20)	38.1 ± 4.0	53.0 ± 0.0	6.5 ± 0.7	7.0 ± 0.4	21.5 ± 2.1	14.5 ± 0.7	1.6 ± 0.3	26.0 ± 1.4	78.5 ± 0.7	22.1 ± 2.4
DDPC/PSM (75:25)	41.2 ± 0.2	63.5 ± 0.7	15.5 ± 4.9	12.4 ± 3.8	22.0 ± 4.2	18.0 ± 2.8	2.0 ± 0.0	14.0 ± 5.7	67.0 ± 7.1	29.4 ± 1.9
DDPC/PSM (70:30)	41.8 ± 1.1	68.5 ± 6.4	23.5 ± 0.7	15.0 ± 1.1	23.5 ± 6.4	22.0 ± 5.7	2.1 ± 0.0	8.0 ± 1.4	54.5 ± 4.9	32.4 ± 1.9
DDPC/PSM (65:35)	42.8 ± 1.0	70.5 ± 3.5	25.0 ± 2.8	15.4 ± 0.1	22.0 ± 2.8	22.0 ± 1.4	2.2 ± 0.1	7.5 ± 0.7	53.5 ± 0.7	33.6 ± 1.8
DDPC/PSM (60:40)	42.8 ± 0.9	69.5 ± 4.9	26.5 ± 3.5	15.8 ± 0.2	23.5 ± 4.9	24.5 ± 2.1	2.3 ± 0.0	7.5 ± 0.7	49.5 ± 2.1	33.6 ± 2.1
DDPC/PSM (55:45)	43.6 ± 0.1	73.0 ± 2.8	31.5 ± 3.5	16.4 ± 0.2	21.5 ± 2.1	24.5 ± 0.7	2.3 ± 0.1	5.5 ± 0.7	44.5 ± 3.5	35.4 ± 0.9

Each value is the average from at least two separate experiments ± SEM. τ , lifetimes (ns); f , fractional intensities (%); α , fractional amplitudes (%); τ_{AV} , intensity-weighted average lifetimes (ns).

Table S3

Comparison of time-resolved fluorescence decays of tPA (1 mol%) in different bilayers at 23 °C

Sample	τ_1	f_1	α_1	τ_2	f_2	α_2	τ_3	f_3	α_3	τ_{AV}
POPC				5.7 ± 0.1	47.0 ± 4.2	33.0 ± 2.8	3.2 ± 0.2	53.0 ± 4.2	67.0 ± 2.8	4.4 ± 0.0
POPC/DPPC (90:10)				6.2 ± 0.0	48.0 ± 1.4	33.0 ± 1.4	3.4 ± 0.0	52.0 ± 1.4	67.0 ± 1.4	4.7 ± 0.1
POPC/DPPC (85:15)				6.6 ± 0.1	47.0 ± 1.4	31.5 ± 0.7	3.5 ± 0.0	53.0 ± 1.4	68.5 ± 0.7	5.0 ± 0.1
POPC/DPPC (80:20)	15.2 ± 2.4	4.5 ± 0.7	1.5 ± 0.7	5.3 ± 0.1	83.0 ± 1.4	69.5 ± 0.7	1.9 ± 0.4	12.5 ± 0.7	29.0 ± 1.4	5.3 ± 0.0
POPC/DPPC (75:25)	17.6 ± 0.5	4.0 ± 0.0	1.0 ± 0.0	5.7 ± 0.0	79.0 ± 0.0	65.5 ± 0.7	2.4 ± 0.0	17.0 ± 0.0	33.5 ± 0.7	5.7 ± 0.1
POPC/DPPC (70:30)	34.0 ± 2.4	10.5 ± 3.5	1.5 ± 0.7	6.8 ± 0.4	62.0 ± 5.7	49.5 ± 4.9	3.0 ± 0.2	27.5 ± 2.1	49.0 ± 4.2	8.7 ± 1.3
POPC/DPPC (65:35)	42.1 ± 0.3	32.5 ± 0.7	6.0 ± 0.0	9.4 ± 0.4	34.5 ± 0.7	28.0 ± 1.4	3.8 ± 0.1	32.5 ± 0.7	66.0 ± 1.4	18.2 ± 0.3
POPC/DPPC (60:40)	45.5 ± 0.3	49.5 ± 2.1	12.0 ± 1.4	13.3 ± 0.7	24.5 ± 0.7	20.5 ± 0.7	4.1 ± 0.1	25.5 ± 0.7	68.0 ± 0.0	27.0 ± 0.9
POPC/DPPC (55:45)	46.7 ± 0.1	56.0 ± 1.4	16.5 ± 0.7	16.2 ± 0.4	23.0 ± 0.0	19.0 ± 0.0	4.3 ± 0.0	20.5 ± 0.7	65.0 ± 1.4	30.9 ± 0.4
PLPC				5.4 ± 0.2	43.5 ± 3.5	30.0 ± 2.8	3.0 ± 0.1	56.5 ± 3.5	70.0 ± 2.8	4.1 ± 0.1
PLPC/DPPC (90:10)				5.6 ± 0.0	47.5 ± 4.9	33.5 ± 4.9	3.1 ± 0.0	52.5 ± 4.9	66.5 ± 4.9	4.3 ± 0.1
PLPC/DPPC (85:15)				6.2 ± 0.5	41.5 ± 9.2	28.0 ± 8.5	3.3 ± 0.2	58.5 ± 9.2	72.0 ± 8.5	4.5 ± 0.0
PLPC/DPPC (80:20)	16.9 ± 4.8	4.0 ± 1.4	1.0 ± 0.0	4.8 ± 0.1	83.0 ± 2.8	70.5 ± 3.5	1.9 ± 0.3	14.0 ± 4.2	29.0 ± 4.2	4.8 ± 0.1
PLPC/DPPC (75:25)	27.4 ± 3.4	3.0 ± 0.0	0.0 ± 0.0	5.4 ± 0.1	73.0 ± 2.8	58.5 ± 2.1	2.6 ± 0.1	24.0 ± 2.8	41.0 ± 2.8	5.4 ± 0.3
PLPC/DPPC (70:30)	35.8 ± 1.5	9.0 ± 1.4	1.0 ± 0.0	5.9 ± 0.0	66.5 ± 0.7	54.5 ± 0.7	2.7 ± 0.0	24.5 ± 0.7	44.5 ± 0.7	7.8 ± 0.5
PLPC/DPPC (65:35)	42.7 ± 1.7	20.5 ± 3.5	2.5 ± 0.7	7.6 ± 0.6	38.5 ± 7.8	30.0 ± 7.1	3.5 ± 0.2	41.0 ± 4.2	67.5 ± 6.4	13.2 ± 1.7
PLPC/DPPC (60:40)	45.7 ± 0.2	40.5 ± 0.7	7.0 ± 0.0	9.0 ± 0.1	28.5 ± 0.7	24.5 ± 0.7	3.6 ± 0.0	31.0 ± 1.4	68.5 ± 0.7	22.2 ± 0.3
PLPC/DPPC (55:45)	46.9 ± 0.1	49.5 ± 0.7	10.5 ± 0.7	12.0 ± 0.3	22.0 ± 0.0	18.0 ± 0.0	3.9 ± 0.0	28.5 ± 0.7	72.0 ± 0.0	27.0 ± 0.5
PAPC				6.6 ± 0.5	20.0 ± 1.4	10.0 ± 1.4	2.9 ± 0.0	80.0 ± 1.4	90.0 ± 1.4	3.7 ± 0.0
PAPC/DPPC (90:10)				5.7 ± 0.0	36.0 ± 0.0	22.0 ± 0.0	2.9 ± 0.0	64.0 ± 0.0	78.0 ± 0.0	3.9 ± 0.0
PAPC/DPPC (85:15)				6.2 ± 0.6	32.5 ± 6.4	19.5 ± 4.9	3.1 ± 0.2	67.5 ± 6.4	80.5 ± 4.9	4.1 ± 0.1
PAPC/DPPC (80:20)	17.9 ± 4.8	3.0 ± 0.0	1.0 ± 0.0	4.8 ± 0.1	70.0 ± 1.4	55.0 ± 0.0	2.3 ± 0.1	27.0 ± 1.4	44.5 ± 0.7	4.5 ± 0.2
PAPC/DPPC (75:25)	20.2 ± 6.3	3.0 ± 0.0	1.0 ± 0.0	5.1 ± 0.2	69.5 ± 3.5	53.5 ± 4.9	2.4 ± 0.1	27.5 ± 3.5	46.0 ± 4.2	4.8 ± 0.3
PAPC/DPPC (70:30)	41.7 ± 3.3	19.5 ± 7.8	2.5 ± 0.7	6.7 ± 0.5	44.0 ± 9.9	34.0 ± 7.1	2.9 ± 0.2	36.0 ± 2.8	63.5 ± 6.4	12.2 ± 3.5
PAPC/DPPC (65:35)	46.2 ± 0.4	38.0 ± 2.8	5.5 ± 0.7	8.9 ± 0.3	26.0 ± 0.0	20.5 ± 0.7	3.3 ± 0.0	35.5 ± 2.1	74.0 ± 1.4	21.1 ± 1.1
PAPC/DPPC (60:40)	47.5 ± 0.5	52.0 ± 1.4	10.0 ± 0.0	11.1 ± 0.9	20.5 ± 2.1	17.0 ± 2.8	3.4 ± 0.2	27.0 ± 1.4	73.0 ± 1.4	28.0 ± 0.9
PAPC/DPPC (55:45)	48.6 ± 0.1	59.0 ± 1.4	13.5 ± 0.7	14.2 ± 0.7	19.0 ± 0.0	15.5 ± 0.7	3.5 ± 0.1	22.0 ± 1.4	71.0 ± 1.4	32.1 ± 0.6
PDPC				5.6 ± 0.2	30.0 ± 1.4	17.0 ± 0.0	2.7 ± 0.0	70.0 ± 1.4	83.0 ± 0.0	3.5 ± 0.1
PDPC/DPPC (90:10)				5.9 ± 0.5	34.0 ± 5.7	20.0 ± 4.2	2.8 ± 0.1	66.0 ± 5.7	80.0 ± 4.2	3.9 ± 0.0
PDPC/DPPC (85:15)				8.0 ± 0.1	20.0 ± 0.0	9.0 ± 0.0	3.2 ± 0.1	80.0 ± 0.0	91.0 ± 0.0	4.2 ± 0.1
PDPC/DPPC (80:20)	23.5 ± 0.8	3.0 ± 0.0	0.5 ± 0.7	4.8 ± 0.0	69.5 ± 2.1	52.5 ± 2.1	2.2 ± 0.1	28.0 ± 2.8	46.5 ± 2.1	4.7 ± 0.1
PDPC/DPPC (75:25)	28.6 ± 7.4	5.5 ± 3.5	0.5 ± 0.7	5.2 ± 0.0	67.5 ± 0.7	50.5 ± 0.7	2.2 ± 0.2	27.0 ± 2.8	49.0 ± 0.0	5.7 ± 1.2
PDPC/DPPC (70:30)	35.8 ± 7.7	15.0 ± 7.1	2.5 ± 0.7	6.5 ± 0.3	50.5 ± 6.4	38.0 ± 4.2	2.8 ± 0.0	34.5 ± 0.7	60.5 ± 3.5	9.9 ± 3.5
PDPC/DPPC (65:35)	41.1 ± 4.0	27.0 ± 7.1	4.0 ± 1.4	8.6 ± 1.0	35.0 ± 7.1	24.5 ± 4.9	3.2 ± 0.2	37.5 ± 0.7	71.5 ± 3.5	15.5 ± 3.9
PDPC/DPPC (60:40)	46.5 ± 0.3	47.0 ± 0.0	9.0 ± 0.0	10.8 ± 0.9	24.5 ± 0.7	19.5 ± 2.1	3.4 ± 0.1	28.0 ± 1.4	72.0 ± 1.4	25.6 ± 0.2
PDPC/DPPC (55:45)	48.2 ± 0.3	58.0 ± 1.4	13.5 ± 0.7	13.6 ± 0.3	20.5 ± 0.7	17.0 ± 1.4	3.5 ± 0.1	21.5 ± 0.7	69.5 ± 0.7	31.5 ± 0.5

Each value is the average from at least two separate experiments ± SEM. τ , lifetimes (ns); f , fractional intensities (%); α , fractional amplitudes (%); τ_{AV} , intensity-weighted average lifetimes (ns).

Table S4

Comparison of time-resolved fluorescence decays of tPA (1 mol%) in different bilayers at 23 °C

Sample		τ_1	f_1	α_1	τ_2	f_2	α_2	τ_3	f_3	α_3	τ_{AV}
DOPC					5.4 ± 0.2	26.0 ± 5.7	15.0 ± 4.2	2.8 ± 0.1	74.0 ± 5.7	85.0 ± 4.2	3.4 ± 0.1
DOPC/DPPC (90:10)					5.8 ± 0.4	28.5 ± 2.1	17.5 ± 2.1	3.0 ± 0.1	71.5 ± 2.1	82.5 ± 2.1	3.8 ± 0.1
DOPC/DPPC (85:15)					7.2 ± 1.0	19.5 ± 6.4	10.0 ± 4.2	3.3 ± 0.2	80.5 ± 6.4	90.0 ± 4.2	4.0 ± 0.1
DOPC/DPPC (80:20)	30.2 ± 2.4	4.0 ± 0.0	0.0 ± 0.0	4.6 ± 0.2	69.5 ± 0.7	55.5 ± 0.7	2.3 ± 0.1	27.0 ± 0.0	43.5 ± 0.7	4.9 ± 0.3	
DOPC/DPPC (75:25)	34.9 ± 1.8	6.0 ± 1.4	1.0 ± 0.0	4.8 ± 0.2	68.0 ± 8.5	55.5 ± 9.2	2.3 ± 0.2	26.0 ± 7.1	44.0 ± 8.5	6.0 ± 0.5	
DOPC/DPPC (70:30)	44.2 ± 0.3	19.5 ± 0.7	2.0 ± 0.0	5.7 ± 0.2	46.0 ± 2.8	39.0 ± 4.2	2.7 ± 0.1	34.0 ± 2.8	59.0 ± 4.2	12.3 ± 0.3	
DOPC/DPPC (65:35)	47.2 ± 0.5	45.0 ± 4.2	6.5 ± 0.7	7.8 ± 0.5	23.0 ± 1.4	21.5 ± 3.5	3.1 ± 0.2	32.0 ± 5.7	72.0 ± 4.2	23.9 ± 2.1	
DOPC/DPPC (60:40)	49.3 ± 0.3	58.5 ± 3.5	12.5 ± 2.1	14.7 ± 1.3	15.0 ± 0.0	10.5 ± 0.7	3.6 ± 0.0	26.5 ± 3.5	77.0 ± 2.8	32.1 ± 2.2	
DOPC/DPPC (55:45)	50.0 ± 1.3	61.5 ± 2.1	15.0 ± 1.4	17.0 ± 2.0	16.0 ± 0.0	11.5 ± 0.7	3.7 ± 0.1	22.5 ± 0.7	73.5 ± 0.7	34.4 ± 1.8	
DLPC					5.1 ± 0.3	30.5 ± 2.1	13.0 ± 1.4	1.8 ± 0.0	69.5 ± 2.1	87.0 ± 1.4	2.8 ± 0.0
DLPC/DPPC (90:10)					5.5 ± 0.0	30.0 ± 1.4	13.0 ± 0.0	2.0 ± 0.1	70.0 ± 1.4	87.0 ± 0.0	3.0 ± 0.0
DLPC/DPPC (85:15)					5.8 ± 0.6	30.5 ± 6.4	13.5 ± 3.5	2.1 ± 0.2	69.5 ± 6.4	86.5 ± 3.5	3.2 ± 0.1
DLPC/DPPC (80:20)	16.4 ± 2.2	4.0 ± 0.0	1.0 ± 0.0	3.7 ± 0.2	63.0 ± 1.4	42.5 ± 0.7	1.5 ± 0.2	33.5 ± 2.1	57.0 ± 1.4	3.5 ± 0.2	
DLPC/DPPC (75:25)	31.6 ± 7.4	7.5 ± 3.5	0.5 ± 0.7	4.1 ± 0.0	57.0 ± 4.2	37.0 ± 2.8	1.5 ± 0.0	36.0 ± 0.0	62.5 ± 2.1	5.3 ± 1.6	
DLPC/DPPC (70:30)	45.2 ± 0.8	34.5 ± 0.7	3.0 ± 0.0	5.0 ± 0.2	34.0 ± 1.4	27.0 ± 2.8	1.8 ± 0.0	31.5 ± 2.1	70.0 ± 2.8	17.8 ± 0.8	
DLPC/DPPC (65:35)	46.8 ± 0.3	52.0 ± 1.4	6.0 ± 0.0	6.2 ± 0.2	22.0 ± 1.4	20.0 ± 0.0	2.0 ± 0.1	26.5 ± 0.7	74.0 ± 0.0	26.1 ± 0.7	
DLPC/DPPC (60:40)	47.2 ± 0.9	59.5 ± 2.1	8.5 ± 0.7	7.6 ± 0.6	17.0 ± 1.4	16.0 ± 1.4	2.1 ± 0.1	23.0 ± 0.0	75.5 ± 0.7	29.9 ± 1.4	
DLPC/DPPC (55:45)	48.0 ± 0.6	65.5 ± 0.7	12.5 ± 0.7	11.4 ± 1.9	15.5 ± 0.7	12.5 ± 0.7	2.4 ± 0.1	19.5 ± 0.7	75.0 ± 0.0	33.5 ± 0.3	
DAPC					6.7 ± 0.1	18.0 ± 0.0	6.5 ± 0.7	2.1 ± 0.0	82.0 ± 0.0	93.5 ± 0.7	3.0 ± 0.0
DAPC/DPPC (90:10)					13.2 ± 3.9	11.5 ± 2.1	3.0 ± 1.4	2.6 ± 0.0	88.5 ± 2.1	97.0 ± 1.4	3.8 ± 0.2
DAPC/DPPC (85:15)					18.7 ± 1.6	10.0 ± 0.0	2.0 ± 0.0	2.8 ± 0.0	90.0 ± 0.0	98.0 ± 0.0	4.3 ± 0.2
DAPC/DPPC (80:20)	33.4 ± 4.0	6.0 ± 1.4	1.0 ± 0.0	4.6 ± 0.1	42.0 ± 2.8	27.0 ± 1.4	2.1 ± 0.1	52.0 ± 1.4	73.0 ± 1.4	5.1 ± 0.6	
DAPC/DPPC (75:25)	44.4 ± 2.9	13.5 ± 3.5	1.0 ± 0.0	5.1 ± 0.1	39.5 ± 0.7	26.5 ± 0.7	2.2 ± 0.0	47.0 ± 2.8	72.5 ± 0.7	9.1 ± 1.7	
DAPC/DPPC (70:30)	53.4 ± 1.1	60.5 ± 0.7	9.0 ± 0.0	8.7 ± 0.9	13.5 ± 0.7	12.5 ± 2.1	2.6 ± 0.1	26.0 ± 1.4	79.0 ± 1.4	34.2 ± 1.1	
DAPC/DPPC (65:35)	54.4 ± 0.6	76.0 ± 0.0	19.5 ± 0.7	13.8 ± 0.0	10.0 ± 0.0	10.0 ± 0.0	2.7 ± 0.1	14.0 ± 0.0	70.5 ± 0.7	43.2 ± 0.7	
DAPC/DPPC (60:40)	54.8 ± 1.0	78.5 ± 0.7	22.5 ± 0.7	14.5 ± 1.3	10.0 ± 1.4	10.5 ± 0.7	2.7 ± 0.0	11.5 ± 0.7	67.0 ± 1.4	44.9 ± 0.8	
DAPC/DPPC (55:45)	54.7 ± 0.3	81.0 ± 1.4	30.0 ± 2.8	17.5 ± 0.1	10.5 ± 0.7	12.0 ± 0.0	2.8 ± 0.0	8.0 ± 1.4	57.5 ± 2.1	46.6 ± 0.5	
DDPC					7.2 ± 1.7	23.5 ± 2.1	7.0 ± 1.4	1.7 ± 0.2	76.5 ± 2.1	93.0 ± 1.4	3.0 ± 0.5
DDPC/DPPC (90:10)	21.1 ± 4.0	8.5 ± 2.1	1.0 ± 0.0	3.5 ± 0.1	51.0 ± 2.8	31.5 ± 4.9	1.3 ± 0.0	40.5 ± 4.9	67.5 ± 4.9	4.0 ± 0.1	
DDPC/DPPC (85:15)	31.8 ± 2.7	11.5 ± 0.7	1.0 ± 0.0	4.0 ± 0.2	46.5 ± 2.1	27.5 ± 0.7	1.4 ± 0.1	42.0 ± 1.4	71.5 ± 0.7	6.1 ± 0.1	
DDPC/DPPC (80:20)	51.1 ± 0.6	63.5 ± 3.5	6.5 ± 0.7	4.9 ± 0.4	17.5 ± 2.1	18.5 ± 2.1	1.4 ± 0.0	20.0 ± 1.4	75.0 ± 1.4	33.4 ± 1.3	
DDPC/DPPC (75:25)	52.2 ± 1.1	77.5 ± 0.7	14.5 ± 0.7	8.0 ± 0.7	9.5 ± 0.7	11.5 ± 0.7	1.6 ± 0.0	13.0 ± 0.0	74.5 ± 0.7	41.5 ± 0.5	
DDPC/DPPC (70:30)	52.3 ± 0.6	82.0 ± 0.0	20.5 ± 0.7	10.8 ± 0.6	9.0 ± 0.0	11.0 ± 0.0	1.8 ± 0.0	9.5 ± 0.7	69.0 ± 0.0	43.8 ± 0.4	
DDPC/DPPC (65:35)	53.4 ± 1.1	82.5 ± 2.1	23.5 ± 2.1	13.5 ± 1.0	9.5 ± 0.7	10.5 ± 0.7	1.9 ± 0.0	8.0 ± 1.4	66.0 ± 1.4	45.5 ± 1.8	
DDPC/DPPC (60:40)	51.7 ± 1.7	84.0 ± 0.0	30.0 ± 0.0	15.1 ± 1.2	10.0 ± 0.0	12.0 ± 0.0	1.9 ± 0.0	6.0 ± 0.0	58.0 ± 0.0	45.2 ± 1.7	
DDPC/DPPC (55:45)	54.2 ± 0.1	85.0 ± 0.0	32.0 ± 2.8	16.5 ± 1.9	9.5 ± 0.7	12.0 ± 0.0	1.9 ± 0.0	5.5 ± 0.7	56.0 ± 2.8	47.7 ± 0.5	

Each value is the average from at least two separate experiments ± SEM. τ , lifetimes (ns); f , fractional intensities (%); α , fractional amplitudes (%); τ_{AV} , intensity-weighted average lifetimes (ns).

Table S5

Comparison of time-resolved fluorescence decays of tPA (1 mol%) in different bilayers at 23 °C

Sample		τ_1	f_1	α_1	τ_2	f_2	α_2	τ_3	f_3	α_3	τ_{AV}
POPC					6.9 ± 0.3	41.0 ± 5.7	25.0 ± 5.7	3.3 ± 0.4	59.0 ± 5.7	75.0 ± 5.7	4.8 ± 0.6
POPC/SSM (90:10)					8.1 ± 0.5	40.5 ± 2.1	24.0 ± 2.8	3.8 ± 0.6	59.5 ± 2.1	76.0 ± 2.8	5.5 ± 0.6
POPC/SSM (85:15)	38.3 ± 1.5	7.0 ± 0.0	1.0 ± 0.0	6.7 ± 0.7	70.5 ± 0.7	55.0 ± 2.8	2.7 ± 0.4	22.5 ± 0.7	44.0 ± 2.8	8.0 ± 0.8	
POPC/SSM (80:20)	32.1 ± 3.8	8.5 ± 0.7	1.5 ± 0.7	7.3 ± 0.6	68.5 ± 3.5	53.5 ± 4.9	2.9 ± 0.3	23.0 ± 2.8	44.5 ± 4.9	8.5 ± 0.2	
POPC/SSM (75:25)	42.7 ± 1.9	22.5 ± 2.1	4.0 ± 1.4	9.6 ± 0.4	49.5 ± 3.5	39.0 ± 5.7	3.6 ± 0.2	28.0 ± 5.7	57.5 ± 6.4	15.3 ± 0.7	
POPC/SSM (70:30)	48.5 ± 0.6	52.5 ± 2.1	15.5 ± 0.7	15.0 ± 0.4	28.5 ± 0.7	26.5 ± 0.7	4.6 ± 0.2	19.0 ± 1.4	58.0 ± 1.4	30.6 ± 1.1	
POPC/SSM (65:35)	49.4 ± 0.3	64.0 ± 0.0	24.0 ± 1.4	17.0 ± 0.6	24.0 ± 0.0	26.0 ± 1.4	4.4 ± 0.5	12.0 ± 0.0	50.5 ± 2.1	36.2 ± 0.3	
POPC/SSM (60:40)	50.6 ± 0.7	72.5 ± 0.7	35.5 ± 0.7	19.4 ± 1.6	20.5 ± 0.7	26.0 ± 0.0	4.4 ± 0.6	6.5 ± 0.7	38.5 ± 0.7	41.0 ± 0.4	
POPC/SSM (55:45)	52.1 ± 1.1	73.0 ± 0.0	41.0 ± 0.0	22.8 ± 1.3	21.0 ± 0.0	26.5 ± 0.7	5.2 ± 0.1	6.0 ± 0.0	32.5 ± 0.7	43.2 ± 1.0	
PLPC					7.6 ± 1.2	27.0 ± 8.5	15.0 ± 7.1	3.5 ± 0.2	73.0 ± 8.5	85.0 ± 7.1	4.5 ± 0.1
PLPC/SSM (90:10)					9.1 ± 1.1	31.0 ± 1.4	16.5 ± 0.7	4.1 ± 0.5	69.0 ± 1.4	83.5 ± 0.7	5.6 ± 0.7
PLPC/SSM (85:15)	42.6 ± 6.4	9.0 ± 2.8	1.0 ± 0.0	6.5 ± 0.1	62.5 ± 0.7	48.0 ± 0.0	2.8 ± 0.1	28.5 ± 2.1	51.0 ± 0.0	8.9 ± 1.7	
PLPC/SSM (80:20)	46.1 ± 0.9	14.5 ± 0.7	2.0 ± 0.0	7.7 ± 0.1	53.5 ± 0.7	40.5 ± 0.7	3.2 ± 0.0	31.5 ± 0.7	57.5 ± 0.7	12.0 ± 0.5	
PLPC/SSM (75:25)	46.2 ± 2.3	35.0 ± 10.1	6.7 ± 2.5	9.9 ± 0.6	40.7 ± 6.8	34.7 ± 3.2	3.6 ± 0.3	24.3 ± 3.5	58.7 ± 2.3	21.2 ± 4.8	
PLPC/SSM (70:30)	48.4 ± 0.5	54.0 ± 2.8	15.0 ± 0.0	13.6 ± 1.3	28.5 ± 2.1	27.5 ± 0.7	4.1 ± 0.5	17.5 ± 0.7	57.5 ± 0.7	30.8 ± 1.0	
PLPC/SSM (65:35)	48.7 ± 0.2	65.5 ± 2.1	24.5 ± 0.7	15.7 ± 0.4	23.5 ± 2.1	27.0 ± 1.4	4.0 ± 0.4	10.5 ± 0.7	48.5 ± 0.7	36.1 ± 0.9	
PLPC/SSM (60:40)	50.8 ± 0.9	73.0 ± 0.0	35.0 ± 1.4	18.8 ± 0.9	20.5 ± 0.7	26.0 ± 0.0	4.2 ± 0.5	7.0 ± 0.0	39.0 ± 1.4	41.2 ± 1.0	
PLPC/SSM (55:45)	52.0 ± 0.7	76.5 ± 0.7	42.0 ± 1.4	21.0 ± 1.1	18.5 ± 0.7	25.5 ± 0.7	4.3 ± 0.4	5.0 ± 0.0	32.5 ± 0.7	43.9 ± 0.9	
PAPC					7.6 ± 1.9	20.5 ± 7.8	10.5 ± 6.4	3.2 ± 0.1	79.5 ± 7.8	89.5 ± 6.4	4.0 ± 0.1
PAPC/SSM (90:10)	28.1 ± 2.6	4.0 ± 0.0	1.0 ± 0.0	4.9 ± 0.0	68.0 ± 1.4	52.0 ± 0.0	2.2 ± 0.2	28.0 ± 1.4	47.5 ± 0.7	5.2 ± 0.2	
PAPC/SSM (85:15)	38.0 ± 1.2	7.5 ± 0.7	1.0 ± 0.0	5.6 ± 0.2	63.5 ± 3.5	48.0 ± 4.2	2.4 ± 0.1	29.5 ± 3.5	51.0 ± 4.2	7.0 ± 0.5	
PAPC/SSM (80:20)	46.5 ± 2.7	16.5 ± 2.1	2.0 ± 0.0	6.8 ± 0.3	48.0 ± 4.2	36.0 ± 2.8	2.9 ± 0.2	35.5 ± 2.1	62.5 ± 2.1	12.0 ± 1.6	
PAPC/SSM (75:25)	48.7 ± 2.0	45.0 ± 7.1	7.5 ± 2.1	9.4 ± 1.1	28.5 ± 6.4	25.0 ± 4.2	3.3 ± 0.3	27.0 ± 1.4	67.5 ± 2.1	25.4 ± 4.1	
PAPC/SSM (70:30)	49.9 ± 0.8	63.5 ± 0.7	17.0 ± 0.0	13.2 ± 1.3	20.0 ± 0.0	21.0 ± 1.4	3.5 ± 0.3	16.5 ± 0.7	62.5 ± 0.7	35.0 ± 0.6	
PAPC/SSM (65:35)	52.8 ± 4.8	73.3 ± 3.5	30.3 ± 9.3	17.4 ± 4.1	18.7 ± 0.6	23.3 ± 3.2	3.6 ± 0.7	8.0 ± 3.6	46.3 ± 12.4	38.9 ± 0.4	
PAPC/SSM (60:40)	51.3 ± 0.6	76.0 ± 1.4	35.0 ± 0.0	18.9 ± 0.8	18.0 ± 1.4	22.5 ± 0.7	3.7 ± 0.2	6.5 ± 0.7	42.5 ± 0.7	42.4 ± 0.8	
PAPC/SSM (55:45)	52.0 ± 0.6	79.0 ± 2.8	41.5 ± 0.7	18.9 ± 2.1	16.5 ± 2.1	23.0 ± 1.4	3.4 ± 0.7	4.5 ± 0.7	35.5 ± 2.1	44.5 ± 1.1	
PDPC					6.0 ± 0.2	32.0 ± 2.8	16.5 ± 0.7	2.6 ± 0.1	68.0 ± 2.8	83.5 ± 0.7	3.7 ± 0.1
PDPC/SSM (90:10)	30.6 ± 10.3	5.5 ± 2.1	1.0 ± 0.0	4.8 ± 0.1	64.0 ± 2.8	46.0 ± 2.8	2.0 ± 0.0	30.5 ± 0.7	53.0 ± 2.8	5.6 ± 1.1	
PDPC/SSM (85:15)	51.1 ± 5.1	15.5 ± 3.5	1.5 ± 0.7	6.5 ± 0.8	47.0 ± 2.8	33.0 ± 4.2	2.6 ± 0.5	37.5 ± 6.4	65.0 ± 4.2	11.9 ± 0.6	
PDPC/SSM (80:20)	44.1 ± 2.2	21.5 ± 0.7	2.5 ± 0.7	7.0 ± 0.1	45.0 ± 1.4	32.5 ± 0.7	2.6 ± 0.2	33.5 ± 2.1	65.0 ± 1.4	13.4 ± 0.0	
PDPC/SSM (75:25)	48.4 ± 0.5	60.5 ± 4.9	13.5 ± 2.1	10.9 ± 0.2	22.0 ± 1.4	21.0 ± 0.0	2.8 ± 0.2	18.0 ± 2.8	65.5 ± 2.1	32.2 ± 2.3	
PDPC/SSM (70:30)	49.1 ± 0.7	70.5 ± 3.5	22.5 ± 2.1	14.2 ± 0.4	19.0 ± 1.4	21.0 ± 0.0	2.9 ± 0.3	10.5 ± 2.1	56.5 ± 2.1	37.6 ± 1.9	
PDPC/SSM (65:35)	50.2 ± 0.4	75.0 ± 0.0	32.0 ± 1.4	17.5 ± 0.7	18.0 ± 0.0	21.5 ± 0.7	3.2 ± 0.1	7.0 ± 0.0	46.5 ± 2.1	41.0 ± 0.1	
PDPC/SSM (60:40)	51.2 ± 0.7	78.0 ± 1.4	38.0 ± 0.0	18.2 ± 1.5	17.0 ± 1.4	23.5 ± 0.7	3.1 ± 0.2	5.0 ± 0.0	38.5 ± 0.7	43.3 ± 0.9	
PDPC/SSM (55:45)	52.1 ± 0.7	79.5 ± 0.7	43.5 ± 0.7	20.3 ± 0.5	17.0 ± 0.0	24.0 ± 0.0	3.3 ± 0.2	4.0 ± 0.0	33.0 ± 1.4	44.8 ± 0.4	

Each value is the average from at least two separate experiments ± SEM. τ , lifetimes (ns); f , fractional intensities (%); α , fractional amplitudes (%); τ_{AV} , intensity-weighted average lifetimes (ns).

Table S6

Comparison of time-resolved fluorescence decays of tPA (1 mol%) in different bilayers at 23 °C

Sample	τ_1	f_1	α_1	τ_2	f_2	α_2	τ_3	f_3	α_3	τ_{AV}
DOPC				5.6 ± 0.1	21.0 ± 1.4	12.0 ± 1.4	2.8 ± 0.0	79.0 ± 1.4	88.0 ± 1.4	3.4 ± 0.0
DOPC/SSM (90:10)	17.6 ± 7.9	3.5 ± 0.7	0.5 ± 0.7	4.6 ± 0.5	69.5 ± 10.6	55.5 ± 12.0	2.2 ± 0.4	27.0 ± 11.3	44.0 ± 12.7	4.4 ± 0.3
DOPC/SSM (85:15)	39.6 ± 1.5	5.0 ± 0.0	1.0 ± 0.0	5.7 ± 0.1	57.0 ± 0.0	40.5 ± 0.7	2.7 ± 0.0	38.5 ± 0.7	59.0 ± 0.0	6.2 ± 0.2
DOPC/SSM (80:20)	46.9 ± 0.2	8.5 ± 0.7	1.0 ± 0.0	6.9 ± 0.2	52.0 ± 0.0	35.0 ± 0.0	2.9 ± 0.1	40.0 ± 0.0	64.0 ± 0.0	8.7 ± 0.1
DOPC/SSM (75:25)	49.7 ± 1.0	16.0 ± 1.4	2.0 ± 0.0	8.7 ± 0.2	45.0 ± 1.4	30.5 ± 0.7	3.4 ± 0.1	39.0 ± 1.4	67.5 ± 0.7	13.2 ± 1.1
DOPC/SSM (70:30)	53.8 ± 0.3	44.5 ± 0.7	8.0 ± 0.0	11.8 ± 0.2	28.0 ± 0.0	22.5 ± 0.7	3.7 ± 0.0	27.5 ± 0.7	69.5 ± 0.7	28.3 ± 0.2
DOPC/SSM (65:35)	55.7 ± 0.4	63.0 ± 0.0	17.5 ± 0.7	15.2 ± 0.6	21.5 ± 0.7	21.5 ± 0.7	3.9 ± 0.1	15.5 ± 0.7	60.5 ± 0.7	39.1 ± 0.4
DOPC/SSM (60:40)	56.7 ± 0.1	70.5 ± 0.7	25.5 ± 0.7	17.9 ± 0.1	19.5 ± 0.7	23.0 ± 0.0	4.0 ± 0.1	10.0 ± 0.0	52.0 ± 1.4	43.7 ± 0.3
DOPC/SSM (55:45)	57.3 ± 0.2	75.0 ± 0.0	33.0 ± 0.0	19.4 ± 0.6	18.0 ± 0.0	24.0 ± 0.0	4.1 ± 0.1	7.0 ± 0.0	43.0 ± 0.0	46.7 ± 0.1
DLPC				4.9 ± 0.0	29.0 ± 0.0	12.5 ± 0.7	1.7 ± 0.0	71.0 ± 0.0	87.5 ± 0.7	2.7 ± 0.0
DLPC/SSM (90:10)	47.3 ± 2.3	9.5 ± 0.7	1.0 ± 0.0	4.2 ± 0.2	47.0 ± 2.8	29.0 ± 2.8	1.6 ± 0.0	43.5 ± 2.1	70.5 ± 3.5	7.1 ± 0.6
DLPC/SSM (85:15)	52.9 ± 0.2	20.5 ± 0.7	1.0 ± 0.0	4.6 ± 0.4	44.0 ± 2.8	30.0 ± 2.8	1.6 ± 0.2	35.0 ± 2.8	68.5 ± 2.1	13.6 ± 0.4
DLPC/SSM (80:20)	56.2 ± 1.3	49.5 ± 3.5	5.0 ± 0.0	6.3 ± 0.6	24.5 ± 0.7	21.5 ± 2.1	1.9 ± 0.2	26.0 ± 2.8	73.5 ± 2.1	30.1 ± 2.4
DLPC/SSM (75:25)	56.4 ± 0.2	65.0 ± 1.4	11.0 ± 1.4	10.3 ± 0.7	16.5 ± 0.7	15.0 ± 0.0	2.3 ± 0.1	18.5 ± 0.7	74.5 ± 0.7	38.8 ± 1.1
DLPC/SSM (70:30)	56.2 ± 0.0	72.0 ± 0.0	16.0 ± 0.0	12.5 ± 0.4	15.5 ± 0.7	16.0 ± 0.0	2.3 ± 0.0	12.5 ± 0.7	68.0 ± 0.0	42.7 ± 0.2
DLPC/SSM (65:35)	56.2 ± 0.4	74.5 ± 0.7	20.0 ± 1.4	13.7 ± 0.6	15.5 ± 0.7	17.0 ± 0.0	2.3 ± 0.1	10.0 ± 0.0	63.0 ± 1.4	44.2 ± 0.2
DLPC/SSM (60:40)	56.5 ± 0.4	77.5 ± 0.7	25.0 ± 1.4	14.9 ± 0.2	15.0 ± 0.0	18.5 ± 0.7	2.3 ± 0.0	7.5 ± 0.7	56.5 ± 2.1	46.2 ± 0.2
DLPC/SSM (55:45)	57.8 ± 0.2	79.5 ± 0.7	29.0 ± 1.4	16.2 ± 1.0	15.0 ± 1.4	19.5 ± 0.7	2.4 ± 0.1	6.0 ± 0.0	51.5 ± 2.1	48.3 ± 0.3
DAPC				6.5 ± 0.3	18.0 ± 5.7	6.5 ± 2.1	2.0 ± 0.0	82.0 ± 5.7	93.5 ± 2.1	2.8 ± 0.3
DAPC/SSM (90:10)	46.4 ± 0.1	9.0 ± 0.0	1.0 ± 0.0	4.4 ± 0.3	41.5 ± 4.9	26.0 ± 4.2	1.8 ± 0.1	49.0 ± 5.7	73.0 ± 4.2	7.1 ± 0.0
DAPC/SSM (85:15)	57.6 ± 0.7	52.0 ± 5.7	5.5 ± 2.1	7.3 ± 1.8	19.0 ± 5.7	16.0 ± 5.7	2.2 ± 0.2	29.5 ± 0.7	78.5 ± 4.9	31.8 ± 2.9
DAPC/SSM (80:20)	57.4 ± 1.5	69.5 ± 0.7	14.0 ± 0.0	13.0 ± 0.4	13.5 ± 0.7	12.0 ± 1.4	2.6 ± 0.1	17.0 ± 0.0	74.5 ± 0.7	42.1 ± 1.6
DAPC/SSM (75:25)	57.6 ± 1.5	77.5 ± 0.7	23.0 ± 1.4	15.3 ± 1.3	13.5 ± 0.7	15.0 ± 1.4	2.6 ± 0.1	9.5 ± 0.7	62.0 ± 0.0	46.7 ± 1.7
DAPC/SSM (70:30)	57.9 ± 1.4	78.5 ± 0.7	28.5 ± 0.7	17.2 ± 0.2	14.5 ± 0.7	18.5 ± 0.7	2.7 ± 0.1	7.0 ± 0.0	53.0 ± 0.0	48.2 ± 1.5
DAPC/SSM (65:35)	58.0 ± 0.7	79.0 ± 0.0	33.0 ± 1.4	18.4 ± 0.7	15.5 ± 0.7	20.5 ± 0.7	2.8 ± 0.2	5.0 ± 0.0	46.5 ± 0.7	48.9 ± 0.9
DAPC/SSM (60:40)	58.5 ± 0.4	80.0 ± 0.0	37.0 ± 1.4	18.7 ± 0.8	16.0 ± 0.0	22.5 ± 0.7	2.8 ± 0.1	4.0 ± 0.0	40.5 ± 0.7	49.9 ± 0.5
DAPC/SSM (55:45)	58.7 ± 1.0	81.0 ± 0.0	40.5 ± 0.7	19.4 ± 0.7	15.5 ± 0.7	24.0 ± 0.0	3.0 ± 0.3	4.0 ± 0.0	36.0 ± 1.4	50.6 ± 1.0
DDPC				8.5 ± 0.3	21.0 ± 1.4	5.5 ± 0.7	1.9 ± 0.0	79.0 ± 1.4	94.5 ± 0.7	3.3 ± 0.1
DDPC/SSM (95:5)	18.3 ± 2.5	10.5 ± 2.1	1.0 ± 0.0	3.4 ± 0.4	47.5 ± 6.4	28.5 ± 4.9	1.2 ± 0.3	42.5 ± 9.2	70.5 ± 4.9	4.0 ± 0.1
DDPC/SSM (90:10)	60.3 ± 0.6	71.0 ± 1.4	8.5 ± 0.7	6.3 ± 0.9	11.5 ± 0.7	14.0 ± 2.8	1.7 ± 0.0	17.0 ± 1.4	77.0 ± 4.2	44.0 ± 1.1
DDPC/SSM (85:15)	58.6 ± 1.0	82.5 ± 3.5	19.5 ± 3.5	11.0 ± 0.3	9.5 ± 2.1	11.5 ± 0.7	1.7 ± 0.0	9.0 ± 1.4	69.0 ± 2.8	49.3 ± 2.6
DDPC/SSM (80:20)	58.3 ± 0.1	83.5 ± 0.7	26.0 ± 1.4	14.5 ± 0.2	10.0 ± 0.0	13.0 ± 0.0	1.9 ± 0.1	6.5 ± 0.7	61.0 ± 1.4	50.2 ± 0.3
DDPC/SSM (75:25)	55.9 ± 1.8	86.0 ± 2.8	31.0 ± 4.2	14.0 ± 0.0	9.0 ± 1.4	13.5 ± 0.7	1.7 ± 0.0	4.5 ± 0.7	56.0 ± 4.2	49.4 ± 0.5
DDPC/SSM (70:30)	56.9 ± 0.9	85.0 ± 1.4	32.0 ± 2.8	14.7 ± 0.2	11.0 ± 1.4	15.5 ± 0.7	1.8 ± 0.1	4.5 ± 0.7	52.0 ± 1.4	50.0 ± 0.0
DDPC/SSM (65:35)	58.4 ± 0.6	85.5 ± 2.1	36.5 ± 2.1	16.4 ± 0.3	11.0 ± 1.4	16.5 ± 0.7	1.9 ± 0.1	3.5 ± 0.7	47.5 ± 0.7	51.7 ± 1.3
DDPC/SSM (60:40)	58.0 ± 0.2	85.0 ± 0.0	39.0 ± 0.0	17.1 ± 0.3	11.5 ± 0.7	18.0 ± 1.4	2.0 ± 0.0	3.0 ± 0.0	44.0 ± 1.4	51.5 ± 0.4
DDPC/SSM (55:45)	58.0 ± 0.5	86.0 ± 0.0	40.5 ± 2.1	17.3 ± 1.1	11.0 ± 0.0	17.0 ± 0.0	2.0 ± 0.2	3.0 ± 0.0	42.5 ± 2.1	51.7 ± 0.5

Each value is the average from at least two separate experiments ± SEM. τ , lifetimes (ns); f , fractional intensities (%); α , fractional amplitudes (%); τ_{AV} , intensity-weighted average lifetimes (ns).

Table S7

Comparison of time-resolved fluorescence decays of tPA (1 mol%) in different bilayers at 23 °C

Sample	τ_1	f_1	α_1	τ_2	f_2	α_2	τ_3	f_3	α_3	τ_{AV}
POPC				6.7 ± 0.1	53.0 ± 1.4	37.0 ± 1.4	3.4 ± 0.0	47.0 ± 1.4	63.0 ± 1.4	5.1 ± 0.0
POPC/PSPC (90:10)	35.5 ± 5.1	5.0 ± 1.4	1.0 ± 0.0	6.4 ± 0.2	74.5 ± 0.7	59.5 ± 0.7	2.7 ± 0.0	20.0 ± 0.0	39.5 ± 0.7	7.1 ± 0.3
POPC/PSPC (85:15)	54.1 ± 1.9	21.5 ± 3.5	2.5 ± 0.7	7.2 ± 0.2	57.5 ± 4.9	51.5 ± 3.5	3.0 ± 0.2	21.0 ± 1.4	46.0 ± 2.8	16.3 ± 2.3
POPC/PSPC (80:20)	58.1 ± 0.9	58.5 ± 0.7	12.0 ± 0.0	8.9 ± 0.1	25.0 ± 0.0	33.0 ± 1.4	3.4 ± 0.1	16.5 ± 0.7	56.0 ± 1.4	36.8 ± 0.9
POPC/PSPC (75:25)	58.9 ± 0.4	69.5 ± 0.7	19.0 ± 0.0	11.4 ± 0.4	16.0 ± 0.0	22.0 ± 1.4	3.9 ± 0.1	14.5 ± 0.7	59.0 ± 1.4	43.4 ± 0.1
POPC/PSPC (70:30)	59.9 ± 0.3	75.0 ± 0.0	24.0 ± 0.0	15.0 ± 0.1	12.5 ± 0.7	16.0 ± 0.0	4.2 ± 0.0	13.0 ± 0.0	59.5 ± 0.7	47.2 ± 0.3
POPC/PSPC (65:35)	60.5 ± 0.0	78.0 ± 0.0	29.0 ± 1.4	16.1 ± 0.5	12.0 ± 0.0	16.5 ± 0.7	4.1 ± 0.0	10.0 ± 0.0	54.5 ± 0.7	49.5 ± 0.4
POPC/PSPC (60:40)	62.2 ± 0.4	78.5 ± 0.7	31.5 ± 0.7	18.7 ± 0.4	12.0 ± 0.0	16.0 ± 0.0	4.3 ± 0.0	9.5 ± 0.7	53.0 ± 1.4	51.6 ± 0.1
POPC/PSPC (55:45)	61.4 ± 0.5	82.5 ± 0.7	37.5 ± 0.7	18.8 ± 1.3	10.5 ± 0.7	16.0 ± 0.0	4.0 ± 0.3	6.5 ± 0.7	45.5 ± 0.7	52.5 ± 0.7
PLPC				7.5 ± 0.1	24.0 ± 1.4	13.5 ± 0.7	3.6 ± 0.0	76.0 ± 1.4	86.5 ± 0.7	4.5 ± 0.0
PLPC/PSPC (90:10)	16.5 ± 0.5	3.3 ± 0.6	1.0 ± 0.0	5.2 ± 0.2	78.7 ± 2.9	65.0 ± 3.5	2.2 ± 0.2	18.0 ± 3.5	34.3 ± 3.8	5.1 ± 0.0
PLPC/PSPC (85:15)	38.5 ± 3.3	4.5 ± 0.7	1.0 ± 0.0	5.9 ± 0.0	70.5 ± 0.7	55.0 ± 0.0	2.7 ± 0.0	26.0 ± 0.0	44.0 ± 0.0	6.5 ± 0.4
PLPC/PSPC (80:20)	60.9 ± 0.2	49.5 ± 2.1	7.0 ± 0.0	7.7 ± 0.4	26.5 ± 2.1	29.5 ± 4.9	3.4 ± 0.2	24.5 ± 4.9	63.0 ± 5.7	32.8 ± 1.3
PLPC/PSPC (75:25)	62.3 ± 0.2	61.5 ± 0.7	11.5 ± 0.7	9.1 ± 0.5	17.5 ± 2.1	22.0 ± 2.8	3.6 ± 0.1	20.5 ± 0.7	66.5 ± 2.1	40.9 ± 0.3
PLPC/PSPC (70:30)	62.5 ± 0.8	73.0 ± 1.4	19.0 ± 1.4	11.9 ± 0.1	11.0 ± 0.0	14.5 ± 0.7	3.8 ± 0.1	16.0 ± 1.4	66.5 ± 2.1	47.6 ± 0.3
PLPC/PSPC (65:35)	62.6 ± 1.0	78.0 ± 1.4	24.0 ± 1.4	14.3 ± 0.2	9.5 ± 0.7	12.5 ± 0.7	4.0 ± 0.0	13.0 ± 1.4	63.5 ± 2.1	50.5 ± 0.0
PLPC/PSPC (60:40)	63.7 ± 0.8	80.0 ± 0.0	28.5 ± 0.7	18.4 ± 0.5	9.0 ± 0.0	11.5 ± 0.7	4.1 ± 0.1	11.0 ± 0.0	60.5 ± 0.7	53.0 ± 0.4
PLPC/PSPC (55:45)	64.4 ± 1.0	81.0 ± 0.0	31.5 ± 0.7	20.1 ± 0.6	9.5 ± 0.7	12.0 ± 0.0	4.2 ± 0.0	9.5 ± 0.7	56.5 ± 0.7	54.5 ± 0.6
PAPC				6.8 ± 0.2	25.5 ± 0.7	13.5 ± 0.7	3.2 ± 0.1	74.5 ± 0.7	86.5 ± 0.7	4.1 ± 0.0
PAPC/PSPC (90:10)	45.5 ± 1.1	8.0 ± 0.0	1.0 ± 0.0	5.2 ± 0.1	62.5 ± 0.7	49.0 ± 1.4	2.4 ± 0.1	29.5 ± 0.7	50.5 ± 2.1	7.6 ± 0.0
PAPC/PSPC (85:15)	58.3 ± 0.6	32.5 ± 2.1	3.0 ± 0.0	6.1 ± 0.2	37.0 ± 4.2	34.5 ± 3.5	2.8 ± 0.1	30.5 ± 2.1	62.5 ± 3.5	22.2 ± 1.3
PAPC/PSPC (80:20)	61.3 ± 0.1	58.5 ± 2.1	9.5 ± 0.7	9.4 ± 0.9	15.0 ± 2.8	15.5 ± 3.5	3.4 ± 0.1	26.5 ± 0.7	76.0 ± 2.8	38.2 ± 1.0
PAPC/PSPC (75:25)	61.9 ± 0.5	70.5 ± 0.7	15.0 ± 0.0	11.6 ± 0.2	10.5 ± 0.7	42.5 ± 43.1	3.4 ± 0.0	19.0 ± 0.0	72.5 ± 0.7	45.4 ± 0.1
PAPC/PSPC (70:30)	62.6 ± 0.8	76.0 ± 0.0	20.5 ± 0.7	15.1 ± 3.1	9.5 ± 0.7	11.0 ± 1.4	3.5 ± 0.2	14.0 ± 0.0	68.5 ± 0.7	49.6 ± 1.1
PAPC/PSPC (65:35)	63.0 ± 0.5	78.5 ± 0.7	25.0 ± 1.4	16.9 ± 0.6	9.0 ± 0.0	11.0 ± 0.0	3.6 ± 0.0	11.5 ± 0.7	65.0 ± 1.4	51.6 ± 0.1
PAPC/PSPC (60:40)	63.9 ± 0.5	82.0 ± 0.0	31.0 ± 1.4	18.5 ± 1.3	9.0 ± 0.0	12.0 ± 0.0	3.6 ± 0.1	8.5 ± 0.7	57.0 ± 1.4	54.4 ± 0.8
PAPC/PSPC (55:45)	63.8 ± 0.1	83.0 ± 0.0	33.5 ± 0.7	19.9 ± 1.0	9.5 ± 0.7	12.0 ± 0.0	3.7 ± 0.0	8.0 ± 0.0	54.5 ± 0.7	54.9 ± 0.1
PDPC				5.4 ± 0.2	43.5 ± 2.1	14.5 ± 0.7	1.2 ± 0.0	56.5 ± 2.1	85.5 ± 0.7	3.0 ± 0.0
PDPC/PSPC (90:10)	13.6 ± 4.2	12.0 ± 2.8	1.5 ± 0.7	3.3 ± 0.3	48.5 ± 0.7	22.5 ± 0.7	0.8 ± 0.0	39.5 ± 2.1	76.5 ± 2.1	3.5 ± 0.3
PDPC/PSPC (85:15)	50.9 ± 1.8	30.5 ± 4.9	1.5 ± 0.7	4.2 ± 0.2	36.0 ± 2.8	19.0 ± 0.0	0.9 ± 0.0	33.5 ± 2.1	80.0 ± 0.0	17.5 ± 2.9
PDPC/PSPC (80:20)	54.8 ± 0.0	54.5 ± 2.1	3.5 ± 0.7	4.4 ± 0.4	23.5 ± 0.7	18.0 ± 1.4	0.9 ± 0.1	21.5 ± 2.1	78.5 ± 2.1	31.1 ± 1.4
PDPC/PSPC (75:25)	55.3 ± 0.9	64.5 ± 10.6	5.0 ± 2.8	4.7 ± 0.4	18.5 ± 4.9	17.5 ± 0.7	0.9 ± 0.1	17.0 ± 5.7	77.5 ± 3.5	36.6 ± 6.3
PDPC/PSPC (70:30)	55.5 ± 0.7	77.5 ± 0.7	10.0 ± 0.0	5.5 ± 0.5	12.0 ± 0.0	16.5 ± 0.7	1.0 ± 0.1	10.5 ± 0.7	73.5 ± 0.7	43.7 ± 0.1
PDPC/PSPC (65:35)	56.3 ± 0.1	81.5 ± 2.1	13.0 ± 2.8	6.1 ± 1.1	9.5 ± 0.7	15.0 ± 1.4	1.1 ± 0.1	8.5 ± 0.7	72.0 ± 1.4	46.8 ± 1.0
PDPC/PSPC (60:40)	56.3 ± 0.9	87.0 ± 1.4	21.5 ± 3.5	8.0 ± 0.7	7.5 ± 0.7	13.0 ± 0.0	1.2 ± 0.0	6.0 ± 1.4	65.5 ± 3.5	49.5 ± 1.6
PDPC/PSPC (55:45)	57.1 ± 0.8	87.5 ± 0.7	22.0 ± 1.4	7.9 ± 0.4	7.0 ± 0.0	12.5 ± 0.7	1.1 ± 0.0	5.5 ± 0.7	65.5 ± 0.7	50.7 ± 0.2

Each value is the average from at least two separate experiments ± SEM. τ , lifetimes (ns); f , fractional intensities (%); α , fractional amplitudes (%); τ_{AV} , intensity-weighted average lifetimes (ns).

Table S8

Comparison of time-resolved fluorescence decays of tPA (1 mol%) in different bilayers at 23 °C

Sample	τ_1	f_1	α_1	τ_2	f_2	α_2	τ_3	f_3	α_3	τ_{AV}
DOPC				6.7 ± 0.1	21.0 ± 0.0	11.0 ± 0.0	3.1 ± 0.0	79.0 ± 0.0	89.0 ± 0.0	3.8 ± 0.0
DOPC/PSPC (90:10)	15.2 ± 0.8	4.0 ± 0.0	1.0 ± 0.0	4.3 ± 0.0	79.0 ± 2.8	66.0 ± 2.8	1.9 ± 0.1	17.0 ± 2.8	33.0 ± 2.8	4.3 ± 0.0
DOPC/PSPC (85:15)	45.3 ± 3.8	7.0 ± 1.4	1.0 ± 0.0	5.0 ± 0.1	64.0 ± 2.8	51.5 ± 2.1	2.4 ± 0.1	29.0 ± 1.4	48.0 ± 1.4	7.1 ± 1.0
DOPC/PSPC (80:20)	60.3 ± 0.1	65.0 ± 1.4	11.0 ± 1.4	7.8 ± 1.3	13.0 ± 4.2	18.0 ± 7.1	3.1 ± 0.3	22.0 ± 2.8	71.5 ± 6.4	40.8 ± 1.0
DOPC/PSPC (75:25)	61.4 ± 0.3	74.0 ± 1.4	16.0 ± 1.4	8.6 ± 0.9	10.5 ± 2.1	16.0 ± 4.2	3.1 ± 0.2	16.0 ± 1.4	68.0 ± 2.8	46.7 ± 0.5
DOPC/PSPC (70:30)	63.3 ± 0.1	78.5 ± 0.7	20.0 ± 1.4	12.3 ± 0.8	7.5 ± 0.7	9.5 ± 0.7	3.3 ± 0.0	14.5 ± 0.7	70.0 ± 0.0	50.9 ± 0.5
DOPC/PSPC (65:35)	64.3 ± 0.3	81.5 ± 0.7	25.5 ± 0.7	16.8 ± 1.3	7.0 ± 0.0	8.5 ± 0.7	3.5 ± 0.1	11.5 ± 0.7	65.5 ± 0.7	54.0 ± 0.0
DOPC/PSPC (60:40)	62.0 ± 1.6	88.0 ± 1.4	42.0 ± 5.7	19.1 ± 1.7	6.0 ± 0.0	9.0 ± 0.0	3.6 ± 0.1	6.0 ± 1.4	49.0 ± 5.7	55.9 ± 0.5
DOPC/PSPC (55:45)	64.5 ± 1.0	86.0 ± 1.4	35.5 ± 3.5	19.4 ± 0.2	7.5 ± 0.7	10.0 ± 0.0	3.5 ± 0.1	7.5 ± 0.7	54.5 ± 3.5	56.9 ± 0.1
DLPC				5.6 ± 0.1	27.5 ± 0.7	10.5 ± 0.7	1.7 ± 0.0	72.5 ± 0.7	89.5 ± 0.7	2.8 ± 0.0
DLPC/PSPC (95:5)	9.3 ± 0.3	6.5 ± 0.7	1.5 ± 0.7	2.9 ± 0.0	65.5 ± 2.1	47.5 ± 2.1	1.1 ± 0.0	27.5 ± 2.1	51.0 ± 2.8	2.8 ± 0.1
DLPC/PSPC (90:10)	56.6 ± 0.3	29.5 ± 3.5	2.0 ± 0.0	4.0 ± 0.1	36.0 ± 1.4	28.5 ± 0.7	1.5 ± 0.1	34.5 ± 2.1	70.5 ± 0.7	18.8 ± 1.5
DLPC/PSPC (85:15)	60.4 ± 0.5	59.5 ± 3.5	5.5 ± 0.7	5.2 ± 0.4	17.0 ± 0.0	18.5 ± 2.1	1.8 ± 0.0	23.5 ± 3.5	75.5 ± 3.5	37.2 ± 1.9
DLPC/PSPC (80:20)	60.1 ± 0.0	73.5 ± 2.1	10.5 ± 0.7	5.6 ± 0.5	11.5 ± 2.1	17.5 ± 3.5	1.7 ± 0.1	15.0 ± 0.0	72.5 ± 2.1	45.2 ± 1.2
DLPC/PSPC (75:25)	61.5 ± 1.0	78.0 ± 1.4	13.0 ± 0.0	6.7 ± 0.5	9.0 ± 0.0	14.0 ± 1.4	1.8 ± 0.1	13.0 ± 1.4	73.0 ± 1.4	48.8 ± 1.3
DLPC/PSPC (70:30)	61.8 ± 0.0	83.0 ± 0.0	18.0 ± 1.4	8.7 ± 2.5	7.5 ± 0.7	11.5 ± 3.5	1.9 ± 0.1	10.0 ± 0.0	70.0 ± 2.8	51.8 ± 0.1
DLPC/PSPC (65:35)	62.1 ± 0.7	85.5 ± 2.1	22.0 ± 0.0	9.0 ± 3.3	6.5 ± 0.7	12.5 ± 3.5	1.9 ± 0.2	8.0 ± 1.4	66.0 ± 4.2	53.9 ± 0.0
DLPC/PSPC (60:40)	62.2 ± 0.9	87.0 ± 1.4	24.5 ± 0.7	9.2 ± 3.9	6.5 ± 0.7	13.0 ± 4.2	1.9 ± 0.2	6.5 ± 0.7	62.5 ± 3.5	54.7 ± 0.4
DLPC/PSPC (55:45)	62.2 ± 0.1	87.5 ± 0.7	26.0 ± 1.4	9.4 ± 4.1	6.0 ± 0.0	13.5 ± 4.9	1.8 ± 0.2	6.0 ± 0.0	60.0 ± 2.8	55.3 ± 0.1
DAPC				6.8 ± 0.0	19.5 ± 2.1	6.5 ± 0.7	2.1 ± 0.0	80.5 ± 2.1	93.5 ± 0.7	3.0 ± 0.0
DAPC/PSPC (95:5)	14.2 ± 5.2	30.0 ± 35.4	11.0 ± 14.1	6.9 ± 5.2	57.0 ± 2.8	30.0 ± 12.7	1.8 ± 0.7	41.0 ± 5.7	70.0 ± 12.7	3.3 ± 0.2
DAPC/PSPC (90:10)	59.1 ± 1.4	35.5 ± 2.1	2.0 ± 0.0	6.2 ± 0.2	17.0 ± 0.0	11.0 ± 0.0	2.2 ± 0.1	48.0 ± 1.4	87.0 ± 0.0	22.9 ± 1.5
DAPC/PSPC (85:15)	61.4 ± 1.1	72.5 ± 3.5	11.0 ± 1.4	8.3 ± 0.7	8.0 ± 1.4	9.0 ± 0.0	2.3 ± 0.0	20.0 ± 2.8	80.5 ± 2.1	45.4 ± 1.1
DAPC/PSPC (80:20)	61.2 ± 0.2	85.5 ± 0.7	22.0 ± 0.0	9.4 ± 1.4	5.0 ± 0.0	9.0 ± 1.4	2.2 ± 0.1	9.5 ± 0.7	69.0 ± 1.4	52.8 ± 0.3
DAPC/PSPC (75:25)	62.2 ± 0.9	85.0 ± 1.4	23.5 ± 0.7	10.8 ± 4.4	6.0 ± 0.0	10.0 ± 2.8	2.3 ± 0.2	8.5 ± 0.7	66.0 ± 2.8	53.9 ± 0.4
DAPC/PSPC (70:30)	63.2 ± 0.5	87.5 ± 0.7	32.0 ± 1.4	16.7 ± 0.3	6.0 ± 0.0	8.5 ± 0.7	2.5 ± 0.0	6.5 ± 0.7	60.0 ± 1.4	56.6 ± 0.1
DAPC/PSPC (65:35)	64.1 ± 0.3	87.5 ± 0.7	34.0 ± 4.2	17.5 ± 2.9	6.5 ± 0.7	9.0 ± 0.0	2.5 ± 0.1	5.5 ± 0.7	57.0 ± 4.2	57.5 ± 0.2
DAPC/PSPC (60:40)	63.8 ± 0.2	88.5 ± 0.7	38.0 ± 5.7	18.6 ± 3.0	7.0 ± 0.0	10.0 ± 0.0	2.6 ± 0.2	4.5 ± 0.7	51.5 ± 4.9	57.7 ± 0.9
DAPC/PSPC (55:45)	64.1 ± 0.0	88.5 ± 0.7	41.5 ± 3.5	19.5 ± 0.4	7.0 ± 0.0	11.0 ± 0.0	2.6 ± 0.1	4.5 ± 0.7	47.5 ± 3.5	58.3 ± 0.6
DDPC				5.6 ± 0.0	31.5 ± 0.7	11.5 ± 0.7	1.6 ± 0.1	68.5 ± 0.7	88.5 ± 0.7	2.8 ± 0.0
DDPC/PSPC (95:5)	40.3 ± 1.9	12.0 ± 1.4	1.0 ± 0.0	3.6 ± 0.0	43.5 ± 0.7	24.0 ± 0.0	1.2 ± 0.0	44.5 ± 0.7	76.0 ± 0.0	6.9 ± 0.8
DDPC/PSPC (90:10)	59.4 ± 0.2	63.5 ± 2.1	5.5 ± 0.7	5.1 ± 0.5	15.5 ± 2.1	16.0 ± 1.4	1.4 ± 0.2	21.0 ± 0.0	78.5 ± 0.7	38.7 ± 1.2
DDPC/PSPC (85:15)	61.1 ± 0.6	79.5 ± 3.5	12.0 ± 2.8	6.0 ± 1.0	8.5 ± 2.1	13.5 ± 2.1	1.4 ± 0.1	11.0 ± 1.4	74.5 ± 0.7	49.5 ± 2.6
DDPC/PSPC (80:20)	61.2 ± 0.1	84.0 ± 1.4	16.5 ± 3.5	7.8 ± 2.2	7.0 ± 1.4	11.0 ± 2.8	1.5 ± 0.2	8.5 ± 0.7	72.0 ± 1.4	52.2 ± 1.0
DDPC/PSPC (75:25)	60.9 ± 0.4	88.5 ± 0.7	27.0 ± 1.4	10.8 ± 0.2	5.5 ± 0.7	9.5 ± 0.7	1.6 ± 0.0	5.5 ± 0.7	63.5 ± 2.1	54.8 ± 0.1
DDPC/PSPC (70:30)	61.9 ± 0.6	88.5 ± 0.7	25.5 ± 4.9	10.5 ± 2.2	6.0 ± 0.0	10.5 ± 0.7	1.6 ± 0.1	5.5 ± 0.7	64.0 ± 4.2	55.4 ± 0.1
DDPC/PSPC (65:35)	62.1 ± 0.1	89.5 ± 0.7	30.0 ± 2.8	12.0 ± 0.6	6.0 ± 0.0	10.0 ± 0.0	1.6 ± 0.0	4.5 ± 0.7	60.0 ± 2.8	56.3 ± 0.3
DDPC/PSPC (60:40)	61.7 ± 0.5	90.5 ± 0.7	38.5 ± 3.5	15.6 ± 0.6	6.0 ± 0.0	10.0 ± 0.0	1.8 ± 0.0	3.5 ± 0.7	51.0 ± 2.8	56.8 ± 0.1
DDPC/PSPC (55:45)	62.4 ± 0.3	90.5 ± 0.7	38.5 ± 4.9	15.3 ± 1.7	6.0 ± 0.0	10.5 ± 0.7	1.8 ± 0.1	3.5 ± 0.7	51.0 ± 5.7	57.4 ± 0.2

Each value is the average from at least two separate experiments ± SEM. τ , lifetimes (ns); f , fractional intensities (%); α , fractional amplitudes (%); τ_{AV} , intensity-weighted average lifetimes (ns).

Table S9

Measured polydispersity and Z-average values for multilamellar vesicles prepared from PSPC and the different unsaturated PC:s. The samples were hydrated and bath sonicates as described under Materials and Methods. Each value is the calculated average based on 45 scans of one sample.

<u>Sample Composition</u>	<u>PDI</u>	<u>Z-average (nm)</u>
PSPC (100 %)	0.29	994
PSPC/POPC (45/55 by mol)	0.42	822
PSPC/PLPC (45/55 by mol)	0.36	1002
PSPC/PAPC (45/55 by mol)	0.67	1235
PSPC/PDPC (45/55 by mol)	0.54	423
PSPC/DOPC (45/55 by mol)	0.34	918
PSPC/DLPC (45/55 by mol)	0.29	844
PSPC/DAPC (45/55 by mol)	0.18	502
PSPC/DDPC (45/55 by mol)	0.44	304

Table S10. Phase transition enthalpies for PSM and DPPC, and for their mixtures with unsaturated phosphatidylcholines. The lipid compositions were either 100 % PSM or DPPC; or 45 mol% saturated phospholipid in 55 mol% unsaturated PC. The total lipid concentration was 2-3 mM. In all bilayer systems, the molar enthalpy was calculated based on the saturated PC concentration only. DSC scans were recorded between 0 and 70 °C, with a temperature gradient of 1 °C/min. Data analysis was performed with Origin software. Since the peaks were broad, subtracting the correct baseline was not trivial, and will affect the measured enthalpies (approximately + 20%).

Composition Enthalpy (kJ/mol)

PSM 26.5 (100%)

PSM/POPC 7.5 (28%)

PSM/PLPC 6.6 (25%)

PSM/PAPC 6.8 (26%)

PSM/PDPC 8.7 (33%)

PSM/DOPC 10.7 (40%)

PSM/DLPC 17.0 (64%)

PSM/DAPC 12.3 (47%)

PSM/DDPC 14.0 (53%)

DPPC 34.6 (100%)

DPPC/POPC 7.6 (22%)

DPPC/PLPC 14.9 (43%)

DPPC/PAPC 17.3 (50%)

DPPC/PDPC 13.3 (38%)

DPPC/DOPC 8.6 (25%)

DPPC/DLPC 16.5 (48%)

DPPC/DAPC 12.1 (35%)

DPPC/DDPC 17.9 (52%)

The value in parenthesis is the percentage of the enthalpy relative to the pure saturated PC enthalpy.